Fakultät für Medizin

Institut für Klinische Chemie und Pathobiochemie

Analysis of tumor evolution in a model of T-NHL

Tim Wartewig

Vollständiger Abdruck der von der Fakultät für Medizin der Technischen Universität München zur Erlangung des akademischen Grades eines

Doctor of Philosophy (Ph.D.)

genehmigten Dissertation.

Vorsitzender: Prof. Dr. Stefan Lichtenthaler

Betreuer: Prof. Dr. Jürgen Ruland

Prüfer der Dissertation:

1. Prof. Dr. Radu Roland Rad

2. Prof. Dr. Mathias Heikenwälder

3. Prof. Dr. Oliver Weigert

Die Dissertation wurde am 01.07.2020 bei der Fakultät für Medizin der Technischen Universität München eingereicht und durch die Fakultät für Medizin am 14.10.2020 angenommen.

Teile der vorliegenden Arbeit wurden bereits veröffentlicht unter:

Wartewig, T., Z. Kurgyis, S. Keppler, K. Pechloff, E. Hameister, R. Öllinger, R. Maresch, T. Buch, K. Steiger, C. Winter, R. Rad, and J. Ruland. 2017. '*PD-1 is a haploinsufficient suppressor of T cell lymphomagenesis*', Nature, 552: 121-25.

Wartewig, T., and J. Ruland. 2019. *'PD-1 Tumor Suppressor Signaling in T Cell Lymphomas'*, Trends Immunol, 40: 403-14.

Declaration of co-contribution

The following parts of this thesis were generated independently by co-authors listed in the original publication Wartewig, T. et al. Nature 552, 121–125 (2017):

1) Library preparation and sequencing of RNA samples (Genomics & Proteomics Core Facility, Deutsches Krebsforschungszentrum, Heidelberg)
2) Quantitative insertion site sequencing (R. Öllinger[1], R. Maresch[1], R. Rad[1])
3) Copy number analysis using Control-FREEC (C. Winter[2])
4) Histology and histological evaluation (K. Steiger[3])
5) Generation of CD4CreER^{T2} mice (T. Buch[4])

The following parts of this thesis were done together or with substantial technical help and scientific input of co-authors listed in the original publication Wartewig, T. et al. Nature 552, 121–125 (2017):

1) Preparation of microspheres with subsequent Phosflow analysis (S. Keppler[1])
2) *In vivo* antibody blockade (Z. Kurgyis[1])
3) PI3K inhibitor treatment *in vivo* (K. Pechloff[1], E. Hameister[1])

---

[1] TranslaTUM, Center for Translational Cancer Research, Technische Universität München, 81675 München, Germany

[2] Institut für Klinische Chemie und Pathobiochemie, Klinikum rechts der Isar, Technische Universität München, 81675 München, Germany

[3] Institute of Pathology, Technische Universität München, 81675 München, Germany

[4] Institute of Laboratory Animal Science, University of Zurich, Zurich, Switzerland

Abstract

Peripheral mature T-cells can be the origin of aggressive cancers called T-cell Non-Hodgkin lymphoma (T-NHL). Mostly of CD4 subtype these hematological cancers have poor survival rates and only very few specific therapies exist to date (Lemonnier, Gaulard, and de Leval 2018; Jacobsen and Weinstock 2018; Van Arnam, Lim, and Elenitoba-Johnson 2018). Recent sequencing studies have shown that mutations of T cell receptor (TCR) associated genes play a major role in the pathogenesis of T-NHL (Casulo et al. 2017; Kataoka et al. 2015; Wang et al. 2015; da Silva Almeida et al. 2015). However, detailed insights in the underlying mechanisms of lymphoma development are still lacking. Studying a mouse model of T-NHL, which is based on the expression of ITK-SYK, resulting from a chromosomal translocation that is recurrently found in T-NHL patients, we investigated the evolution of these cancers *in vivo* and found that T cells harbor mechanisms that can block oncogene engaged TCR pathways. We observed that after acute activation of ITK-SYK in single T cells those cells expanded heavily for a few days, but only in a transient manner indicating the existence of counter-regulatory mechanisms. To specify the tumor suppressive pathways, we performed a genome-wide transposon-based screen for co-operative events in which we found *PDCD1* as the statistically most significant inactivated gene. Bioinformatical analysis revealed that PD-1 is also mutated in human T-NHL biopsies in up to 30 percent of the patients depending on the T-NHL subtype. Of note, only a single allele of PD-1 is inactivated in most of the patients. In agreement, we observed that ITK-SYK driven T cells, in the absence of a single or both copies of *PDCD1*, give rise to fully transformed cancers within weeks. Moreover, we treated ITK-SYK mice with Checkpoint Inhibitor therapy (anti-PD-1 and anti-PD-L1 antibodies), which led to an aggressive outgrowth of oncogene driven T cells. Importantly, those cells were unable to expand *in vivo* when we treated the mice with control antibodies. Moreover, we observed that inactivation of PD-1 led to enhanced PI3K and PKC signaling, and pharmacological interference of these pathways prolongs survival of mice harboring PD-1 deficient ITK-SYK lymphomas. Our results provide new insights into the evolution of T-NHL and have an impact on new therapy regimes for these cancers.

Zusammenfassung

Periphere T-Zellen können der Ausgangspunkt für aggressive T-Zell Non-Hodgkin Lymphome (T-NHL) sein, für welche bis jetzt nur wenig gezielte Therapieansätze existieren. Die Überlebenschancen für betroffene Patienten sind schlecht und ein detaillierteres Verständnis der Tumormechanismen ist dringend erforderlich (Lemonnier, Gaulard, and de Leval 2018; Jacobsen and Weinstock 2018; Van Arnam, Lim, and Elenitoba-Johnson 2018). In den vergangenen Jahren haben verschiedene Studien gezeigt, dass Mutationen in T-Zell Rezeptor assoziierte Signalmolekülen eine wesentliche Rolle im Entstehungsprozess dieser Krebsentität spielen (Casulo et al. 2017; Kataoka et al. 2015; Wang et al. 2015; da Silva Almeida et al. 2015). Wir haben anhand eines Mausmodells, welches auf dem wiederholt in T-NHL Patienten auftretenden Fusionsprotein ITK-SYK basiert, den Entstehungsprozess dieser Lymphome studiert und herausgefunden, dass T-Zellen intrinsische Mechanismen besitzen, um einer Onkogen-Transformation entgegenzuwirken. Genauer hat sich gezeigt, dass nach Aktivierung der ITK-SYK Mutation in einer geringen Anzahl peripherer T-Zellen, die betroffenen Zellen zunächst für einige Tage stark expandieren, dann jedoch durch zell-intrinsische Programme gestoppt werden. Um diese suppressiven Signalwege zu identifizieren, haben wir einen genom-weiten Mutagenese Screen mittels Transposons durchgeführt. Hierdurch konnten wir den inhibitorischen Rezeptor PD-1 als entscheidenden Tumor Suppressor auf T-Zellen identifizieren. Bioinformatische Analysen haben zudem gezeigt, dass PD-1 auch in humanen T-NHL in bis zu einem Drittel der Patienten mutiert ist. Interessanterweise ist in betroffenen Patienten typischerweise nur eine Kopie von *PDCD1* inaktiviert. In Übereinstimmung haben wir beobachtet, dass ITK-SYK Aktivierung in T-Zellen, welche kein oder nur ein einzelnes *PDCD1* Allel besitzen, ein unmittelbar transformiertes T-Zell Lymphom zur Folge hat. Darüber hinaus haben wir durch Checkpoint-Inhibitor Behandlung mittels PD-1 oder PD-L1 blockierenden Antikörpern eine massive Proliferation von Onkogen getriebenen T-Zellen beobachtet, welche andernfalls (ohne Antikörper-Behandlung) unfähig waren *in vivo* zu expandieren. Zudem hat sich gezeigt, dass in Abwesenheit von PD-1 die Signalkaskaden von PI3K und PKC in ITK-SYK exprimierenden Zellen verstärkt sind und dass Intervention mit PI3K-Inhibitoren das Überleben von Mäusen mit PD-1

defizienten ITK-SYK Lymphomen verlängert. Diese Ergebnisse liefern neue Einsichten in den Entstehungsprozess und die Behandlung von T-NHL.

Glossary

ATLL, Adult T cell leukemia/lymphoma, is a neoplasm of mature T cells etiologically linked to the human T-cell lymphotropic virus 1. Disease manifestations are subcategorized depending on their clinical course: acute, chronic, smoldering and lymphoma.

ALCL, Anaplastic Large Cell Lymphoma, are distinguished from other lymphomas by their anaplastic cytology and constant surface expression of the CD30.

AITL, Angioimmunoblastic T cell lymphoma, is characterized by generalized lymphadenopathy, high fever, skin rash and autoimmune-like manifestations. AITL tumor cells share characteristics with TFH cells.

Central memory T cell, antigen-experienced T cell that expresses CD45RO, CCR7, and CD62L

CD4-Cre, Cre recombinase under the control of the CD4 promoter

CD4-CreERT2, similar to CD4-Cre but the translocation of the Cre recombinase into the nucleus is dependent on administration of tamoxifen

Cre, Bacteriophage derived recombinase

CTCL, Cutaneous T cell lymphoma (CTCL) represent a heterogeneous group of lymphomas characterized by abnormal accumulation of malignant T cells in the skin resulting in the development of plaques, rashes and tumors.

Exhaustion, T cell exhaustion is a state of T cell dysfunction that develops during cancer and chronic infections. It is defined by poor effector functions, persistent surface expression of inhibitory receptors and a distinct transcriptional profile.

Focal loss is a decrease in copy number of a genomic DNA segment, which is limited to a small fraction of a chromosome.

FTCL, Follicular T-cell lymphoma, is one of several novel forms of peripheral T cell lymphomas recognized in the last decade which is thought to originate from follicular helper T cells.

Frameshift indel is a genetic mutation caused by insertion or deletion of a number of nucleotides in a DNA sequence that is not divisible by three.

Immunological synapse, interface between an antigen-presenting cell or target cell and a lymphocyte such as a T cell, B cell or Natural Killer cell.

ITIM, immunoreceptor tyrosine-based inhibition motif, is a conserved sequence of amino acids that is present in the cytoplasmic tails of many inhibitory receptors

ITK-SYK, Translocation of the interleukin-2 inducible T cell kinase and the spleen tyrosine kinase

ITSM, immunoreceptor tyrosine-based switch motif, is a conserved sequence of amino acids important for signal transduction of multiple tyrosine-phosphorylated receptors

Lipid rafts are combinations of glycosphingolipids and protein receptors organized in glycolipoprotein lipid microdomains in the plasma membrane.

MF, Mycosis fungoides, is the most common form of cutaneous T-cell lymphoma. Symptoms include rash, tumors, skin lesions, and itchy skin.

Nodal peripheral T cell lymphoma is a T-NHL subcategory that includes angioimmunoblastic T-cell lymphoma, nodal peripheral T-cell lymphoma with T follicular helper phenotype, peripheral T-cell lymphoma, not otherwise specified and follicular T-cell lymphoma.

PD-1, Programmed cell death protein 1, is an inhibitory receptor expressed on several immune cell subsets including T cells containing an ITIM and an ITSM.

Pdcd1, Gene encoding mouse PD-1

PDCD1, Gene encoding human PD-1

PD-L1, Programmed Death Ligand 1, is one of the two known ligands for PD-1

PH, Pleckstrin homology domain (PH domain) is a protein domain involved in intracellular signaling

Piggybac, transposase derived from the Cabbage Looper moth

Single nucleotide variant is a variation in a single nucleotide without any limitations of frequency.

SS, Sézary Syndrome, is an aggressive form of cutaneous T cell lymphoma. In SS the cancerous T cells, called Sézary cells, are present in the blood, skin, and lymph nodes.

TCR, T cell receptor

T-follicular helper (TFH) cells are a distinct subset of antigen-experienced $CD4^+$ T cells that regulate the development of antigen-specific B cell immunity.

T lymphoblastic lymphoma is an aggressive neoplasm of precursor T cells that occurs mostly in young adults.

Transposase, enzyme that can change the position of a transposon

Transposon, segment of DNA in the genome which can change its place.

Whole-exome sequencing is genomic technique for sequencing all protein-coding regions in an organism's genome.

Whole-genome sequencing is the process of determining the complete genomic DNA sequence of an organism's genome.

1 Introduction

1.1 Normal and malignant T cells

T cells are key effector lymphocytes of the adaptive immune system. They are critical for the destruction of infectious pathogens and the killing of endogenous cancer cells. Nevertheless, peripheral T cells can also transform into cancer cells and give rise to malignant lymphomas (called T cell non-Hodgkin lymphoma, T-NHL or Peripheral T-cell Lymphoma, PTCL), which represent highly aggressive cancers with a still ill-defined molecular pathogenesis (Lemonnier, Gaulard, and de Leval 2018; Jacobsen and Weinstock 2018; Van Arnam, Lim, and Elenitoba-Johnson 2018). Normal T cells possess clonotypic antigen receptors (T cell receptors, TCRs) that sense diverse types of antigens and subsequently trigger intracellular signaling cascades that drive the clonal expansion, survival and differentiation of naïve T cells to mediate effector functions (Courtney, Lo, and Weiss 2018; Tubo and Jenkins 2014; Weiss and Littman 1994). Intriguingly, recent molecular studies of mature T-cell lymphomas have revealed a large series of oncogenic mutations within the signaling molecules that normally control the TCR and coreceptor pathways that govern physiological T cell activation (Choi et al. 2015; Wang et al. 2015; da Silva Almeida et al. 2015; Vaque et al. 2014; Kataoka et al. 2015).

1.2 T cell lymphomas are a heterogeneous group of malignancies

Mature T cell lymphomas represent a clinical collection of diverse malignancies that depending on the geographic region represent from ten to thirty percent of all human lymphomas (Vose 2008; Park and Ko 2014). T-NHLs usually have a CD4+ T cell origin and are grouped into several subentities based on their histological and phenotypic characteristics (Arber et al. 2016). The T-NHLs that primarily infiltrate the skin are

referred to as cutaneous T cell lymphomas (CTCLs) and include two major entities, mycosis fungoides (MFs) and Sézary syndrome (SS), the latter of which is sometimes considered late-stage MF, which is characterized by the presence of a circulating TCR clone identical to that found in the skin (Arber et al. 2016). MF is a CTCL with an indolent clinical course that shows slow progression and for which the cell of origin is thought to be a tissue-resident CD4+ TCRβ+ TCRγ- T cell (Arber et al. 2016). In contrast, SS is a leukemic form of CTCL with a poor prognosis in which cancerous T cells are also found in the blood and frequently exhibit a CD4+ CD27+ central memory T-cell phenotype but can also express T-follicular helper cell (TFH) signature genes (Arber et al. 2016; Whittaker, Hoppe, and Prince 2016; Jawed et al. 2014b, 2014a).

The most prevalent subgroup of non-CTCLs are angioimmunoblastic T-cell lymphomas, which are malignant CD4+ T cells that also significantly express TFH markers, such as PD-1, CD10, BCL6, CXCL13, ICOS, SAP and CCR5 determined on protein level by immunohistochemistry (IHC) or flow cytometric or on the mRNA level by gene expression profiling and compared to other types of T-cell malignancies (e.g. ALK+ or ALK- Anaplastic Large Cell Lymphoma (ALCL), T lymphoblastic lymphoma) or to healthy control tissue (Dorfman et al. 2006; Zhan et al. 2011; Attygalle et al. 2002; Agostinelli et al. 2011; de Leval et al. 2007; Vose 2008; Arber et al. 2016; Bosisio and Cerroni 2015). While the primary site of disease is the lymph nodes, these cancers also show frequent systemic manifestations. The clinical course is variable but overall poor, with a 32% 5-year median survival rate (Lunning and Vose 2017; Vose 2008). TFH cell marker proteins are also expressed by nodal peripheral T cell lymphomas (PTCLs) with TFH phenotype, as well as follicular T-cell lymphoma which shows an aggressive clinical course with 50% of patients dying within 24 months after diagnosis (Arber et al. 2016).

An additional T cell lymphoma class is adult T-cell leukemia/lymphoma (ATLL), which is frequently caused by T cell infection with the deltaretrovirus HTLV-1 and is characterized by malignant CD4+ cells with a monoclonal HTLV-1 integration pattern (Arber et al. 2016; Ishitsuka and Tamura 2014). Although the virus-encoded Tax and HBZ proteins are thought to play major roles in T-NHL pathogenesis, HTLV-1 infection alone is not sufficient for neoplastic transformation, and further genetic alterations are required to cause malignancy, which typically occurs decades after the initial HTLV-1 infection.

There is a large group of PTCLs that does not match the characteristics of any of the T-cell lymphoma entities defined in the World Health Organization (WHO) classification (Arber et al. 2016). These T-NHLs are therefore referred to as 'PTCL not otherwise specified (PTCL-NOS)', a category often described as a "wastebasket". The prognosis of PTCL-NOS patients is currently dismal due to a lack of effective therapies. Efforts to subclassify PTCL-NOS cases for meaningful disease-stratification models are currently ongoing.

1.3 Oncogenic activation of TCR pathways is a hallmark of T cell lymphomas

Despite the diverse histopathological and clinical presentation of mature T-NHLs and certain subtype-specific pathomechanisms (Broccoli and Zinzani 2017), one emerging hallmark of multiple T-NHL entities is the oncogenic activation of signaling pathways that are physiologically engaged by TCRs (Gaud, Lesourne, and Love 2018; Brownlie and Zamoyska 2013; Choi et al. 2015; Wang et al. 2015; da Silva Almeida et al. 2015; Vaque et al. 2014; Kataoka et al. 2015) (Figure 1). This conclusion was based on a series of independent studies performed using whole-genome sequencing, whole-exome sequencing and mRNA sequencing of primary human T-NHL cases (Choi et al.

2015; Wang et al. 2015; da Silva Almeida et al. 2015; Vaque et al. 2014; Kataoka et al. 2015) and by IHC/flow cytometric analysis of activation markers such as PD-1 and CD25 (Dorfman et al. 2006; O'Malley et al. 2014).

1.3.1 TCR proximal kinases and Phospholipase C, gamma 1 (PLCG1)

Gain-of-function variants, focal amplifications and transcriptional deregulation are recurrently detected in genes that encode for proximal signal transducers of the TCR signaling machinery, such as the SRC family kinases LCK and FYN (Palomero et al. 2014; Kataoka et al. 2015; McGirt et al. 2015; Vallois et al. 2016). After normal antigen sensing, LCK and FYN phosphorylate ITAM motifs located on TCR-associated CD3 chains, leading to the recruitment and activation of the tyrosine kinase ZAP70 and subsequent T cell activation (Rossy, Williamson, and Gaus 2012; Pitcher and van Oers 2003). Oncogenic mutations in FYN have been observed in nodal, cutaneous and leukemic T-NHL cases at a frequency of 3-4% and LCK mutations have, in particular, been reported in AITL patients (Palomero et al. 2014; Kataoka et al. 2015; McGirt et al. 2015; Vallois et al. 2016). LCK normally phosphorylates and activates the interleukin-2-inducible T-cell kinase ITK, which subsequently generates a signalosome complex with LAT, SLP-76, VAV1 and PLCG1, thereby triggering the activation of PLCG1 to convert phosphatidylinositol 4,5-bisphosphate into DAG/IP3 (Finco et al. 1998; Liu et al. 1999). These events are critical for calcium release and PKC activation downstream of the TCR. Copy number variant (CNVs) of ITK have been detected in AITL tumors (Liang et al. 2014), and activating mutations in PLCG1 are frequently observed in the nodal (>10% (Vallois et al. 2016)), cutaneous (>10% (Choi et al. 2015)) and leukemic (>30% (Kataoka et al. 2015)) forms of T-NHL.

1.3.2 ITK-SYK

Moreover, in addition to focal genomic lesions, the recurrent chromosomal translocation t(5;9)(q33;q22), which fuses the regions 5q33 and 9q22 harboring the antigen receptor kinase genes ITK and SYK (Streubel et al. 2006), has been recurrently detected in follicular T-NHL. This translocation generates a fusion transcript, driven by the ITK promoter, which contains exons 1-5 of the ITK gene fused to exon 8-14 of the SYK locus. The resulting protein contains the PH and Tec homology domains of ITK fused to the SYK kinase domain with a size of approximately 55 kDa. *In vitro* studies on this fusion protein have revealed that ITK-SYK has conserved the catalytic activity of a tyrosine kinase in a constitutive active manner, constitutively associates with lipid rafts and induces TCR pathways by activating PI3kinase signaling, PLCγ and PKCθ (Rigby et al. 2009; Pechloff et al. 2010). Moreover, our lab has shown in the past, that transgenic mice, which express ITK-SYK in the T cell lineage, develop T cell lymphomas that mimic human T-NHLs regarding clinical as well as histopathological properties (Pechloff et al. 2010).

1.3.3 Caspase recruitment domain-containing protein 11 (CARD11)

Normal TCR proximal signals are transduced to the NF-κB and JNK pathways via the multidomain scaffold protein CARD11, which plays a key role as a signaling hub during the adaptive immune response (Ruland and Hartjes 2018). After antigen sensing and PKCθ activation, PKCθ directly phosphorylates CARD11, leading to changes in its conformation and an interaction with BCL10 and MALT1 that leads to T cell activation. Gain of function CARD11 mutations that abolish intramolecular autoinhibition and autonomously activate the CARD11 protein have been recurrently observed in cutaneous (>20%) and leukemic (>20%) T-NHL cases as well as in nodal T-NHL

tumors (<10%) (Park and Ko 2014; Chen et al. 2015; Choi et al. 2015; Kataoka et al. 2015; Vallois et al. 2016).

1.3.4 Rho GTPases and GEFs

One critical process during physiological T cell activation is further remodeling of the actin cytoskeleton, which is required not only for early immunological synapse formation and receptor clustering but also for positioning signaling molecules into the proper location. These events depend on Rho GTPases, which are activated by GEFs, such as VAV1 (Rougerie and Delon 2012; Katzav, Martin-Zanca, and Barbacid 1989; Tarakhovsky et al. 1995). VAV1-positive lesions are present in nodal (>10% (Boddicker et al. 2016; Abate et al. 2017)) and leukemic T-NHL forms (>10% (Kataoka et al. 2015)). In addition, VAV1 is often translocated to various other genes, where it causes in-frame fusion transcripts that typically lack the VAV1 inhibitory SH3 domain, resulting in enhanced VAV1 signaling (Abate et al. 2017). Similarly, RHOA is mutated in nodal T-NHL (50% (Palomero et al. 2014; Vallois et al. 2016; Abate et al. 2017; Odejide et al. 2014; Lemonnier et al. 2012) and leukemic (<10% (Kataoka et al. 2015)) T-NHL entities in which the lesions are postulated to enhance AKT signaling (Yoo et al. 2014).

The enforced activation of TCR pathways observed in T-NHL also occurs as a result of loss-of-function lesions in inhibitory genes such as TNFAIP3, which encodes the ubiquitin modifying enzyme A20 that provides feedback regulation to the NF-kB pathway (Ma and Malynn 2012). Inactivating mutations in TNFAIP3 have been found in cutaneous (>20% (Choi et al. 2015)) and leukemic (<10% (Kataoka et al. 2015)) T-NHL, which likely stimulate this signaling cascade. Another negative ubiquitin regulator of T-cell activation is the E3 ubiquitin–protein ligase CBLB, which is recruited to the

plasma membrane after T cell activation and subsequently degrades TCR signaling components, including TCRs. Inactivating mutations in CBLB have been reported in ATLL (10% (Kataoka et al. 2015)).

1.3.5 PI3K/AKT pathway

The PI3K/AKT pathway is also recurrently affected by T-NHL mutations. In normal T cells, TCRs and several T cell coreceptors activate PI3K signaling, which is critical for T cell proliferation, survival, differentiation, metabolism and migration (Wieman, Wofford, and Rathmell 2007; Juntilla and Koretzky 2008; Han, Patterson, and Levings 2012). In T-cells class I, PI3K phosphorylates phosphatidylinositol-4,5-bisphosphate to form phosphatidylinositol-3,4,5-triphosphate (PIP3) on the inner membrane of the cell, thus initiating the recruitment and activation of downstream effectors, such as PDK1 and its substrate AKT (Okkenhaug and Vanhaesebroeck 2003). Gain-of-function lesions for PI3K/AKT elements have been detected at varying prevalence in all T-NHL entities (including cutaneous (Papadavid et al. 2014), leukemic (Kataoka et al. 2015), and nodal T-NHL (Vallois et al. 2016)). The affected genes include PIK3CA, PIK3CD, PIK3R1, PIK3R5, PIK3CA, PDK1 and AKT1. Several phosphatases, including the lipid phosphatases PTEN and INPP4B, which antagonize PI3K activity, negatively regulate the PI3K signaling axis. Similarly, mutations in these negative regulators were detected in up to 36% (PTEN (Cristofoletti et al. 2013; da Silva Almeida et al. 2015)) of CTCL specimens and have been reported in PTCL-NOS (Dahia et al. 1999) and ATLL (INPP4B (Kataoka et al. 2015)) patients.

1.3.6 Co-receptors CD28, ICOS, CTLA4

Normal T cell activation requires not only antigen sensing by TCRs but also costimulation by CD28 upon binding to B7 family ligands (CD80 or CD86), which

induces the activation of the p85 subunit of PI3K. Activating mutations in CD28 have been detected in patients with nodal T-NHL (>10%) (Vallois et al. 2016; Rohr et al. 2016), leukemic T-NHL (20%) (Kataoka et al. 2015; Chen et al. 2015) and cutaneous T-NHL (>10% (Choi et al. 2015)). In addition to focal amplifications and translocations, the amino acids F51 and D124 are hotspots for single nucleotide variants (SNVs), which presumably enhance the activity of the CD28 ligand-binding domains. In addition, in-frame gene fusions between CTLA4 or ICOS and CD28 have been described for CTCL (Ungewickell et al. 2015; Chen et al. 2015; Vallois et al. 2018), ATLL (Kataoka et al. 2015; Vallois et al. 2018) and AITL (Ungewickell et al. 2015; Vallois et al. 2018). These translocations result in the fusion of the extracellular CTLA4 or ICOS domains with the cytoplasmic tail of CD28 and is thought to aberrantly enhance coreceptor signaling.

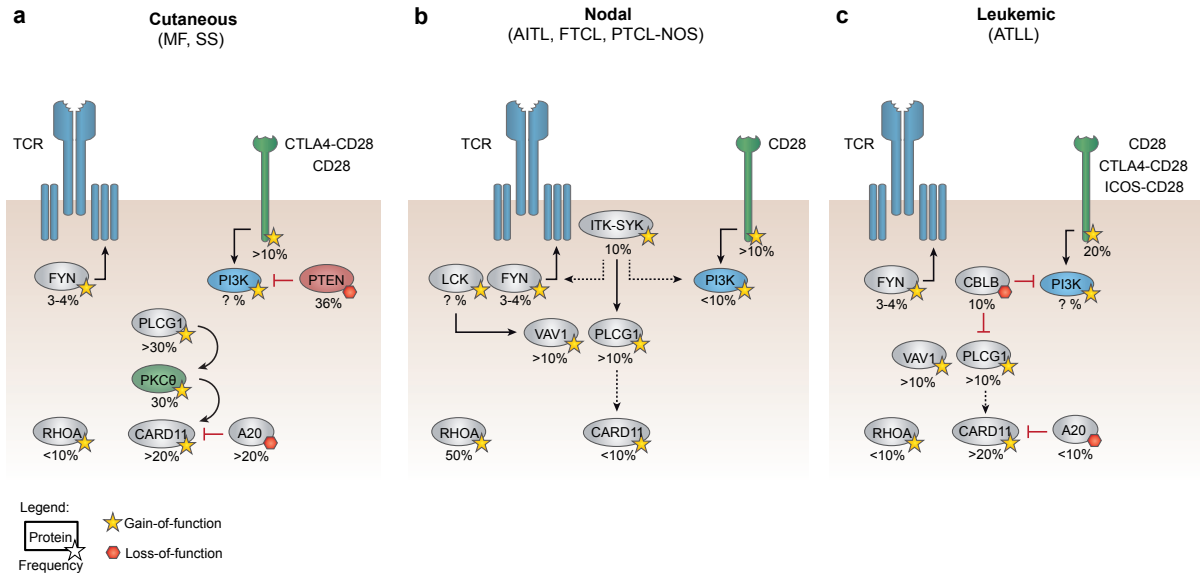

Figure 1 T-NHL oncogenic drivers in TCR pathways

The receptors and signaling pathway components that are recurrently mutated in T-NHL are depicted. Gain-of-function (yellow stars) and loss-of-function (red stars) mutational landscape within T cell receptor signaling pathways in cutaneous T-NHL (a), nodal T-NHL

(b) and leukemic T-NHL (c) with annotated frequencies.
? denotes lack of sufficient data for frequency estimation. Mycosis fungoides (MF), Sézary Syndrome (SS), Angioimmunoblastic T-cell lymphoma (AITL), Follicular T-cell lymphoma (FTCL), Peripheral T-cell lymphoma not otherwise specified (PTCL-NOS). CTLA4-CD28 and ICOS-CD28 denote recurrent in-frame fusion genes which are generated by translocation of the CTLA4 or ICOS loci to the CD28 locus.

2 Methods

2.1 Mice

Mice of both sexes aged 6-12 weeks were used for all experiments. Littermate controls were used whenever possible. Randomization and blinding were not used. $Rosa26^{LSL\text{-}ITK\text{-}SYK}$ mice (Pechloff et al. 2010) were backcrossed for more than 12 generations on a C57BL/6 genetic background. CD4Cre-ERT2 (Sledzinska et al. 2013) mice were crossed to the $Rosa26^{LSL\text{-}ITK\text{-}SYK}$ strain to generate the ITK-$SYK^{CD4Cre\text{-}ERT2}$ mice. $Rosa26^{LSL\text{-}PB}$ mice (Rad et al. 2015) were crossed to $Rosa26^{LSL\text{-}ITK\text{-}SYK}$ mice to generate the $Rosa26^{LSL\text{-}ITK\text{-}SYK}$;$Rosa26^{LSL\text{-}PB}$ strain, and ATP2-H32 (Rad et al. 2010) mice were crossed to CD4-Cre mice to generate the ATP2;CD4-Cre transgenic animals. Both resulting lines were crossed again to generate the quadruple-transgenic $Rosa26^{LSL\text{-}ITK\text{-}SYK}$;$Rosa26^{LSL\text{-}PB}$;ATP2;CD4-Cre mice and the control cohorts. C57BL/6, Nod Scid $Il2rg^{-/-}$ (NSG, 005557), CD4-Cre (022071 (Lee et al. 2001)) and PD-$1^{-/-}$ (028276 (Keir, Freeman, and Sharpe 2007)) mice were purchased from the Jackson Laboratory, Bar Harbor, Maine, USA. CD4-Cre and PD-$1^{-/-}$ mice were backcrossed on a C57BL/6 genetic background. All animal experiments were performed according to local guidelines (Regierung von Oberbayern, Munich, Germany).

2.2 Flow cytometry

The flow cytometric analyses were performed using standard protocols. Primary cell suspensions from the spleen, lymph nodes, or peripheral blood were directly labelled. Single-cell suspensions from the liver, kidney, or lung were first purified by Percoll gradient centrifugation. Fluorescently labelled antibodies against the following surface proteins were used for mouse cell staining: TCRβ (APC/Cy7 anti-mouse TCR β chain Antibody, 10922), CD4 (Pacific Blue anti-mouse CD4 Antibody, 100428), CD44 (PE

anti-mouse/human CD44 Antibody, 103008), and PD-1 (APC anti-mouse CD279 (PD-1) Antibody, 135210). For the Jurkat and primary human T cells, a PD-1 (APC anti-human CD279 (PD-1) Antibody, 329908) antibody was used. Fc receptor blocking was performed with anti-CD16/32 antibodies (101320 or 422302). All antibodies were purchased from BioLegend, San Diego, California, USA. The data were acquired using a FACSCanto II flow cytometer (Becton, Dickinson and Company, Franklin Lakes, New Jersey, USA). FlowJo software (FlowJo LLC, Ashland, Oregon, USA) was used for the data analyses.

2.3 GeneScan analysis for TCR gene rearrangements

Genomic DNA from magnetically purified (130104454, Miltenyi Biotec, Bergisch Gladbach, Germany) $CD4^+$ T cells from C57BL/6 mice (Control), young ITK-$SYK^{CD4\text{-}Cre}$ mice and ITK-$SYK^{CD4\text{-}Cre}$ mice with lymphoma was extracted (DNeasy, Qiagen, Venlo, Netherlands). The GeneScan analysis for TCR gene rearrangements was performed as previously described in detail(Pechloff et al. 2010). In summary, VDJ rearrangements of the TCRβ and TCRγ loci were amplified in five PCR reactions containing 26 primers in total, with three primers labelled with 5'-FAM fluorochromes. Fluorochrome-labelled PCR products were then size separated and scanned via capillary electrophoresis.

2.4 Induction of spontaneous ITK-SYK expression in peripheral T cells

Tamoxifen (T5648, Sigma-Aldrich, St. Louis, Missouri, USA) was dissolved in pure ethanol (with heating) and subsequently diluted in migliol (3274, Caesar & Loretz, Hilden, Germany) to a final concentration of 10 mg/ml. To induce the expression of ITK-SYK in a small fraction of the peripheral $CD4^+$ T cells, ITK-$SYK^{CD4\text{-}CreERT2}$ or ITK-

SYK$^{CD4\text{-}CreERT2}$;PD-1$^{-/-}$ mice received tamoxifen via intraperitoneal (i.p.) injection of the indicated doses.

2.5 RNA

For the RNAseq experiments, ITK-SYK$^{CD4\text{-}CreERT2}$ mice were i.p. injected with single doses of 1 mg tamoxifen per mouse (T5648, Sigma-Aldrich). Forty-eight hours after injection, the spleens and lymph nodes were harvested, single-cell suspensions underwent CD4+ T cell purification by magnetic depletion (130104454, Miltenyi Biotec), and the cells were cultured *in vitro*. At the indicated time points, the T cells were FACS-sorted (FACSAria, Becton, Dickinson and Company) again for viability, and eGFP. Total RNA was extracted, typically from approximately 100,000 cells, using spin columns (RNeasy Micro Plus Kit, Qiagen). Library preparation from 1 ng total RNA was performed with the SMART-Seq v2 Ultra Low Input RNA Kit (Takara Bio Inc., Kusatsu, Shiga, Japan), and SE-50 bp sequencing was performed on Illumina HiSeq2000 machines (Illumina, San Diego, California, USA). Read alignment to the mm10 genome and transcriptome assembly were performed using HISAT2 (Kim, Langmead, and Salzberg 2015) and StringTie (Pertea et al. 2015). Differential expression was assessed with ballgown (Frazee et al. 2015). GSEA was performed with BubbleGUM (Spinelli et al. 2015); to assess proliferation, the following signatures were selected: Whitfield_cell_cycle_literature (Whitfield et al. 2002), Ishida_E2F_targets (Ishida et al. 2001) and Hallmark_G2M_checkpoint (Liberzon et al. 2015). RNAseq data for the naïve murine CD4+ T cells were retrieved from the Gene Expression Omnibus data repository series GSE83315 (van der Veeken et al. 2016) (samples 83,84,85), re-aligned to the mm10 genome using HISAT2 and then processed in a manner similar to that applied to the other samples.

For *Pdcd1* mRNA quantification within the Rosa26$^{LSL\text{-}ITK\text{-}SYK}$;Rosa26$^{LSL\text{-}PB}$;ATP2;CD4-Cre lymphomas, total RNA was extracted from eGFP+ FACS-sorted (FACSAria, Becton, Dickinson and Company) spleen derived lymphocytes using spin-columns (RNeasy Micro Plus Kit, Qiagen) and then reverse transcribed (M0368L, NEB, Ipswich, Massachusetts, USA). The Pdcd1 and eGFP cDNA amount was simultaneously quantified using transcript specific probes (4331182, Mm01285676_m1, FAM-MGB and 4448484, Mr03989638_mr, VIC-MGB_PL, Thermo Fisher Scientific) on a ddPCR sytem (QX200 Droplet Digital PCR System, 1864001, Biorad, Hercules, California, USA). Subsequently, the eGFP-normalized Pdcd1 cDNA amount was categorized based on the presence of transposon cassettes within the Pdcd1 locus.

For the identification of Pdcd1 mRNA-transposon splice junctions the following primers were used (Dupuy et al. 2005) for amplification:

Antisense orientation:	Ex1f	ATGTGGGTCCGGCA
	En2ASAr	CATCTTTCACATACCGGCTA
Sense orientation:	LunSDf	CTACTAGCACCAGAACGCCC
	Ex2r	AGGCCGCCTTCTGTAATGGTT

2.6 Quantitative insertion site sequencing

Lymphomas from moribund Rosa26$^{LSL\text{-}ITK\text{-}SYK}$;Rosa26$^{LSL\text{-}BP}$;ATP2;CD4-Cre mice were harvested by generating single-cell suspensions from the spleens and lymph nodes and then sorting for 5x10^6 viable eGFP$^+$CD4$^+$ T cells on a FACSAria sorter (Becton, Dickinson and Company). Genomic DNA was extracted using spin columns (DNeasy, Qiagen). Recovery of transposon insertion sites was performed using QiSeq, a splinkerette-PCR based method for semi-quantitative insertion site sequencing(Boeva et al. 2012). Bioinformatics data processing, mapping of sequence reads and statistical analyses to identify CIS using TAPDANCE were described earlier (Boeva et al. 2012).

CISs that were also detected in the data from the control animals without the ITK-SYK transgene were excluded from the analysis.

2.7 Genomic *PDCD1* alterations in human T cell lymphoma

PubMed and Google Scholar were searched for published studies on human T cell malignancies that included whole-genome, whole-exome, or targeted sequencing that included the *PDCD1* locus. The supplementary data from the identified studies were searched for single nucleotide variants, small indels, and copy number aberrations (CNAs) that affected the *PDCD1* locus. Whole-genome sequencing data (aligned BAM files, 47 tumor-normal pairs, (Kataoka et al. 2015)) were downloaded from the European Genome-phenome Archive after data access was granted. Whole exome sequencing data (aligned BAM files, 34 tumor-normal pairs (Choi et al. 2015)) were downloaded from the Sequence Read Archive (accession PRJNA285408). The BAM files were subjected to a copy number analysis using Control-FREEC (Boeva et al. 2012). The copy numbers were calculated in windows of 3 kb with steps of 1 kb for each tumor using the tumors and corresponding normal samples as inputs. A breakpoint analysis, segmentation, and absolute copy number calling were performed with Control-FREEC. The resulting segments and copy number ratios (tumor/normal) were log2-transformed and plotted for all tumors along chromosome 2 for visual inspection.

2.8 GSVA and *PDCD1* FPKM analyses in human T cell lymphoma

RNAseq data of human T-NHL patients was downloaded from the Sequence Read Archive (accession PRJNA285408, (Choi et al. 2015)) and the European Genome-phenome Archive (Kataoka et al. 2015). Reads in fasta format were extracted from sra

or bam files and re-aligned to the hg19 genome with hisat2 (Kim, Langmead, and Salzberg 2015) and processed with stringtie (Pertea et al. 2015) and ballgown (Frazee et al. 2015). All samples for which genomic data (WES or WGS) was available were included in the analysis. Using GSVA (Hanzelmann, Castelo, and Guinney 2013) for each sample an enrichment score was calculated based on the geneset from the MSigDB: GO_ANTIGEN_RECEPTOR_MEDIATED_SIGNALING_PATHWAY (195 genes). Twenty-eight of fifty samples enriched positive and were included in the subsequent analysis. FPKM values for *PDCD1* were extracted and statistically compared based on the *PDCD1* copy number status.

2.9 Cloning

For generation of the PD-1 vector, first, the 3' LTR of the lentiGuide-Puro Plasmid (52963, Addgene, Cambridge, Massachusetts, USA) was replaced by an HIV/MSCV hybrid LTR. The LTR-modified backbone and the central polypurine tract (cPPT) sequence was then amplified with the BsmBI restriction site containing oligos BBf, BBr or CPPTf, CPPTr. Finally, the *PDCD1* cDNA was cloned together with an IRES-GFP and the cPPT sequence into the modified backbone by Golden Gate Assembly using the PDCD1f, PDCD1r primers for the cDNA and the IRESGFPf, IRESGFPr primers for the IRES-GFP sequence. The PD-1 YFYF plasmid was subsequently generated using sequential site-directed-mutagenesis with the Y223F and Y248F primer pairs.

PD-1-IRES-GFP	BBf	CTAGCGTCTCGTTTTAATCAACCTCTGGATTACAAAATTTGT
	BBr	CTTGGCGTCTCCGCCGTGGGAGGTGGGTCTGA
	CPPTf	CTAGCGTCTCGCGGCACTAGATCTTGAGACAAATGGCA
	CPPTr	TTGGCGTCTCCGTTGCCCTCGAGCCGGCG
	PDCD1f	CTAGCGTCTCGCAACGCCACCATGCAGATCCCACAGGCG
	PDCD1r	TTGGCGTCTCCTTTGTCAGAGGGGCCAAGAGCA
	IRESGFPf	CTAGCGTCTCGCAAACTCGAGGGTACCCCAATTC

	IRESGFPr	TTGGCGTCTCCAAAATTACTTGTACAGCTCGTCCAT
PD-1YFYF-IRES-GFP	Y223Ff	TTTGGGGAGCTGGATTTCC
	Y223Fr	GTCCACAGAGAACACAGGC
	Y248Ff	TTTGCCACCATTGTCTTTCCT
	Y248Fr	CTCCGTCTGCTCAGGG

2.10 Cell culture

T cells were cultured in RPMI-1640 containing 20% FCS in the case of the primary cells or in 5% FCS in the case of the Jurkat-Eco T cells. For the Phoenix-Eco and Phoenix-Ampho packaging cells, we used DMEM with 10% FCS. No authentication of the cell lines was performed. All cell lines were routinely tested for mycoplasma infection.

For the generation of dendritic cells, Ficoll (Ficoll-Paque PLUS, 17144002, GE Healthcare) gradient seperated PBMCs from healthy donors were magnetically enriched for monocytes (130050201, Miltenyi). Next, the cells were cultured for six days in presence of recombinant IL-4 (20 ng/ml, 20004, Peprotech, Rocky Hill, New Jersey, USA) and GM-CSF (100 ng/ml, 30003, Peprotech). Finally, PD-L1 was induced on the differentiated dendritic cells with a 24-hours-incubation in presence of recombinant Interferon-γ (100 ng/ml, 30002, Peprotech).

For the Idelalisib *in vitro* treatment, the inhibitor was dissolved in DMSO and the cell culture medium was supplemented with the indicated concentration of the compound or DMSO only as a control.

2.11 Retroviral infections

Generation of ecotropic viral particles based on the GFP, ITK-SYK or ITK-SYK^{KD} constructs and infection of Jurkat-Eco cells was done as previously described (Pechloff et al. 2010). For generation of amphotropic retrovirus Phoenix-Ampho cells were grown

in 15 cm dishes and transfected with Fugene (Promega, Madison, Wisconsin, USA) and 10 µg ITK-SYK or ITK-SYK^{KD}. The media was changed 8 h after transfection. The viral supernatant was collected 36 h after transfection, passed through a 0.45 µm filter and used either fresh or snap-frozen. Activated primary human CD4 T-cells were spin-infected with RetroNectin (Takara Bio Inc.) coated 6-well plates (5 mg/ml).

For the production of lentiviral particles, we used HEK293FT cells. Fugene (Promega) based transfection was done with 17 µg pCMV delta R8.2, 10 µg pHCMV-10A1 and 10 µg PD-1 or PD-1 YFYF. HH cells were spin-infected with the lentivirus on RetroNectin (Takara Bio Inc.) coated 6-well plates (5 mg/ml).

2.12 Primary human T-cells

Human PBMCs were isolated by ficoll density centrifugation of fresh blood from healthy donors. CD4 T-cells were enriched by magnetic depletion (130096533, Miltenyi Biotec) and stimulated with anti-CD3/anti-CD28 beads (11161D, Thermo Fisher Scientific Inc., Waltham, Massachusetts, USA) and 10 ng/ml IL-2 (20002, Peprotech, Rocky Hill, New Jersey, USA). After 48 hours, the cells were infected with retrovirus. Five days later the T-cells were stimulated again with 2 µg/ml soluble anti-CD28 (302933, Biolegend) and analyzed for PD-1 expression by flow cytometry.

2.13 Transplantation experiments

For the transplantation experiments into the NSG recipients, splenocytes from the donor mice were harvested at day 7 after tamoxifen (T5648, Sigma-Aldrich; 0.25 mg) induction, subjected to CD8 T cell depletion (11447D, Thermo Fisher Scientific) and then transferred into NSG mice via injection. For the C57BL/6 transplantation experiments, splenocytes from Rosa26$^{LSL\text{-}ITK\text{-}SYK}$ and Rosa26$^{LSL\text{-}ITK\text{-}SYK}$:PD-1$^{-/-}$ mice

were harvested, and the $CD4^+$ T cells were purified and subsequently incubated for one hour in non-serum-containing media (31985062, Thermo Fisher Scientific) supplemented with 1 µM recombinant TAT-CRE protein (EG1001, Excellgen Inc., Rockville, Maryland, USA). After washing, cells were i.v. injected into C57BL/6 recipients. For transplantation into tertiary C57BL/6 recipient mice the spleens from moribund secondary recipients were harvested, FACS-sorted for eGFP, washed and i.v. injected ($1x10^5$ cells/recipient) into wild-type C57BL/6 mice. For the PI3K inhibitor treatment the NSG recipient mice received $5x10^4$ $eGFP^+$ T-cells together with CD8 depleted (11447D, Thermo Fisher Scientific) splenocytes from ITK-$SYK^{CD4\text{-}CreERRT2}$;$PD\text{-}1^{-/-}$ mice, which had been tamoxifen (T5648, Sigma-Aldrich; 0.25 mg) treated five days earlier. Five days after transplantation the NSG mice received Idelalisib (CAL-101, GS-1101, PI3Kδ inhibitor; S2226, Selleckchem, Houston, Texas, USA) or vehicle (0.5% carboxymethylcellulose, 0.05% Tween 80 in ultra-pure water, C5678 and P4780, Sigma-Aldrich) by oral gavage (10 mg per kg per day), 5 days a week.

2.14 PI3K inhibitor treatment *in vivo*

For the PI3K inhibitor treatment the NSG recipient mice received $5x10^4$ $eGFP^+$ T-cells together with CD8 depleted (11447D, Thermo Fisher Scientific) splenocytes from ITK-$SYK^{CD4\text{-}CreERRT2}$;$PD\text{-}1^{-/-}$ mice, which had been tamoxifen (T5648, Sigma-Aldrich; 0.25 mg) treated five days earlier. Five days after transplantation the NSG mice received Idelalisib (S2226, Selleckchem) or vehicle (0.5% carboxymethylcellulose, 0.05% Tween 80 in ultra-pure water, C5678 and P4780, Sigma-Aldrich) by oral gavage (10 mg per kg per day), 5 days a week.

2.15 Phosflow

ITK-SYK$^{CD4\text{-}CreERT2}$ mice were i.p. injected with single doses of 2 mg tamoxifen (TAM) per mouse (T5648, Sigma-Aldrich). Forty-eight hours post-injection, single-cell suspensions were generated from the spleens and lymph nodes, CD4$^+$ T cells were magnetically purified (130104454, Miltenyi Biotec), and eGFP expression was assessed by flow cytometry. The stimulations were performed using recombinant PD-L1-Fc chimaera protein (758208, Biolegend)-coated microspheres (CS01N, Bangs Laboratories Inc., Fishers, Indiana, USA). In brief, streptavidin-coated microspheres were first incubated with a saturating amount of biotinylated anti-human IgG antibody (409302, BioLegend) according to the manufacturer's instructions for one hour at 37 ºC. After extensive washing, these pre-coated microspheres were loaded with either PD-L1-Fc chimeric protein or recombinant human Fc fragments (AG714, Merck Group, Darmstadt, Germany) as a control. Efficient coating was ensured by flow cytometry. After 48 hours, the cells were fixed in 4% PFA followed by methanol permeabilization, stained for p-AKT (S473, 48-9715-42, Thermo Fisher Scientific), and p-PKCθ (700043, Thermo Fisher Scientific) and PTEN (9550, Cell Signaling Technology Inc., Danvers, Massachusetts, USA) and measured on a FACSCantoII (Becton, Dickinson and Company).

To assess the PTEN, p-AKT and p-PKCθ status in ITK-SYK$^+$PD-1$^{-/-}$ lymphoma cells, TAT-CRE treated Rosa26$^{LSL\text{-}ITK\text{-}SYK}$ and Rosa26$^{LSL\text{-}ITK\text{-}SYK}$;PD-1$^{-/-}$ cells were explanted from C57BL/6 recipient mice (see Figure 12 b). The single cell suspensions were then stained for the PTEN, p-AKT and p-PKCθ levels and analyzed as above.

To analyze the PTEN, p-AKT and p-PKCθ status in the PD-1 or PD-1 YFYF transduced T-NHL cells, the GFP$^+$ FACS-sorted cells were co-incubated with equal amounts of PD-L1 expressing dendritic cells for 24 hours. Afterwards, the cells were fixed and

permeabilized, and then stained for CD3, PTEN, p-AKT and p-PKCθ and analyzed as before.

For the analyses of the effects of Idelalisib (S2226, Selleckchem) on the AKT phosphorylation status *in vivo*, $5x10^4$ lymphoma cells from TAM (T5648, Sigma-Aldrich; 0.25 mg) treated ITK-SYK$^{CD4\text{-}CreERT2}$;PD-1$^{-/-}$ animals were transferred to NSG recipient mice at day five after TAM injection. Five days later, the NSG mice received a single dose of 10 mg/kg Idelalisib (Selleckchem) or vehicle (0.5 % carboxymethylcellulose, 0.05 % Tween 80 in ultra-pure water, C5678 and P4780, Sigma-Aldrich) per os**.** Four hours later the splenic cells from the NSG mice were extracted, fixed and permeabilized in methanol, stained for p-AKT and analyzed as above.

2.16 *In vivo* antibody blockade

ITK-SYK$^{CD4\text{-}CreERT2}$ mice received single injections of tamoxifen (T5648, Sigma-Aldrich; 0.25 mg). Twenty-four hours later the mice received 200 µg of anti-PDL1 (BE0101, Bioxell, West Lebanon, New Hampshire, USA) or 200 µg anti-IgG2b (BE0090, Bioxcell) control antibody diluted to 200 µl with PBS every second day. For the application scheme in which the antibody treatment was started at day ten after tamoxifen administration, the ITK-SYK$^{CD4\text{-}CreERT2}$ mice received 200 µg of anti-PDL1 or anti-PD-1 (BE0146, Bioxcell) or anti-IgG2b (BE0090, Bioxcell) control antibody diluted to 200 µl with PBS every third day. In all experiments the mice were monitored by flow cytometry of the peripheral blood.

2.17 Histology

All organs were fixed in 4 % formaldehyde and paraffin embedded. 3–5 µm-thick sections were cut and stained with H&E. Immunohistochemistry was performed on an automated immunostainer (Agilent Technologies, Santa Clara, California, USA) using antibodies against CD3 (CI597C002, DCS, Hamburg, Germany) and Ki-67 (ab15580, Abcam, Cambridge, UK). The stained slides were evaluated by an experienced certified pathologist [5] using a BX53 stereomicroscope (Olympus Corp., Shinjuku, Tokyo, Japan), classified according to the classification of lymphoid neoplasms in mice with respect to the most recent immunohistochemical phenotyping description of rodent lymphoid tissue and scanned using a slide scanner (AT-2, Leica Biosystems, Wetzlar, Germany). Representative images were collected using the Aperio Imagescope software (version 12.3, Leica Biosystems).

2.18 Statistics

Unless otherwise stated, all statistical tests were performed using R3.1.3 software (R Foundation for Statistical Computing). In each experiment, the appropriate statistical tests, including non-parametric tests, were applied as indicated in the figure legends. To assess the correlation between the eGFP maxima and the initial tamoxifen doses (Figure 3 a), the local maxima (reached on day 4 for the 1 mg and 0.25 mg doses of tamoxifen and on day 8 for the 0.05 mg dose) of the mean eGFP frequencies were used for Pearson coefficient calculations. The association of the lymphoma development and the initial eGFP frequency (Figure 3 c) was calculated based on the

[5]Dr. med. vet. Katja Steiger, Technische Universität München, Institut für allgemeine Pathologie und Pathologische Anatomie, Trogerstr. 18, 81675 München

pooled data from two experiments. Fisher's exact test was performed on a 2x2 contingency table that was created based on two categorical variables: "lymphoma development" and "eGFP maximum > 5% during initial expansion phase". The variances within the groups within the data shown in Figure 3 were significantly different as determined by F-test. Mouse survival rates in comparison to the indicated control groups were assessed by a log-rank (Mantel-Cox) test. The survival of the $Rosa26^{LSL\text{-}ITK\text{-}SYK}$;$Rosa26^{LSL\text{-}PB}$;ATP2;CD4-Cre mice was compared to that of the $Rosa26^{LSL\text{-}ITK\text{-}SYK}$;CD4-Cre littermate group. The normalized enrichment score (NES), false discovery rate (FDR) and p values for the GSEA were calculated with BubbleGUM (Spinelli et al. 2015). The p values for the common integration sites (CISs) of the PB transposon cassettes were calculated with TAPDANCE (Sarver et al. 2012); the p values "insertions" were used for the CIS ranking. No statistical methods were used to predetermine sample size estimate. $P < 0.05$ were considered to be statistically significant.

3 Results

3.1 Counter-regulation of oncogenic T cell signaling *in vivo*

To generate a genetically tractable model of human T-NHL, we had introduced a patient-derived ITK-SYK together with a eGFP cDNA for cell tracking into the murine *Rosa26* locus preceded by a loxP-flanked STOP cassette (LSL; Rosa26$^{LSL\text{-}ITK\text{-}SYK}$ mice, (Pechloff et al. 2010)). Crossing Rosa26$^{LSL\text{-}ITK\text{-}SYK}$ mice to CD4-Cre transgenic mice for the T cell-specific excision of the STOP cassette and ITK-SYK/eGFP expression induced aggressive T cell lymphomas in the offspring (ITK-SYK$^{CD4\text{-}Cre}$ mice) that exhibited molecular, clinical and pathological features of the human disease (Pechloff et al. 2010). This phenotype is fully penetrant (Pechloff et al. 2010) and conserved on a CB57BL/6 genetic background (Figure 2 a-c).

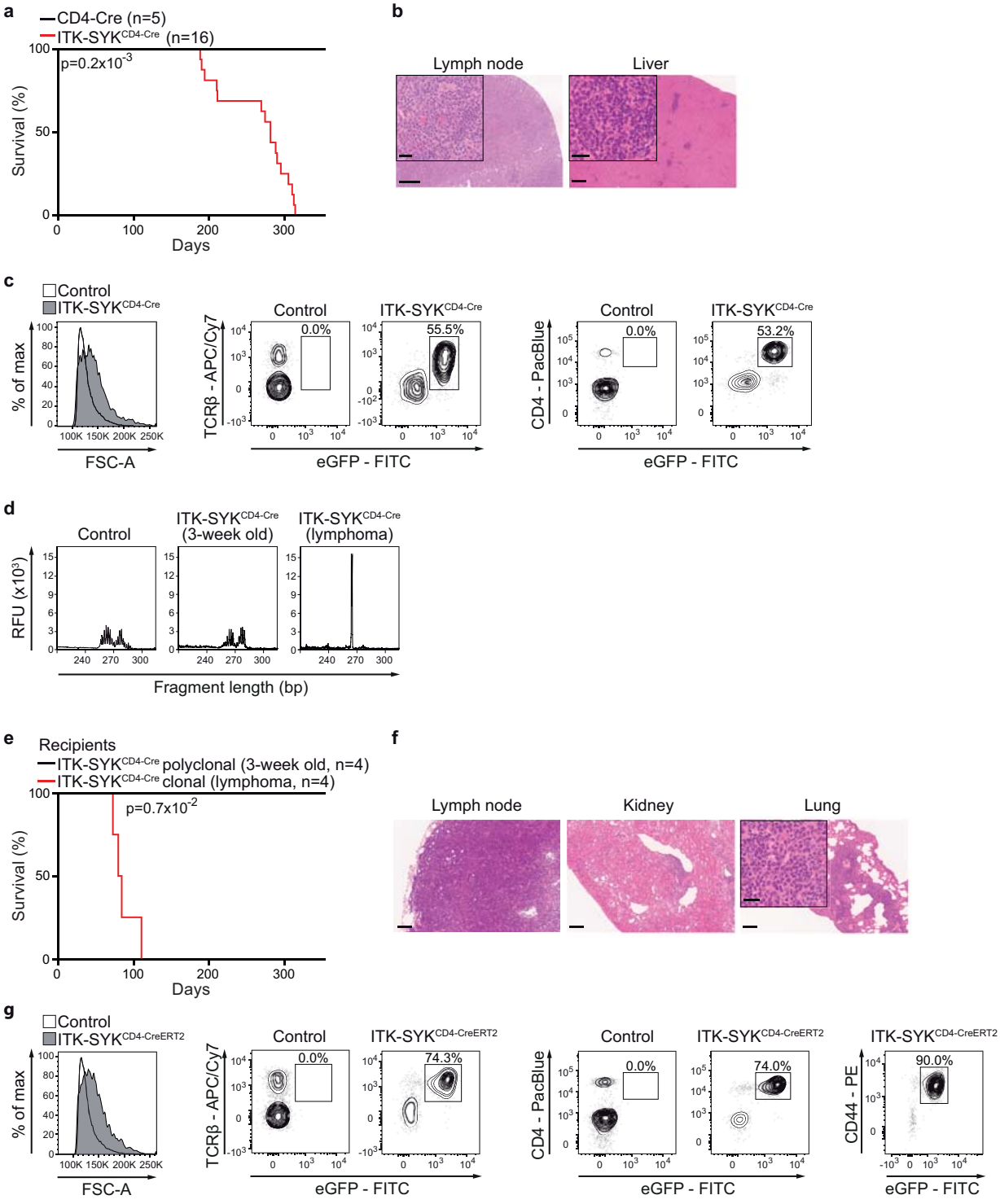

Figure 2 Phenotypic characterization of ITK-SYK-induced lymphomas.

a, Survival curves for the ITK-SYK$^{CD4\text{-}Cre}$ mice and littermate controls (CD4-Cre). The p-value was determined using the two-sided log-rank test, and the median survival was 281 days vs. not reached.

b, Histologies of lymph node and liver after H&E staining of tissues from a sick ITK-SYK$^{CD4\text{-}Cre}$ mouse on a C57BL/6 genetic background. The architecture of the lymph node is disrupted by

a diffuse infiltration of lymphoblastoid cells. Multinodal perivascular infiltrations of lymphoblasts are also detectable in the liver. Scale bars represent 200 µm and 20 µm (insets).

c, Flow cytometric analyses of forward scatter area (FSC-A), which was used as a parameter to detect cell size, and TCRβ, CD4 and eGFP expression in lymphoma tissues from a sick ITK-SYK$^{CD4\text{-}Cre}$ mouse. Peripheral lymphocytes from a CD4-Cre littermate mouse served as the control.

d, GeneScan analysis of TCR gene rearrangements. Fragment size distributions of fluorochrome-labelled PCR products of the Vβ1-20;Jβ2 junction demonstrating polyclonal repertoires of a healthy CD4-Cre mouse (Control), a 3-week-old ITK-SYK$^{CD4\text{-}Cre}$ mouse and clonality of the ITK-SYK$^{CD4\text{-}Cre}$ lymphoma sample. RFU, relative fluorescence unit

e, Survival curves for C57BL/6 mice (n=4 recipients for each donor group) which had received polyclonal ITK-SYK$^{CD4\text{-}Cre}$ cells ($3x10^6$) from 3-week old ITK-SYK$^{CD4\text{-}Cre}$ mice or clonal ITK-SYK$^{CD4\text{-}Cre}$ cells from diseased ITK-SYK$^{CD4\text{-}Cre}$ mice with lymphoma (n=4 donors for each group). P=two-sided log-rank test

f, Histological analysis of lymphoma samples in tamoxifen-induced ITK-SYK$^{CD4\text{-}CreERT2}$ animals. Lymph node with a loss of histomorphological architecture. Multifocal nodular infiltrations of lymphoblasts into kidney and lung are shown. Scale bars represent 100 µm and 20 µm (inset).

g, Flow cytometric analyses of TCRβ-, CD4- and CD44-stained splenic cells in a tamoxifen-induced ITK-SYK$^{CD4\text{-}CreERT2}$ mouse and wild-type littermate (Control).

b, c, **d**, **f**, **g,** Representative data from at least ten analyzed mice.

Although the constitutively active CD4-Cre transgene drives continuous ITK-SYK expression in millions of polyclonal T cells, the final lymphomas are typically clonal (Pechloff et al. 2010), indicating that they have acquired additional genetic alterations that promote malignancy (Figure 2 d).

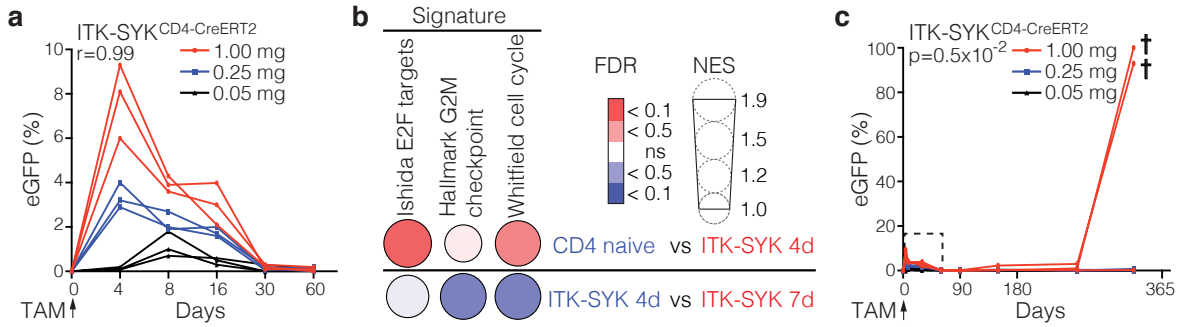

Figure 3 Counter-regulation of oncogenic T cell signaling in vivo.

a, Frequencies of ITK-SYK-expressing eGFP$^+$ lymphocytes in the blood of the ITK-SYK$^{CD4\text{-}CreERT2}$ mice following single injections of tamoxifen (n=3 mice per dose). r=Pearson's correlation coefficient

b, Gene set enrichment analyses of wild-type naïve CD4$^+$ T cells (CD4 naïve) and ITK-SYK$^{CD4\text{-}CreERT2}$ T cells at 4 (ITK-SYK 4d) and 7 days (ITK-SYK 7d) after tamoxifen injection. FDR=color intensity of the circle. NES=circle diameter. Blue/red indicates the group in which a signature was positively enriched; n=3 biological replicates for each group. NES, normalized enrichment score; FDR, false discovery rate

c, Cohorts shown in **a** were followed over one year (n=3 biological replicates per dose). The data in the dashed box correspond to the data in **a**. † indicates animals that had to be euthanized because of lymphoma. P=Fisher's exact test. The test was performed on pooled data from two independent experiments. Representative data from one experiment are shown.

To assess the evolution of these cancers in a controlled manner, we crossed Rosa26$^{LSL\text{-}ITK\text{-}SYK}$ mice with animals that allow inducible Cre activation in CD4$^+$ T cells via tamoxifen (CD4-CreERT2 mice, (Sledzinska et al. 2013)). In the progeny (ITK-SYK$^{CD4\text{-}CreERT2}$ mice), we triggered single pulses of Cre activity in subsets of lymphocytes and followed cohorts of mice for one year (Figure 3 a-c). ITK-SYK and eGFP expression started after 24 h in individual lymphocytes *in vivo* (data not shown), which led to the expansion of these cells (Figure 3 a). The maximal frequencies of ITK-SYK$^+$CD4$^+$ T cells increased with increasing doses of tamoxifen (r=0.992). However, after this expansion phase, the ITK-SYK$^+$ compartments again contracted (Figure 3 a). To characterize the biology of these two phases, we again induced ITK-SYK

expression in T cells *in vivo* by tamoxifen and then FACS-sorted recombinant $CD4^+$ T cells based on eGFP expression for an *in vitro* RNAseq analysis at days 4 and 7 after induction (Figure 3 b). A gene set enrichment analysis (GSEA) revealed the enriched signatures of Ishida_E2F_targets ((Ishida et al. 2001), 67 genes), Hallmark_G2M_checkpoint ((Liberzon et al. 2015), 214 genes) and Whitfield_cell_cycle_literature ((Whitfield et al. 2002), 61 genes) in the ITK-SYK-expressing cells at day 4 compared with that of naïve $CD4^+$ T cells accounting for a highly proliferative phenotype. These signatures were built to identify the different phases during the eukaryotic cell cycle based on the upregulated gene clusters during G1/S entry and S phase (Ishida et al. 2001; Whitfield et al. 2002), G2 phase (Whitfield et al. 2002), and during the G2/M DNA damage checkpoint (Whitfield et al. 2002; Liberzon et al. 2015). However, at day 7, the proliferative signatures were significantly downregulated ($p<0.01$) along with the declining ITK-SYK^+ T cell numbers *in vivo* indicating that T cells possess tumor-suppressive mechanisms that can counteract oncogenic T cell signaling within days. Nevertheless, within one year, two of three mice that received the highest dose of tamoxifen (1 mg) developed ITK-SYK/eGFP-expressing $CD4^+$ T cell lymphomas (Figure 3 c) with activated $CD44^+$ phenotypes and organ infiltration by malignant lymphoblasts (Figure 2 g), which demonstrated that the tumor-suppressive pathways can be disrupted. Because the onset of these lymphomas is associated with the initial frequency of the ITK-SYK-expressing T cells (Figure 3 c; $p=0.0049$), these tumor-enabling secondary events are presumably stochastic in nature.

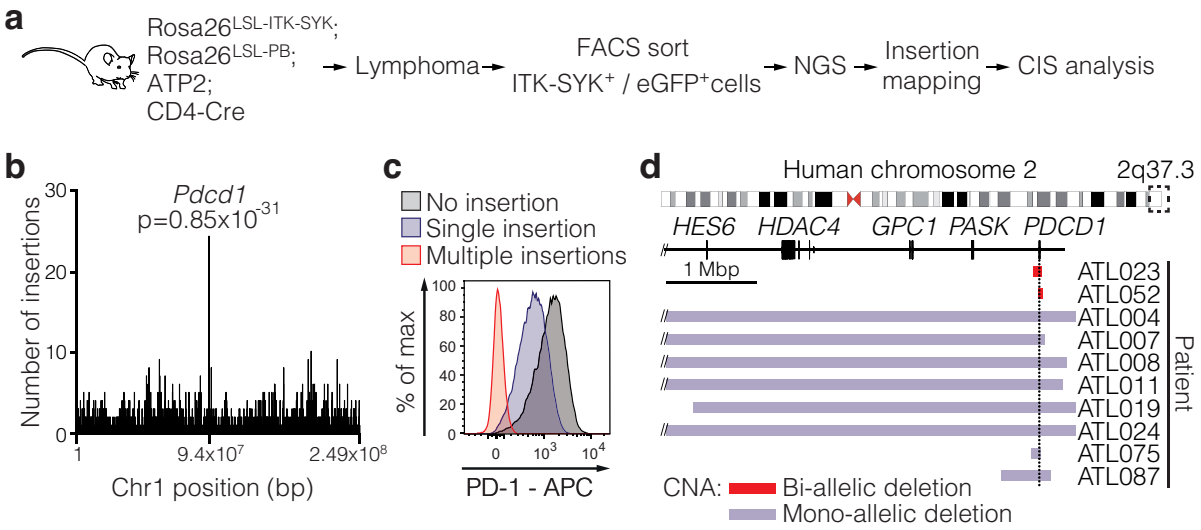

Figure 4 Identification of PDCD1 alterations in T cell lymphoma.

a, Schematic representation of the transposon screen to discover T cell lymphoma genes. Transposons from the ATP2 transgene were mobilized by *piggyBac* in ITK-SYK-expressing T cells. The tumor cells were then FACS-sorted based on eGFP expression, and the transposon insertion sites were identified by next-generation sequencing and bioinformatics analysis.

b, Transposon insertion densities within pooled lymphomas (n=30 mice) for the murine chromosome 1, total: 2732 insertions and *Pdcd1* locus: 23 insertions. The p-value was calculated with a one-sided Poisson distribution-based test, which assumes transposon insertions occurring at a constant rate.

c, Flow cytometric analysis of PD-1 expression on lymphoma cells from diseased Rosa26$^{LSL\text{-}ITK\text{-}SYK}$;Rosa26$^{LSL\text{-}PB}$;ATP2;CD4-Cre mice. Lymphoma sample without any transposon cassette within the *Pdcd1* gene (No insertion), with a single transposon cassette located in the *Pdcd1* locus (Single insertion) or with multiple transposon cassettes within *Pdcd1* (Multiple insertions).

d, The dashed box indicates the genomic region q37.3 on human chromosome 2 that is shown in detail in the lower part of the panel (top). Mono- or bi-allelic deletions of the *PDCD1* gene detected in human T cell lymphoma patients are shown (bottom). The horizontal bars indicate the regions that were affected by the CNAs. The color of the bar indicates the type of CNA. CNA, copy number aberration; Mbp, million base pairs

c, Representative results from at least 15 mice. **d,** Results of an analysis that included all available WGS data within one published dataset.

3.2 Identification of *PDCD1* alterations in T cell lymphoma

We next sought to reveal the mechanisms that enable full T cell transformation after oncogenically enforced TCR signaling. To this end, we designed a genome-wide forward genetic screen in mice (Figure 4 a) using the *piggyBac* (PB) transposition system for insertional mutagenesis (Rad et al. 2010; Friedrich et al. 2017). To achieve spatially restricted transposition in only the ITK-SYK-sensitized T cells, we crossed $Rosa26^{LSL\text{-}ITK\text{-}SYK}$ to CD4-Cre mice and animals conditionally expressing the PB transposase from the Rosa26 locus ($Rosa26^{LSL\text{-}PB}$) and to ATP2-H32 transgenic mice with 25 mutagenic ATP transposon cassettes that could be mobilized by PB (Friedrich et al. 2017; Rad et al. 2015). We engineered a cohort of 30 quadruple-transgenic progeny ($Rosa26^{LSL\text{-}ITK\text{-}SYK}$ transgenic; $Rosa26^{LSL\text{-}PB}$ transgenic; ATP2-H32 transgenic; CD4-Cre transgenic), all of which developed highly aggressive T cell lymphomas after transposon mobilization (Figure 5 a-c). Transposon integration sites were recovered from FACS-sorted $eGFP^{+}$ cancer cells by a splinkerette PCR-based method for multiplexed semi-quantitative insertion site sequencing termed QISeq ((Friedrich et al. 2017), Figure 4 a). Deep sequencing was followed by statistical analyses (Transposon Annotation Poisson Distribution Associated Network Connectivity Environment; TAPDANCE (Sarver et al. 2012)) to identify the genomic regions that were hit by transposons more frequently than expected by chance. Remarkably, the top ranking common insertion site (CIS) (genomic region with the highest transposon insertion density) with the highest significance ($p = 0.8528x10^{-31}$) across the entire mouse genome was located at the *Pdcd1* locus that encodes the inhibitory receptor Programmed Death-1 (PD-1) ((Riley 2009), Figure 4 b). These insertions did not co-exist with common insertions in other loci. The *Pdcd1* transposon insertions were randomly distributed in either sense or anti-sense orientation within the first *Pdcd1*

intron (Figure 5 e) resulting in the generation of *Pdcd1*-transposon fusion transcripts (Figure 5 f). Because the first *Pdcd1* exon contains the ATG start codon and the sequence for the signal peptide for PD-1 membrane localization, all integrations are predicted to disrupt PD-1 function. Some cancers even had multiple *Pdcd1* insertions that most likely reflected bi-allelic inactivation and / or local transposon hopping with gene trapping in subclones. The analysis of lymphomas with transposon insertions into *Pdcd1* confirmed reduced or absent PD-1 protein and *Pdcd1* mRNA expression (Figure 4 c and Figure 5 d).

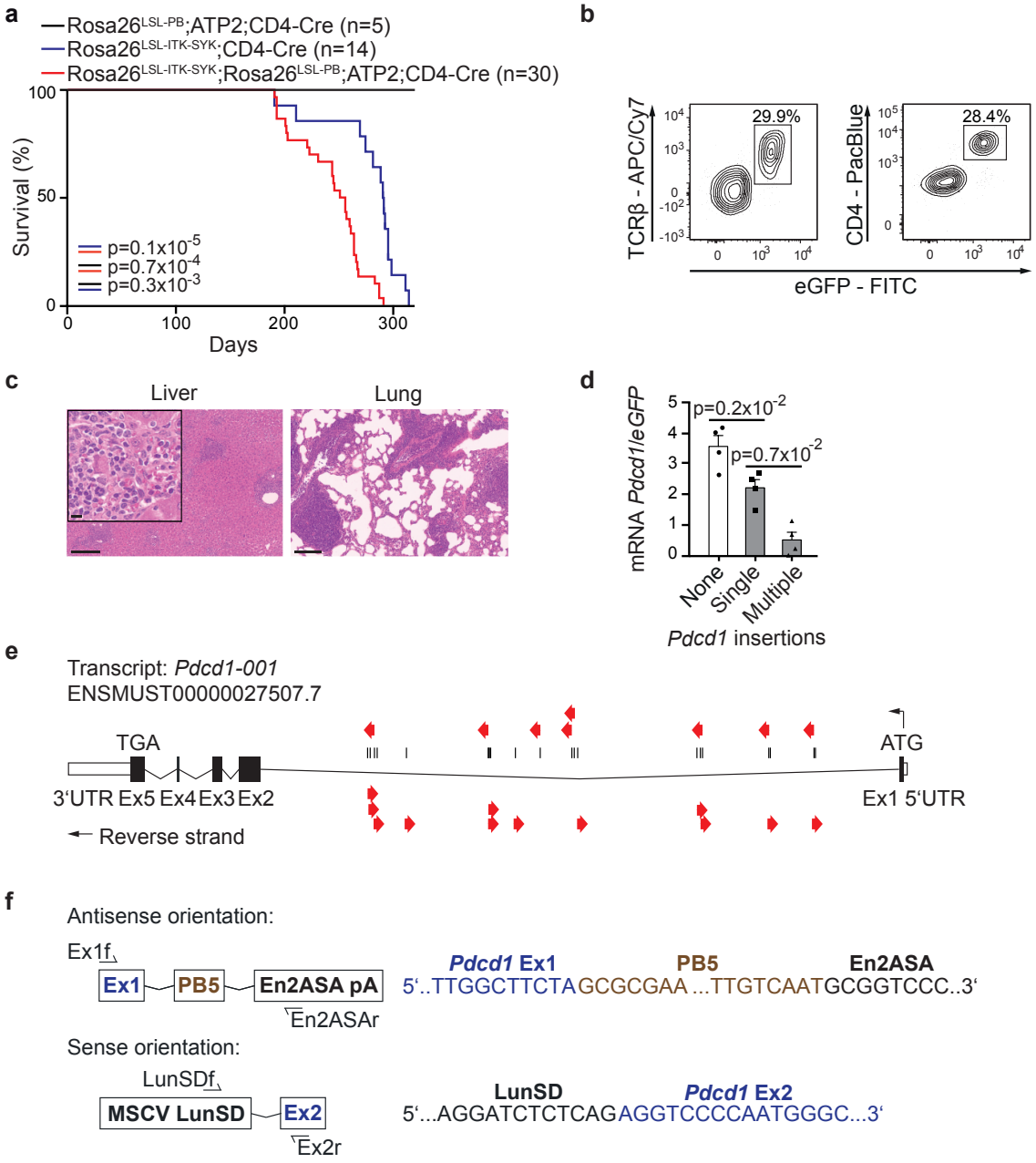

Figure 5 Lymphomas with transposon insertions within *Pdcd1*.

a, Overall survival of the Rosa26$^{LSL\text{-}ITK\text{-}SYK}$;Rosa26$^{LSL\text{-}PB}$;ATP2;CD4-Cre mice (red) and littermate ITK-SYK$^{CD4\text{-}Cre}$ mice (blue). The Rosa26$^{LSL\text{-}PB}$;ATP2;CD4-Cre mice (black) did not display any signs of disease. The p-value was determined using two-sided log-rank test, and the median survival was 255 days vs. 289 days.

b, Flow cytometric analyses of TCRβ, CD4 and eGFP expression in a typical lymphoma sample from a Rosa26$^{LSL\text{-}ITK\text{-}SYK}$;Rosa26$^{LSL\text{-}PB}$;ATP2;CD4-Cre mouse.

c, Histological analysis of the mouse shown in **b** with multinodal perivascular infiltrations of lymphoblasts into the liver (left) and lung (right). Scale bars represent 200 µm and 20 µm

(inset).

d, *Pdcd1* mRNA transcript levels in eGFP^{+} FACS-sorted peripheral lymphocytes from Rosa26$^{LSL\text{-}ITK\text{-}SYK}$;Rosa26$^{LSL\text{-}PB}$;ATP2;CD4-Cre lymphoma samples without any detectable transposon cassettes within the *Pdcd1* locus (None, n=4) or with a single insertion (Single, n=4) or multiple *Pdcd1*-located transposon cassettes (Multiple, n=4). *Pdcd1* expression levels were normalized to *eGFP* transcript levels. P=Tukey's post hoc test. Shown are the mean±s.e.m and individual data points.

e, Twenty unique transposon integration sites mapped to the murine *Pdcd1* locus. The vertical black bars indicate the genomic positions of the insertion. The red arrows indicate the orientations of the transposon cassettes.

f, Nucleotide sequences of the *Pdcd1-piggyBac* mRNA splice junctions as determined by Sanger sequencing of amplified cDNA from Rosa26$^{LSL\text{-}ITK\text{-}SYK}$;Rosa26$^{LSL\text{-}PB}$;ATP2;CD4-Cre lymphoma samples. The cDNA was generated from sorted eGFP^{+} lymphoma cells in which at least one *Pdcd1* transposon cassette could be detected. Note that the 5' *piggyBac* transposon-specific inverted terminal repeat nucleotide sequence (PB5) can function as a cryptic splice acceptor and a splice donor site. Hence, PB5 may act as a gene trapping sequence by itself[14]. En2SA, exon 2 located murine *Engrailed 2* splice acceptor; pA, SV40 polyadenylation signal; MSCV, murine stem cell virus long terminal repeat; LunSD, splice donor from exon 1 of murine *Foxf2.*

b, c, Representative data from at least ten analyzed mice. **f**, The splice junctions were amplified from the cDNA of at least eight lymphomas.

PD-1 is prominently known for its physiological function in restricting antigen induced TCR responses at tolerance checkpoints with persistent antigenic stimulation for the prevention of autoimmunity (Riley 2009). Additionally, PD-1 receives considerable attention because it limits antigen driven T cell proliferation and survival in suppressive microenvironments in cancer and chronic infection (Francisco, Sage, and Sharpe 2010). The results from our genetic screen indicated that PD-1 could in addition possess unrecognized functions as a tumor suppressor in T cell lymphoma.

Title	Journal	Year	Method	Cases	CNV	SNV	Total	Percent
Genomic profiling of Sézary syndrome identifies alterations of key T cell signaling and differentiation genes.	Nature Genetics	2015	WES	36	13*	0	13	36%
Integrated molecular analysis of adult T cell leukemia/lymphoma.	Nature Genetics	2015	WGS	47	11†	1	12	26%
Genomic landscape of cutaneous T cell lymphoma.	Nature Genetics	2015	WES	40	8	0	8	20%
PLCG1 mutations in cutaneous T cell lymphomas.	Blood	2014	TS	11	N/A	1	1	9%
The mutational landscape of cutaneous T cell lymphoma and Sézary syndrome.	Nature Genetics	2015	WES	24	1	1	2	8%

Table 6 Meta-analysis: *PDCD1* alterations in human lymphomas

Meta-analysis of five published studies containing whole-genome and whole-exome sequencing data from patients with peripheral T cell lymphoma and cutaneous T cell lymphoma. *PDCD1* alterations were observed in 36 out of 158 cases (23%) across the five studies. CNA, copy number aberration; SNV, single nucleotide variant; WES, whole-exome sequencing; WGS, whole-genome sequencing; TS, targeted sequencing; *, all CNAs were focal deletions; †, for CNAs see Figure 4 d.

To investigate whether *PDCD1* is altered in human T cell lymphoma, we performed a meta-analysis of five published studies (Kataoka et al. 2015; Wang et al. 2015; da Silva Almeida et al. 2015; Vaque et al. 2014; Choi et al. 2015) and analyzed publicly available whole-genome and whole-exome sequencing and mRNA expression data from patients with T-NHLs. Strikingly, we found genomic *PDCD1* alterations in 36 of 158 cases (23%) in the combined 5 studies (Table 6). Overall, the predominant mutation types were copy number aberrations (33 cases). Among these, focal deletions were prominent with mono- and bi-allelic *PDCD1* loss (Figure 4 d and Figure 7 b).

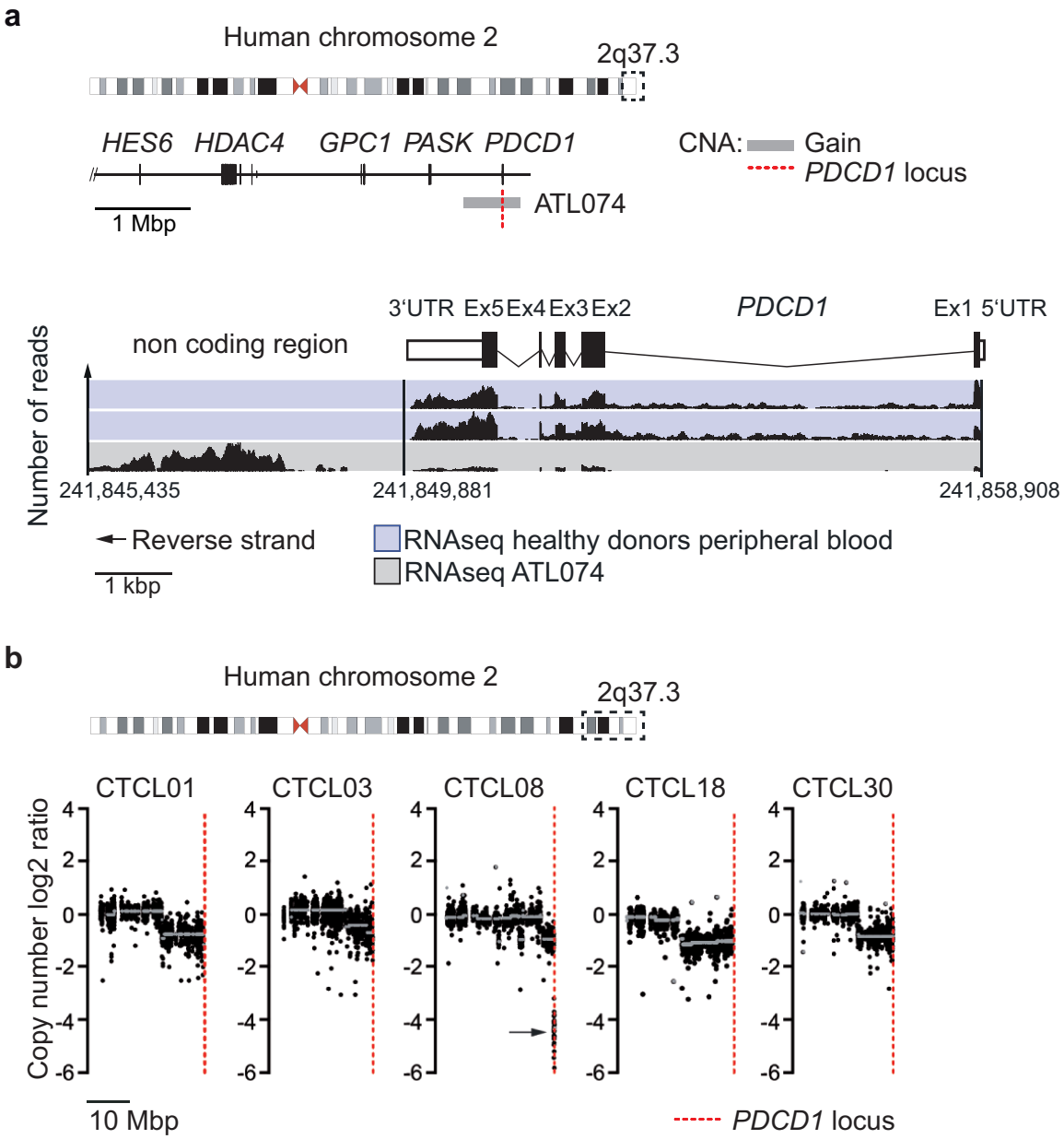

Figure 7 *PDCD1* alterations in human lymphomas

a, The dashed box indicates the genomic region q37.3 on human chromosome 2 that is shown in more detail in the middle of the panel (top). The grey horizontal bar indicates the genomic region that was affected by a *PDCD1* copy number gain in T-NHL patient ATL074 (middle). Histograms showing the number of human genome-aligned RNAseq reads from peripheral blood mononuclear cells (PBMCs) of two healthy donors and lymphoma cells of patient ATL074 at the *PDCD1* locus and a non-coding region near the *PDCD1* 3' UTR (bottom).

b, The dashed box indicates the genomic region on human chromosome 2 that is shown in detail in the lower part of the panel (top). CNAs in *PDCD1* that were detected in CTCL patients are shown (bottom). The vertical dashed lines indicate the genomic position of the

PDCD1 locus. Black dots represent the logarithmic tumor/normal copy number ratio; each dot represents 1 kbp. The grey lines indicate logarithmic value of the median tumor/normal copy number ratio. The arrow indicates a bi-allelic *PDCD1* loss in sample CTCL08.
CNA, copy number aberration; kbp, kilo base pairs; Mbp, million base pairs

The *PDCD1* gene was located within a minimally deleted region on human chromosome 2q37.3 (Figure 4 d). The highest rate of homo- or heterozygous *PDCD1*-deleted cases (36%, 13 out of 36) was found in a series of patients with advanced Stage IV cutaneous T cell lymphoma (Sézary syndrome, (Wang et al. 2015), Table 6). A single T-NHL case with *PDCD1* genomic gains exhibited defective *PDCD1* mRNA expression (Figure 7 a). Together with the results from our genetic *in vivo* screen, these frequent homo- or heterozygous *PDCD1* deletions in human T-NHLs strongly suggest that PD-1 is functionally relevant during lymphoma pathogenesis.

3.3 Oncogenic T cell signaling induces a PD-1 inhibitory loop

In normal non-malignant T cells, PD-1 cell surface expression is upregulated after antigen sensing and T cell receptor ligation (Francisco, Sage, and Sharpe 2010), and it subsequently downregulates TCR responses to provide feedback for T cell homeostasis and the prevention of autoimmunity. To investigate whether PD-1 induction was also responsive to oncogenic T cell signals we introduced ITK-SYK or a kinase-defective version (ITK-SYK^{KD}) together with GFP into Jurkat T cells (Pechloff et al. 2010). ITK-SYK signaling drives PD-1 surface expression in a kinase dependent manner (Figure 9 a). In transduced primary human CD4^{+} T cells we also detected ITK-SYK kinase mediated upregulation of PD-1 surface expression (Figure 9 b).

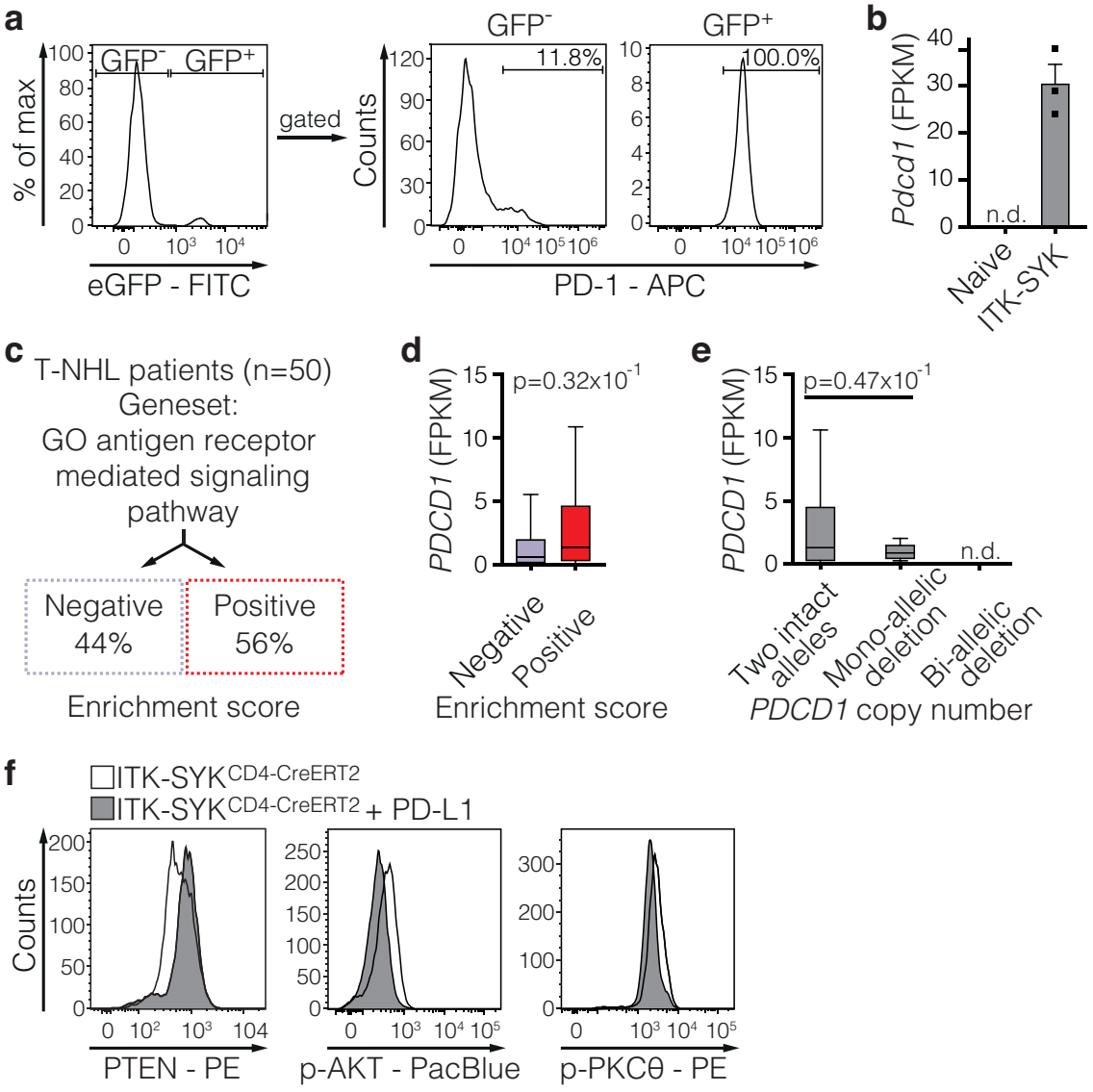

Figure 8 Oncogenic T cell signaling induces a PD-1 inhibitory loop.

a, PD-1 expression on the peripheral blood lymphocytes from an ITK-SYK$^{CD4\text{-}CreERT2}$ mouse as measured by flow cytometry 96 hours after tamoxifen injection.

b, Normalized transcript read counts of reads that were mapped to the *Pdcd1* locus and detected in the RNAseq dataset from naïve CD4^{+} T cells (Naive) or ITK-SYK-expressing eGFP^{+}CD4^{+} T cells from ITK-SYK$^{CD4\text{-}CreERT2}$ mice 4 days after the tamoxifen injection (ITK-SYK). Shown are the mean±s.e.m and individual data points. FPKM, fragments per kilobase of exon per million fragments mapped; n.d., not detectable indicates FPKM<0.1; n=3 mice per group.

c, Gene Set Variation Analysis (GSVA) of fifty primary human T-NHL RNAseq samples is shown. The analysis was performed based on the geneset GO_antigen_receptor_mediated_signaling_pathway.

d, *PDCD1* FPKM distributions from the samples in **a** are shown. The T-NHL patients (n=50)

were classified according to their enrichment score. P=one-sided unequal variances Student's t-test. The FPKM distributions are shown as box plots. The 0.25-, 0.5- and 0.75-quantile is depicted by the box, minimum and maximum by the whiskers.
e, *PDCD1* FPKM distributions from the positive samples in **d** are shown. The lymphomas were classified according to their *PDCD1* copy number status. All T-NHLs with positive enrichment score were included (n=28). P=one-sided unequal variances Student's t-test. The FPKM distributions are shown as box plots. The 0.25-, 0.5- and 0.75-quantile is depicted by the box, minimum and maximum by the whiskers; n.d., not detectable indicates FPKM<0.1.
f, Intracellular flow cytometric analyses of PTEN, p-AKT and p-PKCθ levels in primary ITK-SYK-expressing T cells stimulated with PD-L1 or Fc-fragment-coated microspheres.
a, Representative results from three analyzed mice. **f,** Representative data from three independent experiments with two biological replicates per experiment.

Next, we analyzed PD-1 expression after acute ITK-SYK expression in $CD4^+$ T cells from *in vivo* tamoxifen-treated ITK-$SYK^{CD4\text{-}CreERT2}$ mice. ITK-SYK signaling also drives robust PD-1 surface expression in these cells (Figure 8 a and Figure 9 c). Re-analysis of the RNAseq data presented in Figure 3 b additionally revealed profound upregulation of *Pdcd1* mRNA upon ITK-SYK signaling in primary murine $CD4^+$ T cells (Figure 8 b). Finally, we analyzed *PDCD1* mRNA expression in human T-NHL samples (N=50) with available gene expression data (Kataoka et al. 2015; Choi et al. 2015) that did or did not exhibit activation of the gene expression signature GO_antigen_receptor_mediated_signaling_pathway (195 genes) (Figure 8 c, d). Aberrant activation of TCR signaling pathways within the tumor cells correlated with significantly increased *PDCD1* mRNA expression in primary human T-NHL. We further analyzed *PDCD1* mRNA expression within this patient group in cases with non, homozygous or heterozygous *PDCD1* deletions (Figure 8 e). Loss of one or two *PDCD1* gene loci lead to a significantly reduced or completely absent *PDCD1* mRNA

expression (Figure 8 e). Thus, *PDCD1* expression is upregulated after oncogenic T cell signaling in murine and human cells and the loss of *PDCD1* gene loci in human T-NHL affects *PDCD1* mRNA expression.

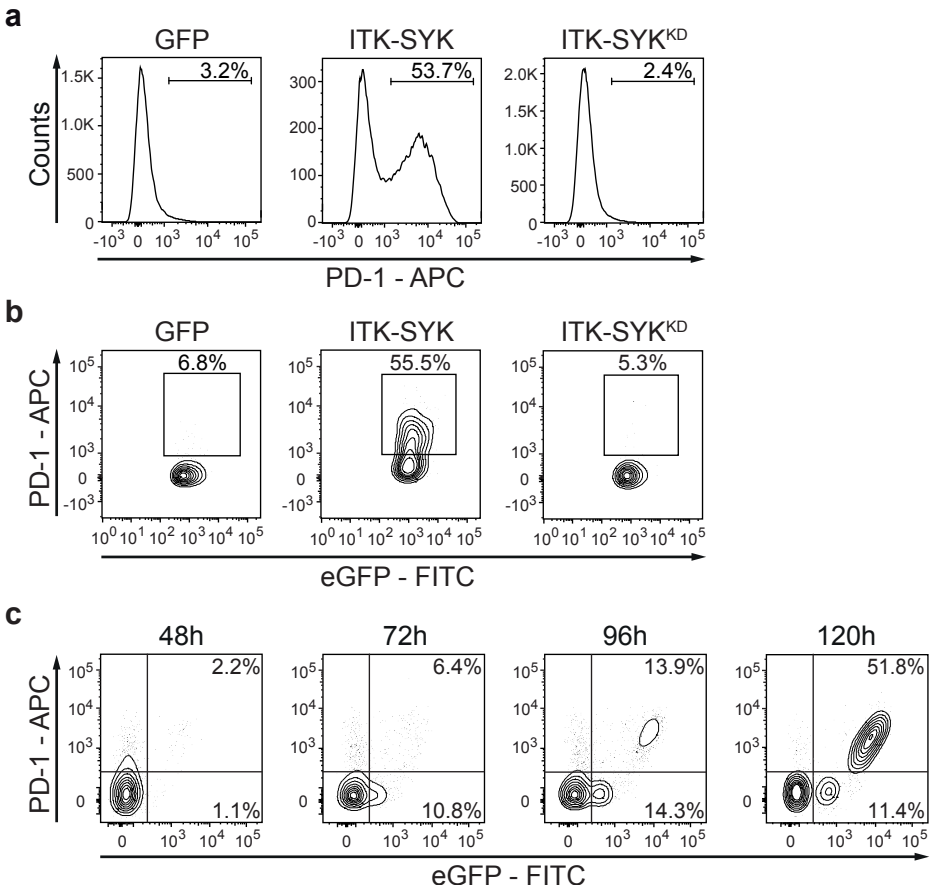

Figure 9 ITK-SYK signaling induces PD-1 expression on human T cells

a, b, Jurkat T cells (**a**) or primary human $CD4^+$ T cells (**b**) were infected with retroviruses carrying ITK-SYK or kinase-defective $ITK\text{-}SYK^{KD}$ together with GFP or GFP alone (control; GFP). PD-1 surface expression was determined by flow cytometry.

c, PD-1 expression after acute ITK-SYK signaling in primary T cells from tamoxifen-treated $ITK\text{-}SYK^{CD4\text{-}CreERT2}$ mice was assessed by a flow cytometric analysis. $ITK\text{-}SYK^{CD4\text{-}CreERT2}$ mice received 1 mg tamoxifen, and the cells were harvested 48 hours later, cultured *in vitro* and analyzed at the indicated time points.

a, b The data from three experiments with similar results. **c** Representative results from three analyzed mice.

The mechanisms of intracellular PD-1 signaling are still not understood in detail. However, PD-1 ligation dampens physiological antigen mediated T cell activation by enhancing the tumor suppressor phosphatase PTEN (Patsoukis et al. 2013) and attenuating the PI3K/AKT (Chemnitz et al. 2004) and PKCθ/NF-κB pathways (Sheppard et al. 2004). Because these two signaling cascades are critical for lymphomagenesis, we tested whether they were sensitive to PD-1 ligation after oncogene induction. To this end, we activated ITK-SYK in $CD4^+$ T cells *in vivo* by injecting tamoxifen into ITK-$SYK^{CD4\text{-}CreERT2}$ mice. Forty-eight hours later, we isolated pre-malignant cells and stimulated them with PD-L1 (Figure 8 f) and subsequently performed an intracellular Phosflow analysis. The engagement of PD-1 on ITK-SYK-induced primary T cells increased the PTEN protein levels and attenuated the AKT and PKCθ activities (Figure 8 f). Thus, oncogenic T cell signaling upregulates PD-1 expression and PD-1 functions subsequently to suppresses certain oncogenic effector pathways.

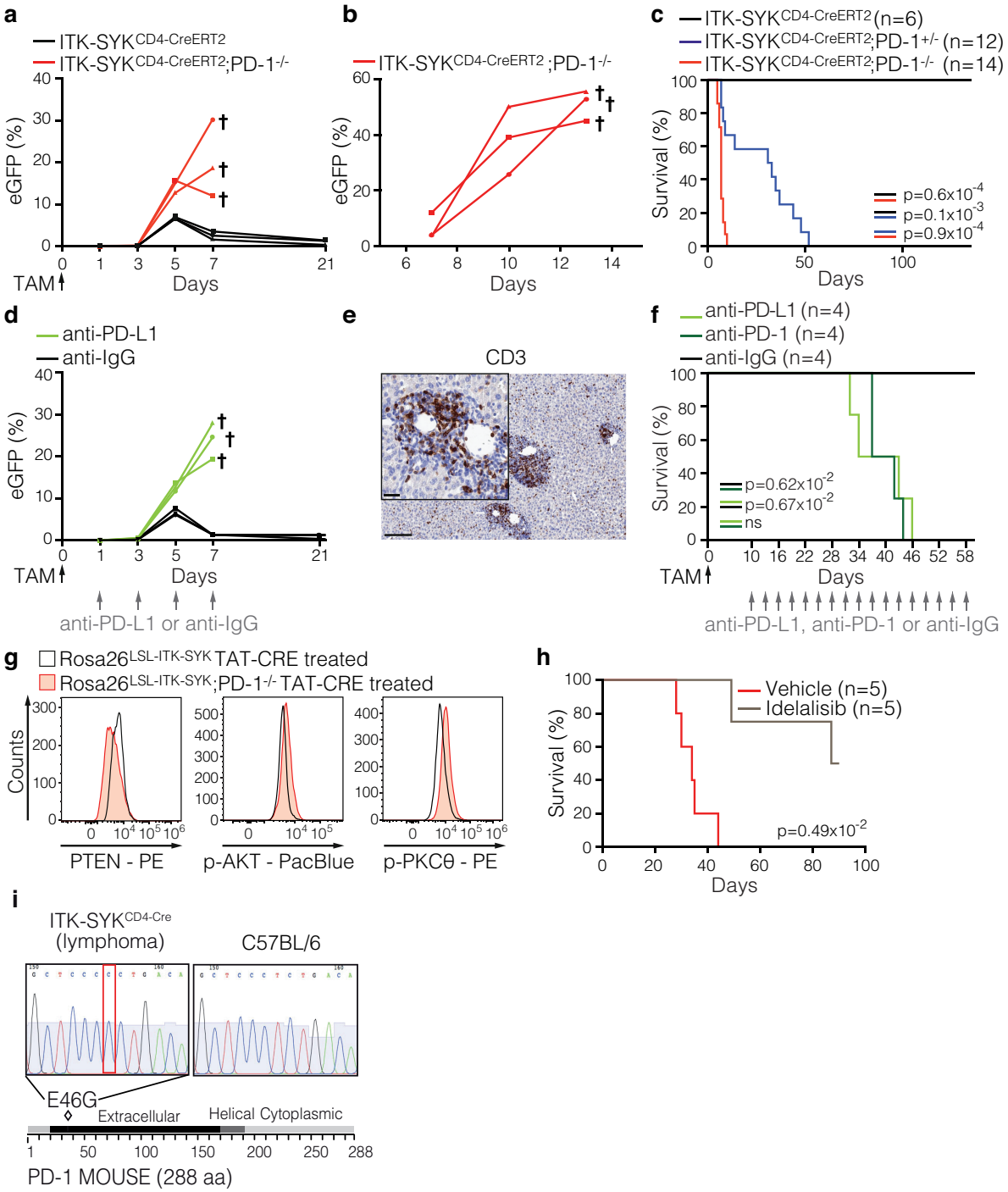

Figure 10 PD-1 is a haploinsufficient tumor suppressor *in vivo.*

a, ITK-SYK$^{CD4\text{-}CreERT2}$ and ITK-SYK$^{CD4\text{-}CreERT2}$;PD-1$^{-/-}$ mice (n=3 mice per genotype) received single injections of tamoxifen (0.25 mg). The fractions of ITK-SYK-expressing eGFP^{+} peripheral blood lymphocytes were determined over time using flow cytometry.

b, Fifty million splenic cells from diseased ITK-SYK$^{CD4\text{-}CreERT2}$;PD-1$^{-/-}$ mice (n=3 donors) were intravenously transferred to NSG mice (n=3 recipients). The frequencies of eGFP^{+} lymphocytes in the peripheral blood of the recipients are indicated. NSG, NOD SCID Il2rg$^{-/-}$

c, Survival curves of ITK-SYK$^{CD4\text{-}CreERT2}$, ITK-SYK$^{CD4\text{-}CreERT2}$;PD-1$^{+/-}$ and ITK-SYK$^{CD4\text{-}CreERT2}$;PD-1$^{-/-}$ mice (n=6, n=12 and n=14). All mice received a single dose of tamoxifen on day zero. P=two-sided log-rank test

d, The fractions of ITK-SYK-expressing eGFP^{+} peripheral blood lymphocytes of checkpoint inhibitor-treated ITK-SYK$^{CD4\text{-}CreERT2}$ mice were determined by flow cytometry. ITK-SYK$^{CD4\text{-}CreERT2}$ mice received single injections of tamoxifen. Beginning twenty-four hours after tamoxifen induction, the mice received 200 µg of anti-PD-L1 or control antibody (n=3 mice per condition) every second day.

e, Anti-CD3 antibody-stained liver section from a diseased anti-PD-L1-treated ITK-SYK$^{CD4\text{-}CreERT2}$ mouse from the experiment shown in **d**, Scale bars represent 100 µm and 20 µm (inset).

f, Survival of ITK-SYK$^{CD4\text{-}CreERT2}$ mice that received checkpoint inhibitor treatment starting ten days after tamoxifen administration. ITK-SYK$^{CD4\text{-}CreERT2}$ mice received single injections of tamoxifen on day zero (0.25 mg). Starting from day ten after injection, the mice were administered 200 µg of anti-PD-L1 or anti-PD-1 antibody or control antibody (n=4 mice per condition) every third day. P=two-sided log-rank test

g, Intracellular flow cytometric analyses of PTEN, p-AKT and p-PKCθ levels in ITK-SYK-expressing T cells isolated from the C57BL/6 recipients presented in Extended Data Figure 6b. The genotype of the transplanted cells is indicated.

h, Survival of the PI3Kδ inhibitor- or vehicle-treated NSG recipient mice. Tamoxifen-induced ITK-SYK$^{CD4\text{-}CreERT2}$;PD-1$^{-/-}$ T cells (n=5 biological replicates, 5x10^{4} cells per transplant) were transplanted into NSG mice (n=5 recipients per group). P=two-sided log-rank test.

i, Sanger sequencing chromatogram of an amplicon derived from the genomic region chr1:94,041,449-94,041,461 of an ITK-SYK$^{CD4\text{-}Cre}$ mouse with lymphoma and a C57BL/6 control animal (top). The red box indicates a T>C missense mutation at position chr1:94,041,455 (top left) leading to a p.E46G amino acid change located in the extracellular domain of mouse PD-1 (bottom).

† indicates animals that had to be euthanized because of lymphomas. **a,** Representative data from three independent experiments, each with three biological replicates. **b,** The data from a single experiment that was independently repeated once with comparable results. **c**, Pooled data from two independent experiments. **d**, Representative data from four independent experiments, each with three biological replicates per antibody. **e**, Representative histology from one out of nine analyzed mice. **f,** The data from a single experiment, which was repeated once with similar results. **g,** Representative results from two out of eight analyzed mice in two independent experiments. **h,** Pooled survival data from two experiments.

3.4 PD-1 is a haploinsufficient tumor suppressor *in vivo*.

To study the biological importance of the oncogene / PD-1 loop in tumor suppression *in vivo*, we crossed the Rosa26$^{LSL\text{-}ITK\text{-}SYK}$ and CD4-CreERT2 alleles on a PD-1 deficient background (Keir, Freeman, and Sharpe 2007). As previously observed, the induction of ITK-SYK by tamoxifen led to a strong expansion of ITK-SYK^{+}/eGFP^{+} T cells in the offspring. In the presence of PD-1, this response was robustly counter-regulated (Figure 10 a). In sharp contrast, without PD-1, the ITK-SYK^{+} T cells expanded vigorously without restriction, and all tamoxifen-treated ITK-SYK$^{CD4\text{-}CreERT2}$;PD-1$^{-/-}$ animals were sacrificed after only one week because of a strong accumulation of ITK-SYK^{+}PD-1$^{-/-}$ CD4^{+} T cells in the lymphoid tissues and invasive growth into the solid organs (Figure 10 a and Figure 11 a-c). Histopathology and flow cytometric analyses revealed the presence of lymphoblastoid CD4^{+} T cells with condensed chromatin and noncohesive growth patterns (Figure 10 a and Figure 11 a-c). Upon transfer onto immunocompromised recipients, these ITK-SYK^{+}/eGFP^{+}PD-1$^{-/-}$ CD4^{+} T cells continued to expand invasively and transmitted the lethal disease, demonstrating that they were fully transformed malignant lymphocytes (Figure 10 b and Figure 11 d-g).

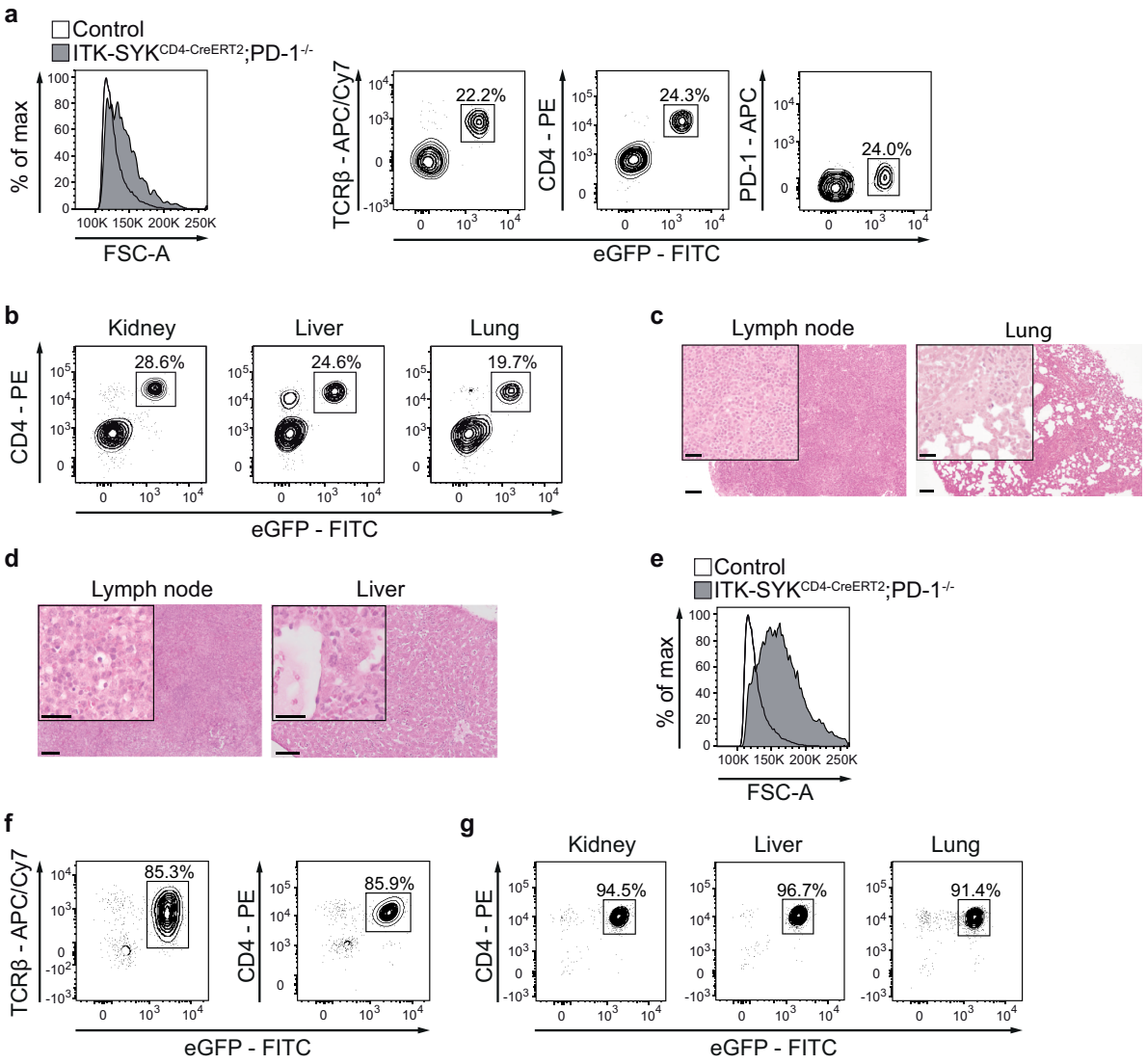

Figure 11 Phenotypic characterization of PD-1 deficient lymphomas.

a, b, Flow cytometric analyses of TCRβ, CD4, PD-1 and eGFP expression in single-cell suspensions from the spleen (**a**) or kidney, liver and lung (**b**) from an ITK-SYK$^{CD4\text{-}CreERT2}$;PD-1$^{-/-}$ mouse at one week after tamoxifen (TAM) injection. Flow cytometric analysis of forward scatter area (FSC-A) was used as a parameter to detect cell size.

c, Lymph node and lung histology by H&E staining of tissues from a diseased ITK-SYK$^{CD4\text{-}CreERT2}$;PD-1$^{-/-}$ mouse one week after tamoxifen induction. The lymph node architecture was disrupted by a diffuse neoplastic lymphoid infiltration. In the lung, neoplastic lymphoid cells were located in intra- and perivascular regions with a multifocal nodal infiltration pattern. Scale bars represent 100 µm and 20 µm (inset). Scale bars represent 100 µm and 20 µm (insets).

d, Histology by H&E staining of lymph node and liver tissues of an NSG recipient mouse 13 days after the transplantation of 5x10^7 lymphomatous ITK-SYK$^{CD4\text{-}CreERT2}$;PD-1$^{-/-}$

splenocytes. Abnormal infiltration of lymphoblastoid cells is visible. Scale bars represent 100 µm and 20 µm (insets).
e, f, g Flow cytometric analysis of FSC-A and TCRβ, CD4 and eGPF expression in lymphoma cells in the spleen (**e, f**), kidney, liver and lung (**g**) from the same mouse as in **d**.
a, b, c Representative data from three independent experiments, each with three biological replicates. **d, e, f, g** Representative results from one of six NSG recipient mice from two independent experiments.

In parallel, we isolated unstimulated peripheral $CD4^+$ T cells from $Rosa26^{LSL\text{-}ITK\text{-}SYK}$ and $Rosa26^{LSL\text{-}ITK\text{-}SYK}$;$PD\text{-}1^{-/-}$ mice without Cre transgenes and incubated these with the recombinant, cell-permeant TAT-CRE fusion recombinase *in vitro* (Nolden et al. 2006). Immediately after, we intravenously injected $5x10^5$ treated cells into syngenic C57BL/6 wild-type mice that did not receive any pre-conditioning treatment (Figure 12 a-f). TAT-CRE deleted the LSL cassette within the recipient *in vivo,* and the treated $CD4^+$ T cells began to express ITK-SYK and eGFP after 24 h (data not shown). The TAT-CRE treated ITK-SYK-expressing $CD4^+$ T cells from PD-1 competent donors ($Rosa26^{LSL\text{-}ITK\text{-}SYK}$) vanished over time (Figure 12 c). In contrast, those from PD-1 deficient donors ($Rosa26^{LSL\text{-}ITK\text{-}SYK}$;$PD\text{-}1^{-/-}$) expanded vigorously and induced lethal infiltrative lymphomas that that could be serially transplanted (Figure 12 a-j). Thus, the absence of PD-1 in peripheral T cells enables an appropriate oncogenic signal to directly create an aggressive cancer.

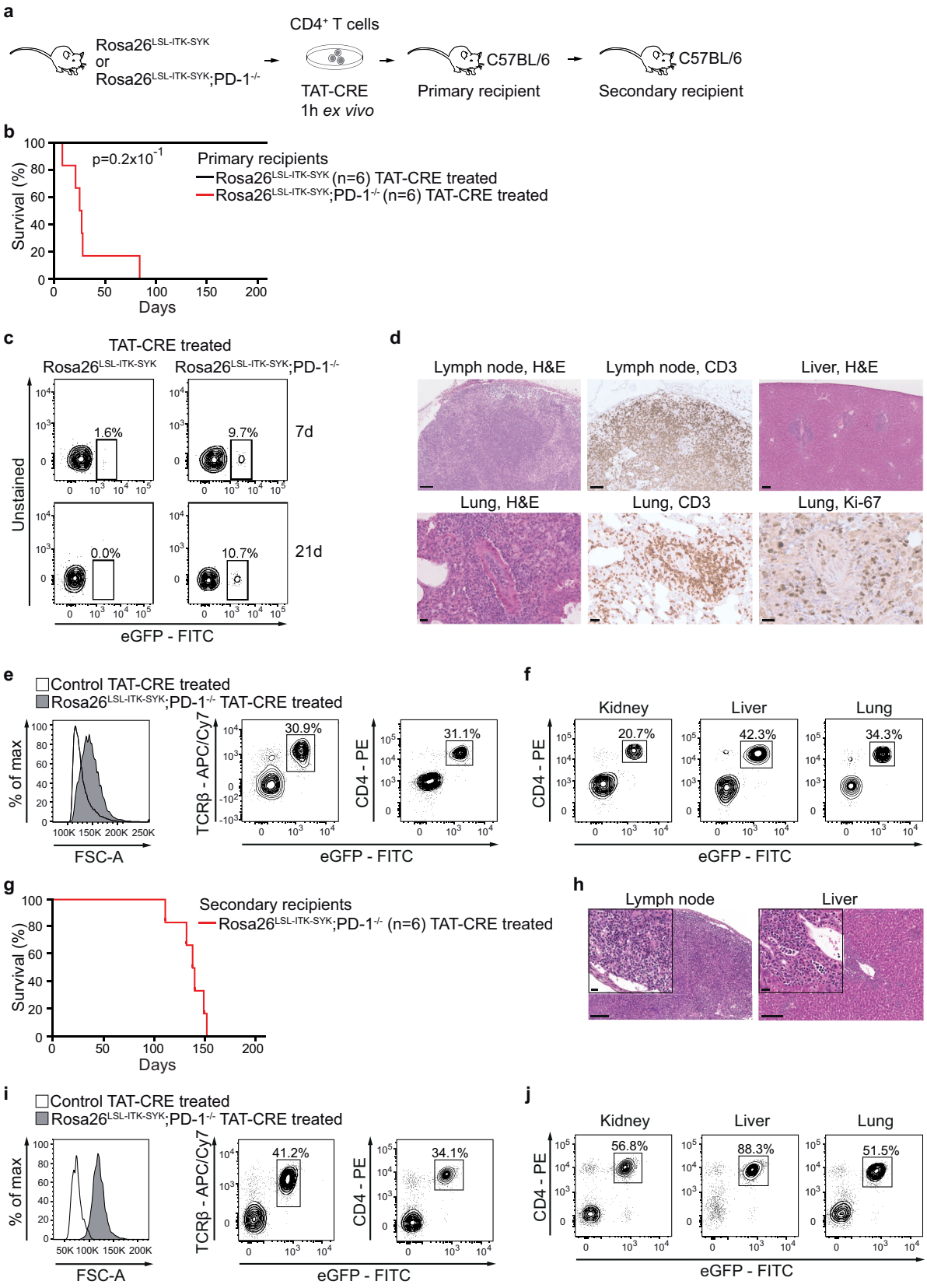

Figure 12 Serial transplantation of PD-1-deficient lymphomas.

a, Representation of the experimental strategy for inducing ITK-SYK expression via TAT-

CRE in PD-1-competent (Rosa26$^{LSL\text{-}ITK\text{-}SYK}$) or PD-1-deficient (Rosa26$^{LSL\text{-}ITK\text{-}SYK}$;PD-1$^{-/-}$) cells for subsequent transfer into wild-type C57BL/6 recipient mice.

b, Survival curves of the C57BL/6 recipients (n=6 recipients per genotype) transplanted with 5x10^5 TAT-CRE-treated Rosa26$^{LSL\text{-}ITK\text{-}SYK}$ or Rosa26$^{LSL\text{-}ITK\text{-}SYK}$;PD-1$^{-/-}$CD4$^+$ T cells (n=6 donor mice per genotype). P=two-sided log-rank test

c, Flow cytometric analysis of ITK-SYK/eGFP expression in peripheral blood lymphocytes from C57BL/6 mice that received TAT-CRE-treated PD-1-competent (Rosa26$^{LSL\text{-}ITK\text{-}SYK}$) or PD-1-deficient (Rosa26$^{LSL\text{-}ITK\text{-}SYK}$;PD-1$^{-/-}$) cells on days 7 and 21 after transplantation. The genotypes of the donor mice are indicated.

d, Histology and immunohistochemistry of the indicated organs from a sick primary recipient mouse after the transfer of TAT-CRE-treated Rosa26$^{LSL\text{-}ITK\text{-}SYK}$;PD-1$^{-/-}$ T cells showing the expansion of a malignant T-lymphocyte population. Scale bars represent 100 µm (top row) and 20 µm (bottom row)**.**

e, f, Flow cytometric analysis of CD4-stained lymphocytes derived from the spleen (**e**) or indicated organs (**f**) of the mouse shown in **d**. FSC-A, forward scatter area, which was used as a parameter to detect cell size of splenic Rosa26$^{LSL\text{-}ITK\text{-}SYK}$;PD-1$^{-/-}$ T cells compared to the TAT-CRE treated C57BL/6 CD4$^+$ T cells (Control).

g, Survival of secondary C57BL/6 recipient mice (n=6) that received 1x10^5 TAT-CRE-induced Rosa26$^{LSL\text{-}ITK\text{-}SYK}$;PD-1$^{-/-}$ lymphoma T-cells from diseased primary C57BL/6 recipients (n=6 biological replicates).

h, H&E-stained histologic sections from lymph node and liver tissues from a diseased C57BL/6 mouse that had received 1x10^5 TAT-CRE-treated Rosa26$^{LSL\text{-}ITK\text{-}SYK}$;PD-1$^{-/-}$ T cells as the secondary recipient from a sick C57BL/6 primary recipient. Scale bars represent 100 µm and 20 µm (insets).

i, j, Flow cytometric analysis as in **e, f** but for the secondary recipient from **h**.

c, Characteristic flow cytometric profiles measured in two independent experiments. **d, e, f, h, i, j**, Representative results from one out of six analyzed mice.

In human T-NHL mono-allelic deletions are the most common *PDCD1* alteration (Figure 4 d). Therefore, we treated a cohort of heterozygous ITK-SYK$^{CD4\text{-}CreERT2}$;PD-1$^{+/-}$ mice with tamoxifen and monitored these animals over time. Intriguingly, all heterozygous ITK-SYK$^{CD4\text{-}CreERT2}$;PD-1$^{+/-}$ mice succumbed to invasive lymphomas within 50 days after tamoxifen injection (Figure 10 c and Figure 13 a-e) and also these

PD-1$^{+/-}$ lymphomas transmitted the aggressive disease to secondary recipients (Figure 13 f-h), establishing PD-1 as an haploinsufficient tumor suppressor.

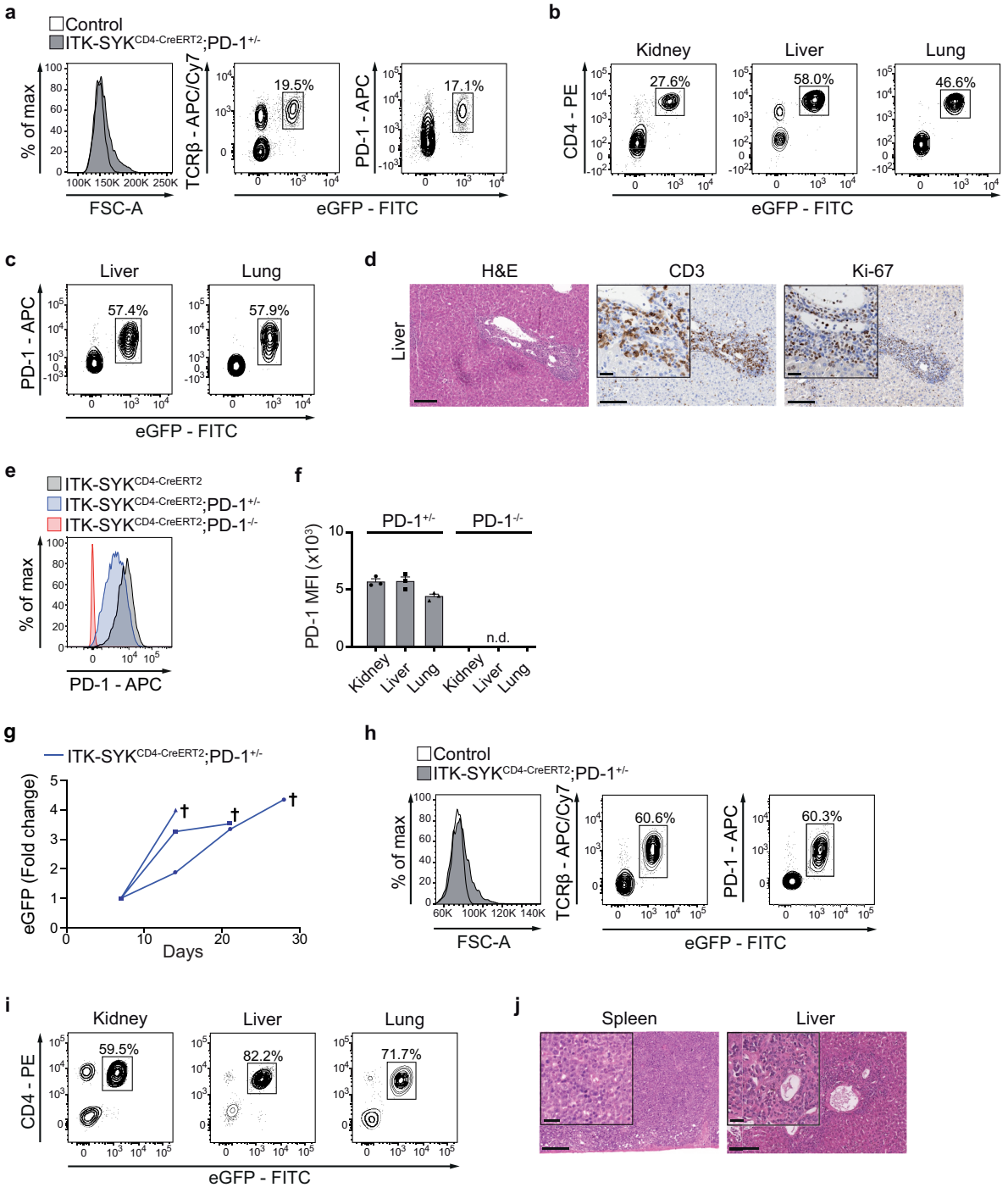

Figure 13 Characterization of Pdcd1-heterozygous lymphomas.

a, Flow cytometric analysis of forward scatter area (FSC-A), which was used as a parameter to detect cell size, and TCRβ, PD-1 and eGPF expression in splenic lymphoma cells from a

diseased ITK-SYK$^{CD4\text{-}CreERT2}$;PD-1$^{+/-}$ mouse at two weeks after tamoxifen injection (0.25 mg). CD4^{+} T cells from an untreated wild-type C57BL/6 mouse (Control) served as control.

b, c, Flow cytometric analysis of CD4, eGFP and PD-1 expression in single-cell suspensions of the indicated dissociated organs from the same mouse as in **a**.

d, Histology after H&E staining and immunohistochemical staining with anti-CD3 or anti-Ki-67 antibody of the liver tissue from the same animal as in **a, b, c**. Abnormal infiltration of lymphoblastoid cells is visible. Scale bars represent 100 µm and 20 µm (insets).

e, Flow cytometric analyses of PD-1 receptor expression on ITK-SYK^{+}/eGFP^{+} T cells from ITK-SYK$^{CD4\text{-}CreERT2}$, ITK-SYK$^{CD4\text{-}CreERT2}$;PD-1$^{+/-}$ and ITK-SYK$^{CD4\text{-}CreERT2}$;PD-1$^{-/-}$ mice are shown.

f, Flow cytometric analysis of PD-1 expression on ITK-SYK^{+}/eGFP^{+} T lymphocytes. Cells isolated from the kidney, liver and lung of diseased ITK-SYK$^{CD4\text{-}CreERT2}$;PD-1$^{+/-}$ (labelled with PD-1$^{+/-}$) or ITK-SYK$^{CD4\text{-}CreERT2}$;PD-1$^{-/-}$ (labelled with PD-1$^{-/-}$) mice from the experiment presented in Figure 10 c. Shown are the mean±s.d. and individual data points; n.d., not detectable.

g, Fifty million splenic cells from diseased ITK-SYK$^{CD4\text{-}CreERT2}$;PD-1$^{+/-}$ mice (n=3 donors) were intravenously transferred to NSG mice (n=3 recipients). The fold changes of ITK-SYK-expressing eGFP^{+} lymphocytes in the peripheral blood of the recipients are indicated. † indicates animals that had to be euthanized because of lymphomas.

h, **i**, Flow cytometric analysis of the FSC-A, TCRβ, PD-1, CD4 and eGFP expression in spleen cell suspension (**h**) or lymphoma cells isolated from the lung, kidney and liver (**i**) of an NSG mouse that received 5x10^{7} splenic cells from a TAM-induced ITK-SYK$^{CD4\text{-}CreERT2}$;PD-1$^{+/-}$ mouse. CD4^{+} T cells from an untreated wild-type C57BL/6 mouse served as control.

j, Spleen and liver histology after H&E staining of organ sections of the NSG recipient mouse presented in **h**, **i.** Infiltration of a lymphoblastoid cell population in the spleen resulting in a complete loss of the normal architecture. Mixed periportal and intrasinusoidal infiltrations of neutrophilic granulocytes, lymphocytes and lymphoblasts into the liver with multifocal periportal hepatocellular necroses. Scale bars represent 100 µm and 20 µm (insets).

a, b, c, d, Representative data from three independent experiments, each with at least three biological replicates. **e,** Histograms representing one out of three analyzed mice per genotype. **f,** PD-1 expression on eGFP^{+} T cells isolated from the lung, kidney, and liver was measured in three biological replicates per genotype. **g**, The data from a single experiment that was independently repeated once with similar results. **h, i**, Representative results from one of six analyzed mice from two independent experiments. **j**, The results are characteristic for three mice that were analyzed in two independent experiments.

The blockage of the PD-1 / PD-L1 interaction with antibodies against PD-1 or PD-L1 is heavily exploited in the clinic to activate of T cell immunity against cancer cells of multiple types (Brahmer et al. 2012). Based on our findings in PD-1 deficient mice, we next treated ITK-SYKCD4-CreERT2 mice with checkpoint inhibitors (anti-PD-L1; anti-PD-1) after tamoxifen induction (Figure 10 d-f and Figure 14 a-c). Strikingly, similar to a genetic PD-1 deletion, anti-PD-L1 treatment starting one day after tamoxifen induction lead to an immediate lethal ITK-SYK+ T cell proliferation with invasive growth (Figure 10 d,e and Figure 14 a-c). Likewise, treatment of ITK-SYKCD4-CreERT2 mice with anti-PD-L1 or anti-PD-1 during the contraction phase of the ITK-SYK+ compartment (ten days after tamoxifen) also induced lethal a lymphoproliferation (Figure 10 f and Figure 14 e). Yet, these cells did not transmit the disease to secondary recipients (Figure 14 d). Thus, although these checkpoint inhibitors accelerate the growth of T cells with oncogenically sensitized TCR pathways in vivo, these pharmacological effects are in contrast to T cell intrinsic *Pdcd1* gene deletion only transient.

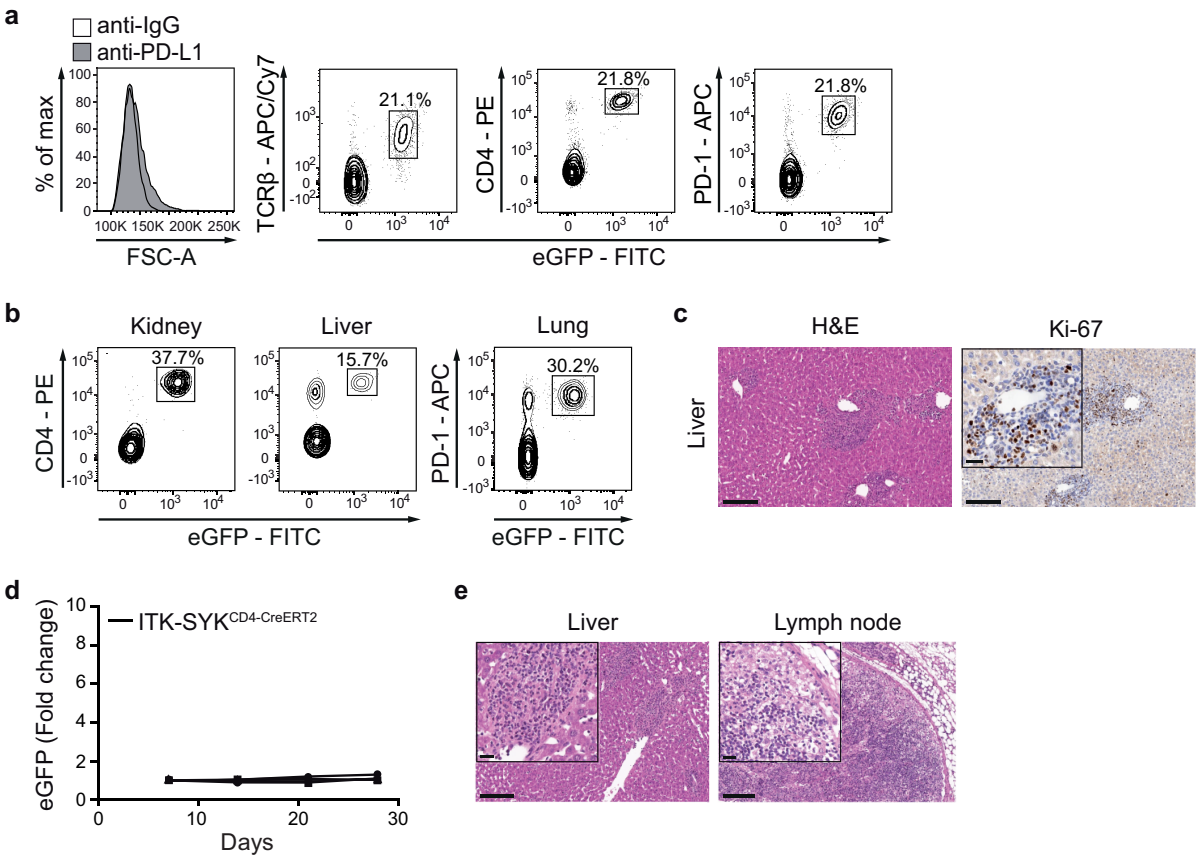

Figure 14 Anti-PD-L1 triggers lethal ITK-SYK+ lymphoproliferation

a, b, c, Analyses of the antibody-treated mice from the experiment shown in Figure 10 d. Flow cytometric data of forward scatter area (FSC-A), which was used as a parameter to detect cell size, and TCRβ, CD4, PD-1 and eGPF expression in lymphomatous cells isolated from the spleen (**a**), kidney, liver and lung (**b**).

c, Histology and immunohistochemistry of liver sections from the same mouse demonstrating the expansion of blastoid T-cells. Scale bars represent 100 µm and 20 µm (inset)**.**

d, Fifty million splenic cells from anti-PD-L1-treated, sick ITK-SYK$^{CD4\text{-}CreERT2}$ mice (n=3 biological replicates) were intravenously transferred to NSG recipient mice (n=3). The fold change of eGFP^{+} lymphocytes in the peripheral blood of recipients over time is shown.

e, Liver and lymph node histology after H&E staining of tissue sections from a diseased ITK-SYK$^{CD4\text{-}CreERT2}$ mouse from the experiment presented in Figure 10 f. The mouse received an anti-PD-1 antibody treatment that started ten days after tamoxifen administration.

a, b, c, Representative data from one out of nine analyzed mice in four independent experiments. **d,** The data from a single experiment that was repeated once with similar results. **e**, Histologies are characteristic for four mice that were analyzed in two independent experiments.

We demonstrated above that the ligation of PD-1 enhances PTEN and attenuates PI3K/AKT and PKCθ function after ITK-SYK signaling (see Figure 8 f). PD-1 signaling in a PD-1 transduced human lymphoma cell line also enhances PTEN and attenuates PI3K/AKT and PKCθ (Figure 15 a-c). In primary PD-1 deficient ITK-SYK^{+} lymphomas we consistently detected reduced PTEN levels and enhanced AKT and PKCθ activity (Figure 10 g) suggesting that the *PDCD1* deletions promote tumorigenesis at least in part via these mechanism. To study the functional relevance of PI3K/AKT enforcement, we incubated PD-1$^{-/-}$ deficient lymphoma cells with the small molecule PI3K inhibitor Idelalisib *in vitro*, that is currently in clinical development for selected B cell malignancies (Gopal et al. 2014). PI3K inhibition downregulated AKT activity and also killed ITK-SYK^{+}PD-1$^{-/-}$ lymphoma cells a dose dependent manner (Figure 15 d). Finally, we also treated mice that harbor ITK-SYK^{+}PD-1$^{-/-}$ lymphomas with Idelalisib *in vivo*. PI3K inhibition significantly extended the life span of these mice demonstrating that the activity of PI3K/AKT signaling is a critical factor in lymphomas with *Pdcd1* deletion (Figure 10 h and Figure 15 e).

Although most PD-1 mutations in human T-NHL are mono-allelic focal deletions (Table 6), two *PDCD1* frameshift mutations and two single nucleotide variants, p.E46X located in the extracellular domain and p.K78R located in the transmembrane region of PD-1, have recently been reported in a cohort of PTCL NOS patients (Watatani et al. 2019). To determine, if spontaneous single nucleotide variants in murine *Pdcd1* gene can give rise to fully transformed ITK-SYK driven lymphomas in the mouse, we additionally performed Whole Exome Sequencing of diseased ITK-SYK$^{CD4\text{-}Cre}$ mice (see Figure 2). Interestingly, we detected a single nucleotide variant at position chr1:94,041,455, which is part of *Pdcd1* exon 2, and leads to a p.E46G amino acid

exchange in the extracellular domain of PD-1, presumably mimicking the human derived p.E46X mutation (Figure 10 i).

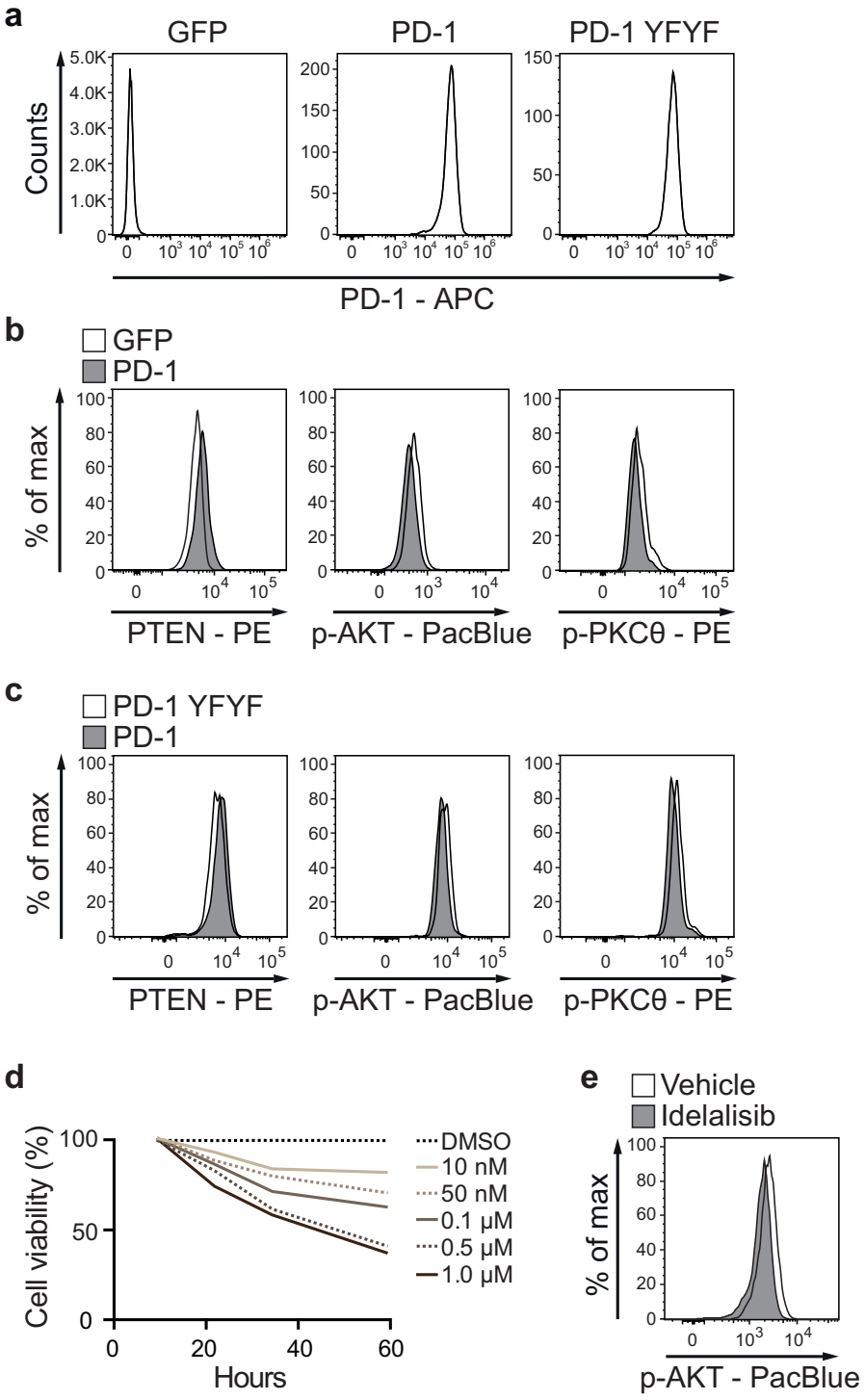

Figure 15 PI3K regulates PI3K signaling.

a, Human T-NHL HuT 78 cells were infected with retroviruses carrying wild-type PD-1 (PD-

1) or a signaling-incompetent variant of PD-1 (PD-1 YFYF; ITIM/ITSM motifs mutated in the PD-1 cytoplasmic tail) together with GFP or GFP alone (control; GFP). PD-1 surface expression was determined by flow cytometry.

b, Intracellular flow cytometric analyses of PTEN, p-AKT and p-PKCθ levels in wild-type PD-1- (PD-1) or GFP only-transduced (GFP) HuT 78 cells that had been co-cultured with PD-L1-expressing human dendritic cells for 24 hours.

c, Intracellular flow cytometric analyses from a similar experiment as in **b** but with wild-type-PD-1 (PD-1) and Y223F/Y248F-mutated-PD-1 (PD-1 YFYF) transduced HuT 78 cells.

d, TAT-CRE-induced $Rosa26^{LSL\text{-}ITK\text{-}SYK}$;$PD\text{-}1^{-/-}$ cells isolated from diseased C57BL/6 recipient mice (Figure 12 b) were cultured *in vitro* in the presence of the indicated concentration of the PI3Kδ inhibitor idelalisib or DMSO. Cell viability was determined over time.

e, *Ex vivo* phosphorylation status of the AKT kinase after the oral administration of idelalisib (10 mg/kg) or vehicle into mice. ITK-$SYK^{CD4\text{-}CreERT2}$;$PD\text{-}1^{-/-}$ T cells were induced *in vivo* with tamoxifen (0.25 mg). On day five after induction, $5x10^4$ $eGFP^+$ T cells were transplanted into NSG recipient mice. Five days later, the mice received a single gavage of idelalisib (10 mg/kg) or vehicle control. Four hours later, spleen-derived single-cell suspensions were analyzed by flow cytometry via Phosflow.

a, Results from two independent experiments with comparable outcomes. **b, c** Experiments were performed three times, each with similar results. **d,** Experiment was performed with four biological replicates; one representative replicate is shown. **e**, Experiment was performed twice with similar results.

4 Discussion

4.1 PD-1 is a key tumor suppressor in T-NHL

While the oncogenic activation of TCRs and coreceptor signaling pathways is an established principle in multiple T-NHL entities, experimental evidence showing that respective signaling variants continuously drive lymphoma cell proliferation and survival remains limited. To explore the direct consequences of oncogenically promoted T-cell pathways *in vivo*, we generated a murine model of human T-NHL in which we conditionally expressed the ITK-SYK fusion kinase in primary CD4+ T cells. While the expression of only ITK-SYK in mature T cells can trigger the massive expansion of these cells, this response is only transient and is insufficient to drive cancer. We therefore performed an unbiased *in vivo* screen to identify cooperating genetic events that could facilitate lymphoma development. We discovered that disrupting the *PDCD-1* gene, which encodes the PD-1 checkpoint receptor, was sufficient to create together with ITK-SYK expression T cell lymphomas with molecular, pathological and clinical features of the human disease. A comprehensive meta-analysis of human datasets of whole-exome, whole-genome, and targeted sequence data obtained from T-NHL patients revealed that additional genomic *PDCD1* gene alterations were present in 23% of all investigated human T-NHL cases (Choi et al. 2015; Kataoka et al. 2015; Wang et al. 2015; da Silva Almeida et al. 2015; Vaque et al. 2014). The most prevalent mutation type was CNVs (8% biallelic deletions and 83% mono-allelic deletions) followed by SNVs (3% missense and 6% nonsense). The T-NHL subtype that was most prominently affected by *PDCD1* alterations was ATLL, in which 26% of the patients carried *PDCD1* mutations, followed by CTCL, in which 22% of the patients carried mutated *PDCD1*. The highest proportion of *PDCD1*-deleted cases (36%) was found in a group of patients with advanced stage IV cutaneous T cell

lymphoma. The most frequently observed variants in human disease are mono-allelic *PDCD1* alterations. In the murine ITK-SYK driven PTCL model, the targeted deletion of only one *PDCD1* allele is sufficient to permit lymphoma genesis, establishing that PD-1 functions as a haplo-insufficient tumor suppressor in T-NHL.

4.2 Tumor suppressor mechanisms of PD-1

Our data shows that PD-1 can act as a tumor suppressor in T cell lymphoma. However, the tumor suppressive signals of PD-1 remain largely unclear. Though, it is conceivable that these effector mechanisms could overlap with the physiological pathways involved in PD-1 signaling, which restrict antigen-induced TCR responses at tolerance checkpoints to prevent autoimmunity (Figure 16). Under physiological conditions, PD-1 expression is upregulated on the cell surface of activated T cells, and PD-1 ligation via its agonists PD-L1 or PD-L2 subsequently counter-regulates TCR and coreceptor pathways at various molecular levels (Dong et al. 1999; Freeman et al. 2000; Latchman et al. 2001; Tseng et al. 2001). To exert this effect, PD-1 possesses a cytoplasmic immunoreceptor tyrosine-based inhibition motif (ITIM, defined as V/I/LxYxxL) followed by an immunoreceptor tyrosine-based switch motif (ITSM, defined as TxYxxL) (Shlapatska et al. 2001). After PD-1 ligation, these ITIM/ITSM moieties are tyrosine-phosphorylated (Sheppard et al. 2004; Hui et al. 2017) and subsequently recruit and activate the tyrosine-protein phosphatase Src homology 2 (SH2) domain-containing tyrosine phosphatase (SHP2) (Yokosuka et al. 2012). Active PD-1 signaling then leads to a reduction in the phosphorylation of CD3ζ, ZAP70 and PKCθ (Sheppard et al. 2004), resulting in the presumably subsequent downmodulation of NF-κB. In addition, PD-1 mediates, via SHP2, the dephosphorylation of the CD28 cytoplasmatic tail (Hui et al. 2017) to counter-regulate PI3K and AKT (PKB) activity.

Moreover, active PD-1 stabilizes the PTEN tumor suppressor lipid phosphatase via unknown mechanisms (Figure 8 f). This increase in PTEN further negatively regulates PI3K-generated levels of PIP3 (Maehama and Dixon 1998; Myers et al. 1998), thereby further inhibiting the AKT survival pathway. In addition, PD-1 ligation negatively regulates the expression of the cell survival factor Bcl-xL in T cells (Parry et al. 2005).

The genetic loss of PD-1 during human T cell lymphomagenesis likely unleashes TCR proximal signals that exert oncogenic effects within the tumor cell in addition to releasing the brakes on the PI3K/AKT and PKCθ/NF-κB signaling pathways, both of which are critical promoters of T cell lymphomas. Consistent with this hypothesis, the experimental deletion of *PDCD1* in the murine PTCL model reduced PTEN expression and subsequently enhanced AKT and PKCθ signaling (Figure 10 g). In addition, in human T cell lymphoma cell lines, the forced overexpression of PD-1 and its subsequent ligation enhanced PTEN expression and attenuated AKT and PKCθ activity in an ITIM/ITSM motif-dependent manner (Figure 15 a-c). These findings indicate that the tumor-suppressive function of PD-1 might be mediated in part via the inhibitory effects on the PI3K/AKT and PKCθ/NF-κB axes. Consistent with the enhancement of PI3K/AKT and PKCθ/NF-κB signaling observed in PD-1-deficient T cell lymphoma cells, these tumors were also sensitive to pharmacological PI3K inhibition (Figure 10 h). Moreover, PI3K inhibition is currently being successfully explored in patients with relapsed or refractory PTCL and CTCL in a clinical setting (Horwitz et al. 2018).

4.3 PD-1 checkpoint inhibition in T cell lymphoma

Many tumors show an increase in regulatory T cell populations, upregulation of PD-L1, and increases in immunomodulatory molecules like IL-10 that suppress T cell

cytotoxicity as tumor evasion mechanisms. The PD-1 checkpoint pathway is currently receiving a great deal of attention in immune oncology because it can trigger exhaustion and dysfunctionality in the T cells directed against cancer cells in suppressive tumor microenvironments (Ribas and Wolchok 2018; Hoos 2016; Gotwals et al. 2017; Sharma et al. 2011).

Clinically approved antibodies (checkpoint inhibitors) directed against either the PD-1 receptor ((Nivolumab (BMS, 2014), Pembrolizumab (Merck, 2014)), or its ligand, PD-L1 (Atezolizumab (Roche, 2016), Avelumab (Merck Serono and Pfizer, 2017) and Durvalumab (AstraZeneca, 2016)), can block PD-1 signaling in patients and enhance T cell immunity against malignant cells with highly successful translation in tumors of various histology, including melanoma (Hodi et al. 2010), non-small-cell lung cancer (Borghaei et al. 2015; Garon et al. 2015), renal-cell carcinoma (Motzer et al. 2015) and Merkel cell carcinoma (Nghiem et al. 2016). Based on the efficiency of these strategies across tumor entities, the blockade of the PD-1 pathway is currently also being explored in lymphoid malignancies (Hude et al. 2017). However, as indicated above, in T cell lymphoma, the tumor cell itself is a T cell. Because *PDCD1* acts as a tumor suppressor gene in these malignancies, we explored the consequences of anti-PD-1 or anti-PD-L1 checkpoint inhibition in the ITK-SYK mouse model (Figure 10 d-f and Figure 14 a-e). Intriguingly, both checkpoint inhibitors massively accelerated the expansion of ITK-SYK-expressing lymphomatous cells, leading to fatal organ infiltration within days; these results indicate that the pharmacological inhibition of the PD-1 pathway can, in principle, accelerate malignant T cell growth under certain conditions. Meanwhile, results obtained in a clinical T-NHL study demonstrate the relevance of this hypothesis in patients (Ratner et al. 2018). Here, *Ratner et al.* report data from three HTLV-1-positive ATLL patients enrolled in an American phase II trial

of Nivolumab treatment in which a single dose of this anti-PD-1 antibody resulted in rapid disease acceleration in all three patients with increased leukocytosis and LDH levels, a marker of disease progression (International Non-Hodgkin's Lymphoma Prognostic Factors 1993; 'Major prognostic factors of patients with adult T-cell leukemia-lymphoma: a cooperative study. Lymphoma Study Group (1984-1987)' 1991; Nosaka et al. 2002). However, in an independent but similar Japanese trial, eight ATLL patients also received nivolumab, and none of these patients exhibited rapid disease acceleration (Ishitsuka, Utsunomiya, and Ishida 2018). One difference between the two studies was the disease state of the patients. Whereas the three cases in the *Ratner et al.* study exhibited smoldering, chronic, and an unusual stable acute ATLL, all eight patients in the *Ishitsuka et al.* trial had aggressive ATLL. This biological difference could explain the different responses of the patients to anti-PD-1 treatment as it is conceivable that ATLL cells with a smoldering, chronic or rather stable phenotype might still be under negative suppressor control by PD-1, which can be released by checkpoint inhibitors, whereas those with an aggressive phenotype might have already corrupted the PD-1 pathway and are as such not further accelerated by anti-PD-1 treatment (Ratner et al. 2018). However, whether this hypothesis will hold true is currently unclear. Thus, further studies are required to define which genetic, immunological and environmental differences among ATLL patients determine the response to PD-1 inhibition. However, although the number of patients in these trials was very small, they provide clinical evidence that there is some concern about the safety of PD-1 inhibition in ATLL (Ratner et al. 2018).

In addition to the acceleration of established T cell malignancies, a patient case report also suggested the possibility that secondary T cell lymphoma development could occur upon PD-1 checkpoint inhibition (Ono et al. 2018). In this study, *Ono et al.*

reported a patient with Hodgkin lymphoma (HL) who was treated with nivolumab. In HL, the cancer cells (Reed-Sternberg cells) are of B cell origin, are typically CD30+CD15+, and frequently express high levels of PD-L1 (Tanaka et al. 2018; Roemer et al. 2016), making this tumor especially responsive to anti-PD-1 checkpoint inhibition (Ansell et al. 2015). Indeed, the HL observed in the patient described by *Ono et al.* responded and regressed upon nivolumab treatment (Ono et al. 2018); however, the patient developed a timely correlated monoclonal hepatosplenic T cell lymphoma with a fatal outcome. The authors therefore concluded that although PD-1 blockade is a promising therapeutic approach for refractory malignancies, attention should be paid to potential secondary T cell lymphoma development (Ono et al. 2018). However, only a single such case was reported, and it is currently unclear whether the secondary T cell lymphoma was indeed caused by PD1-1 inhibition. Thus, the potential frequencies, risk factors and latencies of potential secondary T cell lymphoma development after PD-1 checkpoint inhibition remain to be determined. Moreover, whether hematopoietic malignancies, such as HL, in which early lymphoid progenitors can already harbor genetic founder lesions and the tumor tissue is characterized by highly inflammatory T cell infiltrates, carry a particularly high risk of the development of secondary T cell lymphomas after PD-1 inhibition remains to be uncovered.

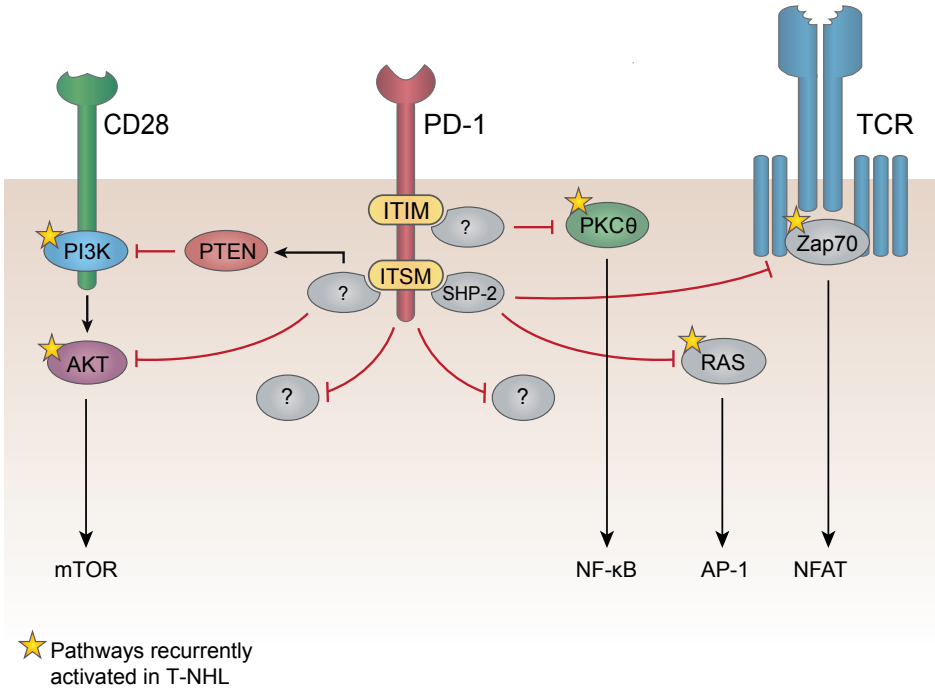

Figure 16 Putative PD-1-mediated tumor suppressive mechanisms in T cell non-Hodgkin lymphoma (T-NHL)

PD-1 can inhibit oncogenic-driven T cell receptor (TCR) pathways by recruiting phosphatases, including SHP-2, to the immunoreceptor tyrosine-based inhibitory (ITIM) and immunoreceptor tyrosine-based switch (ITSM) motifs in the PD1 cytoplasmic tail. These phosphatases can counteract the positive signaling events upon being oncogenically triggered. They inhibit PKCθ and the RAS and phosphoinositide 3 kinase PI3K/AKT signaling pathways. Altogether, these results indicate a decrease in the activation of transcription factors, such as mTOR, nuclear factor-κB (NF κB), activator protein 1 (AP 1) and nuclear factor of activated T cells (NFAT), which are important for driving oncogene-transformed T cell proliferation and survival. ? indicates possible unknown binding partners and molecular targets of PD1.

4.4 Concluding Remarks and Future Perspectives

The last decade has seen tremendous progress in our understanding of PD-1 functions. In addition to the prevention of immunopathologies after chronic antigenic stimulation, this unique receptor has evolved as an important tumor suppressor in the T cell lineage, in which it counteracts the oncogenic signals that are mediated via the PI3K/AKT and PKCθ/NF-κB pathways. These insights provide new routes for exploring the poorly understood pathogenesis of T cell lymphomas and indicate that inhibiting PI3K signaling using inhibitors such as idelalisib or duvelisib might be a promising strategy in a subset of these cancers (Horwitz et al. 2018). Moreover, PKC/NF-κB inhibition could also be an option. However, several open questions remain. Currently, it is unclear how oncogenic events are “sensed” by PD-1 and whether the upregulation of PD-1 surface expression on premalignant T cells follows the same rules as the upregulation of PD-1 on normal antigen activated T cells. It is also unknown whether PD-1 can counteract only oncogenic signals that enforce TCR pathways or whether it plays a broader role in T cell lymphoma suppression. Moreover, PD-1 needs to be ligated by either PD-L1 or PD-L2 to be activated. Currently, it is unknown which cells in the microenvironment of (pre-)cancerous T cells provide the PD-1 ligands that contribute to lymphoma suppression and/or whether such ligands could also be provided by the malignant T cells themselves. The former is a possibility, as PD-L1 is expressed by many cell types including non-transformed naive T-cells following activation. The latter is a potential mechanism as disrupting the 3’ UTR of the PDL1 mRNA frequently led to PD-L1 overexpression in T cell malignancies (Kataoka et al. 2016). However, PD-L1 expression is observed across various T-NHL entities including PTCL (Brown et al. 2003) and CTCL (Kantekure et al. 2012). Moreover, the PD-L1 – PD1 interaction could potentially take place in trans, in cis or both (Zhao et al.

2018). The intracellular pathways that mediate PD-1 tumor suppression are also insufficiently defined, and it is currently unknown whether PD-1 counteracts oncogenesis only by exerting negative effects on the PI3K/AKT and PKCθ/NF-κB axis or whether it also functions via other mechanisms. The identification of such mechanisms is complicated by the fact that the negative regulation of antigen-induced T cell activation by PD-1 is surprisingly still insufficiently understood (Sharpe and Pauken 2018). Moreover, while PD-1 targeting checkpoint inhibitors can, in principle, lead to the progression of T cell malignancies, as has been demonstrated in ATLL (Ratner et al. 2018), inducing PD-1 or PD-L1 blockade with pembrolizumab was highly successful in natural killer cell–T-cell lymphoma (Kwong et al. 2017). Thus, it is very important to identify which T-NHL cases will benefit from or potentially progress upon PD-1 checkpoint blockade. The patient response is probably dependent on specific oncogenic alterations within the tumor T cells, including whether the PD-1 pathway is already corrupted within malignant T cells, and the composition of the immune microenvironment. Thus, many questions regarding the tumor suppressor function of PD-1 signaling in T cell lymphoma remain to be answered and new insights into the mechanisms of PD-1 signaling during T-NHL oncogenesis could improve checkpoint therapies by better tailoring specific therapies to patients. Finding new possibilities to balance suppression of anti-cancer CD8+ cytotoxic activity with enabling natural PD-1 inhibition of oncogenic T cells could provide alternative therapy regimes with enhanced safety profile for patients with T-NHLs sensitive to PD-1 tumor suppressive signaling. Additionally, it is possible that answers to these questions will also shed new light on the pathways involved in PD-1 signaling in nontransformed T cells.

5 References

Abate, F., A. C. da Silva-Almeida, S. Zairis, J. Robles-Valero, L. Couronne, H. Khiabanian, S. A. Quinn, M. Y. Kim, M. A. Laginestra, C. Kim, D. Fiore, G. Bhagat, M. A. Piris, E. Campo, I. S. Lossos, O. A. Bernard, G. Inghirami, S. Pileri, X. R. Bustelo, R. Rabadan, A. A. Ferrando, and T. Palomero. 2017. 'Activating mutations and translocations in the guanine exchange factor VAV1 in peripheral T-cell lymphomas', *Proc Natl Acad Sci U S A*, 114: 764-69.

Agostinelli, C., S. Hartmann, W. Klapper, P. Korkolopoulou, S. Righi, T. Marafioti, P. P. Piccaluga, E. Patsouris, M. L. Hansmann, K. Lennert, and S. A. Pileri. 2011. 'Peripheral T cell lymphomas with follicular T helper phenotype: a new basket or a distinct entity? Revising Karl Lennert's personal archive', *Histopathology*, 59: 679-91.

Ansell, S. M., A. M. Lesokhin, I. Borrello, A. Halwani, E. C. Scott, M. Gutierrez, S. J. Schuster, M. M. Millenson, D. Cattry, G. J. Freeman, S. J. Rodig, B. Chapuy, A. H. Ligon, L. Zhu, J. F. Grosso, S. Y. Kim, J. M. Timmerman, M. A. Shipp, and P. Armand. 2015. 'PD-1 blockade with nivolumab in relapsed or refractory Hodgkin's lymphoma', *N Engl J Med*, 372: 311-9.

Arber, D. A., A. Orazi, R. Hasserjian, J. Thiele, M. J. Borowitz, M. M. Le Beau, C. D. Bloomfield, M. Cazzola, and J. W. Vardiman. 2016. 'The 2016 revision to the World Health Organization classification of myeloid neoplasms and acute leukemia', *Blood*, 127: 2391-405.

Attygalle, A., R. Al-Jehani, T. C. Diss, P. Munson, H. Liu, M. Q. Du, P. G. Isaacson, and A. Dogan. 2002. 'Neoplastic T cells in angioimmunoblastic T-cell lymphoma express CD10', *Blood*, 99: 627-33.

Boddicker, R. L., G. L. Razidlo, S. Dasari, Y. Zeng, G. Hu, R. A. Knudson, P. T. Greipp, J. I. Davila, S. H. Johnson, J. C. Porcher, J. B. Smadbeck, B. W. Eckloff, D. D. Billadeau, P. J. Kurtin, M. A. McNiven, B. K. Link, S. M. Ansell, J. R. Cerhan, Y. W. Asmann, G. Vasmatzis, and A. L. Feldman. 2016. 'Integrated mate-pair and RNA sequencing identifies novel, targetable gene fusions in peripheral T-cell lymphoma', *Blood*, 128: 1234-45.

Boeva, V., T. Popova, K. Bleakley, P. Chiche, J. Cappo, G. Schleiermacher, I. Janoueix-Lerosey, O. Delattre, and E. Barillot. 2012. 'Control-FREEC: a tool for assessing copy number and allelic content using next-generation sequencing data', *Bioinformatics*, 28: 423-5.

Borghaei, H., L. Paz-Ares, L. Horn, D. R. Spigel, M. Steins, N. E. Ready, L. Q. Chow, E. E. Vokes, E. Felip, E. Holgado, F. Barlesi, M. Kohlhaufl, O. Arrieta, M. A. Burgio, J. Fayette, H. Lena, E. Poddubskaya, D. E. Gerber, S. N. Gettinger, C. M. Rudin, N. Rizvi, L. Crino, G. R. Blumenschein, Jr., S. J. Antonia, C. Dorange, C. T. Harbison, F. Graf Finckenstein, and J. R. Brahmer. 2015. 'Nivolumab versus Docetaxel in Advanced Nonsquamous Non-Small-Cell Lung Cancer', *N Engl J Med*, 373: 1627-39.

Bosisio, F. M., and L. Cerroni. 2015. 'Expression of T-follicular helper markers in sequential biopsies of progressive mycosis fungoides and other primary cutaneous T-cell lymphomas', *Am J Dermatopathol*, 37: 115-21.

Brahmer, J. R., S. S. Tykodi, L. Q. Chow, W. J. Hwu, S. L. Topalian, P. Hwu, C. G. Drake, L. H. Camacho, J. Kauh, K. Odunsi, H. C. Pitot, O. Hamid, S. Bhatia, R. Martins, K. Eaton, S. Chen, T. M. Salay, S. Alaparthy, J. F. Grosso, A. J. Korman, S. M. Parker, S. Agrawal, S. M. Goldberg, D. M. Pardoll, A. Gupta, and J. M. Wigginton. 2012. 'Safety and activity of anti-PD-L1 antibody in patients with advanced cancer', *N Engl J Med*, 366: 2455-65.

Broccoli, A., and P. L. Zinzani. 2017. 'Peripheral T-cell lymphoma, not otherwise specified', *Blood*, 129: 1103-12.

Brown, J. A., D. M. Dorfman, F. R. Ma, E. L. Sullivan, O. Munoz, C. R. Wood, E. A. Greenfield, and G. J. Freeman. 2003. 'Blockade of programmed death-1 ligands on dendritic cells enhances T cell activation and cytokine production', *J Immunol*, 170: 1257-66.

Brownlie, R. J., and R. Zamoyska. 2013. 'T cell receptor signalling networks: branched, diversified and bounded', *Nat Rev Immunol*, 13: 257-69.

Casulo, C., O. O'Connor, A. Shustov, M. Fanale, J. W. Friedberg, J. P. Leonard, B. S. Kahl, R. F. Little, L. Pinter-Brown, R. Advani, and S. Horwitz. 2017. 'T-Cell Lymphoma: Recent Advances in Characterization and New Opportunities for Treatment', *J Natl Cancer Inst*, 109.

Chemnitz, J. M., R. V. Parry, K. E. Nichols, C. H. June, and J. L. Riley. 2004. 'SHP-1 and SHP-2 associate with immunoreceptor tyrosine-based switch motif of programmed death 1 upon primary human T cell stimulation, but only receptor ligation prevents T cell activation', *J Immunol*, 173: 945-54.

Chen, Y. W., T. Guo, L. Shen, K. Y. Wong, Q. Tao, W. W. Choi, R. K. Au-Yeung, Y. P. Chan, M. L. Wong, J. C. Tang, W. P. Liu, G. D. Li, N. Shimizu, F. Loong, E. Tse, Y. L. Kwong, and G. Srivastava. 2015. 'Receptor-type tyrosine-protein phosphatase kappa directly targets STAT3 activation for tumor suppression in nasal NK/T-cell lymphoma', *Blood*, 125: 1589-600.

Choi, J., G. Goh, T. Walradt, B. S. Hong, C. G. Bunick, K. Chen, R. D. Bjornson, Y. Maman, T. Wang, J. Tordoff, K. Carlson, J. D. Overton, K. J. Liu, J. M. Lewis, L. Devine, L. Barbarotta, F. M. Foss, A. Subtil, E. C. Vonderheid, R. L. Edelson, D. G. Schatz, T. J. Boggon, M. Girardi, and R. P. Lifton. 2015. 'Genomic landscape of cutaneous T cell lymphoma', *Nat Genet*, 47: 1011-9.

Courtney, A. H., W. L. Lo, and A. Weiss. 2018. 'TCR Signaling: Mechanisms of Initiation and Propagation', *Trends Biochem Sci*, 43: 108-23.

Cristofoletti, C., M. C. Picchio, C. Lazzeri, V. Tocco, E. Pagani, A. Bresin, B. Mancini, F. Passarelli, A. Facchiano, E. Scala, G. A. Lombardo, M. Cantonetti, E. Caprini, G. Russo, and M. G. Narducci. 2013. 'Comprehensive analysis of PTEN status in Sezary syndrome', *Blood*, 122: 3511-20.

da Silva Almeida, A. C., F. Abate, H. Khiabanian, E. Martinez-Escala, J. Guitart, C. P. Tensen, M. H. Vermeer, R. Rabadan, A. Ferrando, and T. Palomero. 2015. 'The mutational landscape of cutaneous T cell lymphoma and Sezary syndrome', *Nat Genet*, 47: 1465-70.

Dahia, P. L., R. C. Aguiar, J. Alberta, J. B. Kum, S. Caron, H. Sill, D. J. Marsh, J. Ritz, A. Freedman, C. Stiles, and C. Eng. 1999. 'PTEN is inversely correlated with the cell survival factor Akt/PKB and is inactivated via multiple mechanismsin haematological malignancies', *Hum Mol Genet*, 8: 185-93.

de Leval, L., D. S. Rickman, C. Thielen, Ad Reynies, Y. L. Huang, G. Delsol, L. Lamant, K. Leroy, J. Briere, T. Molina, F. Berger, C. Gisselbrecht, L. Xerri, and P. Gaulard. 2007. 'The gene expression profile of nodal peripheral T-cell lymphoma demonstrates a molecular link between angioimmunoblastic T-cell lymphoma (AITL) and follicular helper T (TFH) cells', *Blood*, 109: 4952-63.

Dong, H., G. Zhu, K. Tamada, and L. Chen. 1999. 'B7-H1, a third member of the B7 family, co-stimulates T-cell proliferation and interleukin-10 secretion', *Nat Med*, 5: 1365-9.

Dorfman, D. M., J. A. Brown, A. Shahsafaei, and G. J. Freeman. 2006. 'Programmed death-1 (PD-1) is a marker of germinal center-associated T cells and angioimmunoblastic T-cell lymphoma', *Am J Surg Pathol*, 30: 802-10.

Dupuy, A. J., K. Akagi, D. A. Largaespada, N. G. Copeland, and N. A. Jenkins. 2005. 'Mammalian mutagenesis using a highly mobile somatic Sleeping Beauty transposon system', *Nature*, 436: 221-6.

Finco, T. S., T. Kadlecek, W. Zhang, L. E. Samelson, and A. Weiss. 1998. 'LAT is required for TCR-mediated activation of PLCgamma1 and the Ras pathway', *Immunity*, 9: 617-26.

Francisco, L. M., P. T. Sage, and A. H. Sharpe. 2010. 'The PD-1 pathway in tolerance and autoimmunity', *Immunol Rev*, 236: 219-42.

Frazee, A. C., G. Pertea, A. E. Jaffe, B. Langmead, S. L. Salzberg, and J. T. Leek. 2015. 'Ballgown bridges the gap between transcriptome assembly and expression analysis', *Nat Biotechnol*, 33: 243-6.

Freeman, G. J., A. J. Long, Y. Iwai, K. Bourque, T. Chernova, H. Nishimura, L. J. Fitz, N. Malenkovich, T. Okazaki, M. C. Byrne, H. F. Horton, L. Fouser, L. Carter, V. Ling, M. R. Bowman, B. M. Carreno, M. Collins, C. R. Wood, and T. Honjo. 2000.

'Engagement of the PD-1 immunoinhibitory receptor by a novel B7 family member leads to negative regulation of lymphocyte activation', *J Exp Med*, 192: 1027-34.

Friedrich, M. J., L. Rad, I. F. Bronner, A. Strong, W. Wang, J. Weber, M. Mayho, H. Ponstingl, T. Engleitner, C. Grove, A. Pfaus, D. Saur, J. Cadinanos, M. A. Quail, G. S. Vassiliou, P. Liu, A. Bradley, and R. Rad. 2017. 'Genome-wide transposon screening and quantitative insertion site sequencing for cancer gene discovery in mice', *Nat Protoc*, 12: 289-309.

Garon, E. B., N. A. Rizvi, R. Hui, N. Leighl, A. S. Balmanoukian, J. P. Eder, A. Patnaik, C. Aggarwal, M. Gubens, L. Horn, E. Carcereny, M. J. Ahn, E. Felip, J. S. Lee, M. D. Hellmann, O. Hamid, J. W. Goldman, J. C. Soria, M. Dolled-Filhart, R. Z. Rutledge, J. Zhang, J. K. Lunceford, R. Rangwala, G. M. Lubiniecki, C. Roach, K. Emancipator, L. Gandhi, and Keynote- Investigators. 2015. 'Pembrolizumab for the treatment of non-small-cell lung cancer', *N Engl J Med*, 372: 2018-28.

Gaud, G., R. Lesourne, and P. E. Love. 2018. 'Regulatory mechanisms in T cell receptor signalling', *Nat Rev Immunol*, 18: 485-97.

Gopal, A. K., B. S. Kahl, S. de Vos, N. D. Wagner-Johnston, S. J. Schuster, W. J. Jurczak, I. W. Flinn, C. R. Flowers, P. Martin, A. Viardot, K. A. Blum, A. H. Goy, A. J. Davies, P. L. Zinzani, M. Dreyling, D. Johnson, L. L. Miller, L. Holes, D. Li, R. D. Dansey, W. R. Godfrey, and G. A. Salles. 2014. 'PI3Kdelta inhibition by idelalisib in patients with relapsed indolent lymphoma', *N Engl J Med*, 370: 1008-18.

Gotwals, P., S. Cameron, D. Cipolletta, V. Cremasco, A. Crystal, B. Hewes, B. Mueller, S. Quaratino, C. Sabatos-Peyton, L. Petruzzelli, J. A. Engelman, and G. Dranoff. 2017. 'Prospects for combining targeted and conventional cancer therapy with immunotherapy', *Nat Rev Cancer*, 17: 286-301.

Han, J. M., S. J. Patterson, and M. K. Levings. 2012. 'The Role of the PI3K Signaling Pathway in CD4(+) T Cell Differentiation and Function', *Front Immunol*, 3: 245.

Hanzelmann, S., R. Castelo, and J. Guinney. 2013. 'GSVA: gene set variation analysis for microarray and RNA-seq data', *BMC Bioinformatics*, 14: 7.

Hodi, F. S., S. J. O'Day, D. F. McDermott, R. W. Weber, J. A. Sosman, J. B. Haanen, R. Gonzalez, C. Robert, D. Schadendorf, J. C. Hassel, W. Akerley, A. J. van den Eertwegh, J. Lutzky, P. Lorigan, J. M. Vaubel, G. P. Linette, D. Hogg, C. H. Ottensmeier, C. Lebbe, C. Peschel, I. Quirt, J. I. Clark, J. D. Wolchok, J. S. Weber, J. Tian, M. J. Yellin, G. M. Nichol, A. Hoos, and W. J. Urba. 2010. 'Improved survival with ipilimumab in patients with metastatic melanoma', *N Engl J Med*, 363: 711-23.

Hoos, A. 2016. 'Development of immuno-oncology drugs - from CTLA4 to PD1 to the next generations', *Nat Rev Drug Discov*, 15: 235-47.

Horwitz, S. M., R. Koch, P. Porcu, Y. Oki, A. Moskowitz, M. Perez, P. Myskowski, A. Officer, J. D. Jaffe, S. N. Morrow, K. Allen, M. Douglas, H. Stern, J. Sweeney, P. Kelly,

V. Kelly, J. C. Aster, D. Weaver, F. M. Foss, and D. M. Weinstock. 2018. 'Activity of the PI3K-delta,gamma inhibitor duvelisib in a phase 1 trial and preclinical models of T-cell lymphoma', *Blood*, 131: 888-98.

Hude, I., S. Sasse, A. Engert, and P. J. Brockelmann. 2017. 'The emerging role of immune checkpoint inhibition in malignant lymphoma', *Haematologica*, 102: 30-42.

Hui, E., J. Cheung, J. Zhu, X. Su, M. J. Taylor, H. A. Wallweber, D. K. Sasmal, J. Huang, J. M. Kim, I. Mellman, and R. D. Vale. 2017. 'T cell costimulatory receptor CD28 is a primary target for PD-1-mediated inhibition', *Science*, 355: 1428-33.

International Non-Hodgkin's Lymphoma Prognostic Factors, Project. 1993. 'A predictive model for aggressive non-Hodgkin's lymphoma', *N Engl J Med*, 329: 987-94.

Ishida, S., E. Huang, H. Zuzan, R. Spang, G. Leone, M. West, and J. R. Nevins. 2001. 'Role for E2F in control of both DNA replication and mitotic functions as revealed from DNA microarray analysis', *Mol Cell Biol*, 21: 4684-99.

Ishitsuka, K., and K. Tamura. 2014. 'Human T-cell leukaemia virus type I and adult T-cell leukaemia-lymphoma', *Lancet Oncol*, 15: e517-26.

Ishitsuka, K., A. Utsunomiya, and T. Ishida. 2018. 'PD-1 Inhibitor Therapy in Adult T-Cell Leukemia-Lymphoma', *N Engl J Med*, 379: 695.

Jacobsen, E. D., and D. M. Weinstock. 2018. 'Challenges and implications of genomics for T-cell lymphomas', *Hematology Am Soc Hematol Educ Program*, 2018: 63-68.

Jawed, S. I., P. L. Myskowski, S. Horwitz, A. Moskowitz, and C. Querfeld. 2014a. 'Primary cutaneous T-cell lymphoma (mycosis fungoides and Sezary syndrome): part I. Diagnosis: clinical and histopathologic features and new molecular and biologic markers', *J Am Acad Dermatol*, 70: 205 e1-16; quiz 21-2.

———. 2014b. 'Primary cutaneous T-cell lymphoma (mycosis fungoides and Sezary syndrome): part II. Prognosis, management, and future directions', *J Am Acad Dermatol*, 70: 223 e1-17; quiz 40-2.

Juntilla, M. M., and G. A. Koretzky. 2008. 'Critical roles of the PI3K/Akt signaling pathway in T cell development', *Immunol Lett*, 116: 104-10.

Kantekure, K., Y. Yang, P. Raghunath, A. Schaffer, A. Woetmann, Q. Zhang, N. Odum, and M. Wasik. 2012. 'Expression patterns of the immunosuppressive proteins PD-1/CD279 and PD-L1/CD274 at different stages of cutaneous T-cell lymphoma/mycosis fungoides', *Am J Dermatopathol*, 34: 126-8.

Kataoka, K., Y. Nagata, A. Kitanaka, Y. Shiraishi, T. Shimamura, J. Yasunaga, Y. Totoki, K. Chiba, A. Sato-Otsubo, G. Nagae, R. Ishii, S. Muto, S. Kotani, Y. Watatani, J. Takeda, M. Sanada, H. Tanaka, H. Suzuki, Y. Sato, Y. Shiozawa, T. Yoshizato, K.

Yoshida, H. Makishima, M. Iwanaga, G. Ma, K. Nosaka, M. Hishizawa, H. Itonaga, Y. Imaizumi, W. Munakata, H. Ogasawara, T. Sato, K. Sasai, K. Muramoto, M. Penova, T. Kawaguchi, H. Nakamura, N. Hama, K. Shide, Y. Kubuki, T. Hidaka, T. Kameda, T. Nakamaki, K. Ishiyama, S. Miyawaki, S. S. Yoon, K. Tobinai, Y. Miyazaki, A. Takaori-Kondo, F. Matsuda, K. Takeuchi, O. Nureki, H. Aburatani, T. Watanabe, T. Shibata, M. Matsuoka, S. Miyano, K. Shimoda, and S. Ogawa. 2015. 'Integrated molecular analysis of adult T cell leukemia/lymphoma', *Nat Genet*, 47: 1304-15.

Kataoka, K., Y. Shiraishi, Y. Takeda, S. Sakata, M. Matsumoto, S. Nagano, T. Maeda, Y. Nagata, A. Kitanaka, S. Mizuno, H. Tanaka, K. Chiba, S. Ito, Y. Watatani, N. Kakiuchi, H. Suzuki, T. Yoshizato, K. Yoshida, M. Sanada, H. Itonaga, Y. Imaizumi, Y. Totoki, W. Munakata, H. Nakamura, N. Hama, K. Shide, Y. Kubuki, T. Hidaka, T. Kameda, K. Masuda, N. Minato, K. Kashiwase, K. Izutsu, A. Takaori-Kondo, Y. Miyazaki, S. Takahashi, T. Shibata, H. Kawamoto, Y. Akatsuka, K. Shimoda, K. Takeuchi, T. Seya, S. Miyano, and S. Ogawa. 2016. 'Aberrant PD-L1 expression through 3'-UTR disruption in multiple cancers', *Nature*, 534: 402-6.

Katzav, S., D. Martin-Zanca, and M. Barbacid. 1989. 'vav, a novel human oncogene derived from a locus ubiquitously expressed in hematopoietic cells', *EMBO J*, 8: 2283-90.

Keir, M. E., G. J. Freeman, and A. H. Sharpe. 2007. 'PD-1 regulates self-reactive CD8+ T cell responses to antigen in lymph nodes and tissues', *J Immunol*, 179: 5064-70.

Kim, D., B. Langmead, and S. L. Salzberg. 2015. 'HISAT: a fast spliced aligner with low memory requirements', *Nat Methods*, 12: 357-60.

Kwong, Y. L., T. S. Y. Chan, D. Tan, S. J. Kim, L. M. Poon, B. Mow, P. L. Khong, F. Loong, R. Au-Yeung, J. Iqbal, C. Phipps, and E. Tse. 2017. 'PD1 blockade with pembrolizumab is highly effective in relapsed or refractory NK/T-cell lymphoma failing l-asparaginase', *Blood*, 129: 2437-42.

Latchman, Y., C. R. Wood, T. Chernova, D. Chaudhary, M. Borde, I. Chernova, Y. Iwai, A. J. Long, J. A. Brown, R. Nunes, E. A. Greenfield, K. Bourque, V. A. Boussiotis, L. L. Carter, B. M. Carreno, N. Malenkovich, H. Nishimura, T. Okazaki, T. Honjo, A. H. Sharpe, and G. J. Freeman. 2001. 'PD-L2 is a second ligand for PD-1 and inhibits T cell activation', *Nat Immunol*, 2: 261-8.

Lee, P. P., D. R. Fitzpatrick, C. Beard, H. K. Jessup, S. Lehar, K. W. Makar, M. Perez-Melgosa, M. T. Sweetser, M. S. Schlissel, S. Nguyen, S. R. Cherry, J. H. Tsai, S. M. Tucker, W. M. Weaver, A. Kelso, R. Jaenisch, and C. B. Wilson. 2001. 'A critical role for Dnmt1 and DNA methylation in T cell development, function, and survival', *Immunity*, 15: 763-74.

Lemonnier, F., L. Couronne, M. Parrens, J. P. Jais, M. Travert, L. Lamant, O. Tournillac, T. Rousset, B. Fabiani, R. A. Cairns, T. Mak, C. Bastard, O. A. Bernard, L. de Leval, and P. Gaulard. 2012. 'Recurrent TET2 mutations in peripheral T-cell

lymphomas correlate with TFH-like features and adverse clinical parameters', *Blood*, 120: 1466-9.

Lemonnier, F., P. Gaulard, and L. de Leval. 2018. 'New insights in the pathogenesis of T-cell lymphomas', *Curr Opin Oncol*, 30: 277-84.

Liang, P. I., S. T. Chang, M. Y. Lin, Y. C. Hsieh, P. Y. Chu, C. J. Chen, K. J. Lin, Y. C. Jung, W. S. Hwang, W. T. Huang, W. C. Chang, H. Ye, and S. S. Chuang. 2014. 'Angioimmunoblastic T-cell lymphoma in Taiwan shows a frequent gain of ITK gene', *Int J Clin Exp Pathol*, 7: 6097-107.

Liberzon, A., C. Birger, H. Thorvaldsdottir, M. Ghandi, J. P. Mesirov, and P. Tamayo. 2015. 'The Molecular Signatures Database (MSigDB) hallmark gene set collection', *Cell Syst*, 1: 417-25.

Liu, S. K., N. Fang, G. A. Koretzky, and C. J. McGlade. 1999. 'The hematopoietic-specific adaptor protein gads functions in T-cell signaling via interactions with the SLP-76 and LAT adaptors', *Curr Biol*, 9: 67-75.

Lunning, M. A., and J. M. Vose. 2017. 'Angioimmunoblastic T-cell lymphoma: the many-faced lymphoma', *Blood*, 129: 1095-102.

Ma, A., and B. A. Malynn. 2012. 'A20: linking a complex regulator of ubiquitylation to immunity and human disease', *Nat Rev Immunol*, 12: 774-85.

Maehama, T., and J. E. Dixon. 1998. 'The tumor suppressor, PTEN/MMAC1, dephosphorylates the lipid second messenger, phosphatidylinositol 3,4,5-trisphosphate', *J Biol Chem*, 273: 13375-8.

'Major prognostic factors of patients with adult T-cell leukemia-lymphoma: a cooperative study. Lymphoma Study Group (1984-1987)'. 1991. *Leuk Res*, 15: 81-90.

McGirt, L. Y., P. Jia, D. A. Baerenwald, R. J. Duszynski, K. B. Dahlman, J. A. Zic, J. P. Zwerner, D. Hucks, U. Dave, Z. Zhao, and C. M. Eischen. 2015. 'Whole-genome sequencing reveals oncogenic mutations in mycosis fungoides', *Blood*, 126: 508-19.

Motzer, R. J., B. Escudier, D. F. McDermott, S. George, H. J. Hammers, S. Srinivas, S. S. Tykodi, J. A. Sosman, G. Procopio, E. R. Plimack, D. Castellano, T. K. Choueiri, H. Gurney, F. Donskov, P. Bono, J. Wagstaff, T. C. Gauler, T. Ueda, Y. Tomita, F. A. Schutz, C. Kollmannsberger, J. Larkin, A. Ravaud, J. S. Simon, L. A. Xu, I. M. Waxman, P. Sharma, and Investigators CheckMate. 2015. 'Nivolumab versus Everolimus in Advanced Renal-Cell Carcinoma', *N Engl J Med*, 373: 1803-13.

Myers, M. P., I. Pass, I. H. Batty, J. Van der Kaay, J. P. Stolarov, B. A. Hemmings, M. H. Wigler, C. P. Downes, and N. K. Tonks. 1998. 'The lipid phosphatase activity of PTEN is critical for its tumor supressor function', *Proc Natl Acad Sci U S A*, 95: 13513-8.

Nghiem, P. T., S. Bhatia, E. J. Lipson, R. R. Kudchadkar, N. J. Miller, L. Annamalai, S. Berry, E. K. Chartash, A. Daud, S. P. Fling, P. A. Friedlander, H. M. Kluger, H. E. Kohrt, L. Lundgren, K. Margolin, A. Mitchell, T. Olencki, D. M. Pardoll, S. A. Reddy, E. M. Shantha, W. H. Sharfman, E. Sharon, L. R. Shemanski, M. M. Shinohara, J. C. Sunshine, J. M. Taube, J. A. Thompson, S. M. Townson, J. H. Yearley, S. L. Topalian, and M. A. Cheever. 2016. 'PD-1 Blockade with Pembrolizumab in Advanced Merkel-Cell Carcinoma', *N Engl J Med*, 374: 2542-52.

Nolden, L., F. Edenhofer, S. Haupt, P. Koch, F. T. Wunderlich, H. Siemen, and O. Brustle. 2006. 'Site-specific recombination in human embryonic stem cells induced by cell-permeant Cre recombinase', *Nat Methods*, 3: 461-7.

Nosaka, K., T. Miyamoto, T. Sakai, H. Mitsuya, T. Suda, and M. Matsuoka. 2002. 'Mechanism of hypercalcemia in adult T-cell leukemia: overexpression of receptor activator of nuclear factor kappaB ligand on adult T-cell leukemia cells', *Blood*, 99: 634-40.

O'Malley, D. P., V. Chizhevsky, K. E. Grimm, A. Hii, and L. M. Weiss. 2014. 'Utility of BCL2, PD1, and CD25 immunohistochemical expression in the diagnosis of T-cell lymphomas', *Appl Immunohistochem Mol Morphol*, 22: 99-104.

Odejide, O., O. Weigert, A. A. Lane, D. Toscano, M. A. Lunning, N. Kopp, S. Kim, D. van Bodegom, S. Bolla, J. H. Schatz, J. Teruya-Feldstein, E. Hochberg, A. Louissaint, D. Dorfman, K. Stevenson, S. J. Rodig, P. P. Piccaluga, E. Jacobsen, S. A. Pileri, N. L. Harris, S. Ferrero, G. Inghirami, S. M. Horwitz, and D. M. Weinstock. 2014. 'A targeted mutational landscape of angioimmunoblastic T-cell lymphoma', *Blood*, 123: 1293-6.

Okkenhaug, K., and B. Vanhaesebroeck. 2003. 'PI3K in lymphocyte development, differentiation and activation', *Nat Rev Immunol*, 3: 317-30.

Ono, K., Y. Onishi, M. Kobayashi, S. Hatta, K. Nasu, S. Watanabe, S. Ichikawa, Y. Okitsu, N. Fukuhara, and H. Harigae. 2018. 'gammadelta T cell clonal proliferation early after PD-1 blockade', *Ann Hematol*.

Palomero, T., L. Couronne, H. Khiabanian, M. Y. Kim, A. Ambesi-Impiombato, A. Perez-Garcia, Z. Carpenter, F. Abate, M. Allegretta, J. E. Haydu, X. Jiang, I. S. Lossos, C. Nicolas, M. Balbin, C. Bastard, G. Bhagat, M. A. Piris, E. Campo, O. A. Bernard, R. Rabadan, and A. A. Ferrando. 2014. 'Recurrent mutations in epigenetic regulators, RHOA and FYN kinase in peripheral T cell lymphomas', *Nat Genet*, 46: 166-70.

Papadavid, E., P. Korkolopoulou, G. Levidou, A. A. Saetta, T. Papadaki, M. Siakantaris, V. Nikolaou, A. Oikonomidi, I. Chatziandreou, L. Marinos, A. Kolialexi, A. Stratigos, D. Rigopoulos, A. Psyrri, E. Patsouris, and C. Antoniou. 2014. 'In situ assessment of PI3K and PTEN alterations in mycosis fungoides: correlation with clinicopathological features', *Exp Dermatol*, 23: 931-3.

Park, S., and Y. H. Ko. 2014. 'Peripheral T cell lymphoma in Asia', *Int J Hematol*, 99: 227-39.

Parry, R. V., J. M. Chemnitz, K. A. Frauwirth, A. R. Lanfranco, I. Braunstein, S. V. Kobayashi, P. S. Linsley, C. B. Thompson, and J. L. Riley. 2005. 'CTLA-4 and PD-1 receptors inhibit T-cell activation by distinct mechanisms', *Mol Cell Biol*, 25: 9543-53.

Patsoukis, N., L. Li, D. Sari, V. Petkova, and V. A. Boussiotis. 2013. 'PD-1 increases PTEN phosphatase activity while decreasing PTEN protein stability by inhibiting casein kinase 2', *Mol Cell Biol*, 33: 3091-8.

Pechloff, K., J. Holch, U. Ferch, M. Schweneker, K. Brunner, M. Kremer, T. Sparwasser, L. Quintanilla-Martinez, U. Zimber-Strobl, B. Streubel, A. Gewies, C. Peschel, and J. Ruland. 2010. 'The fusion kinase ITK-SYK mimics a T cell receptor signal and drives oncogenesis in conditional mouse models of peripheral T cell lymphoma', *J Exp Med*, 207: 1031-44.

Pertea, M., G. M. Pertea, C. M. Antonescu, T. C. Chang, J. T. Mendell, and S. L. Salzberg. 2015. 'StringTie enables improved reconstruction of a transcriptome from RNA-seq reads', *Nat Biotechnol*, 33: 290-5.

Pitcher, L. A., and N. S. van Oers. 2003. 'T-cell receptor signal transmission: who gives an ITAM?', *Trends Immunol*, 24: 554-60.

Rad, R., L. Rad, W. Wang, J. Cadinanos, G. Vassiliou, S. Rice, L. S. Campos, K. Yusa, R. Banerjee, M. A. Li, J. de la Rosa, A. Strong, D. Lu, P. Ellis, N. Conte, F. T. Yang, P. Liu, and A. Bradley. 2010. 'PiggyBac transposon mutagenesis: a tool for cancer gene discovery in mice', *Science*, 330: 1104-7.

Rad, R., L. Rad, W. Wang, A. Strong, H. Ponstingl, I. F. Bronner, M. Mayho, K. Steiger, J. Weber, M. Hieber, C. Veltkamp, S. Eser, U. Geumann, R. Ollinger, M. Zukowska, M. Barenboim, R. Maresch, J. Cadinanos, M. Friedrich, I. Varela, F. Constantino-Casas, A. Sarver, J. Ten Hoeve, H. Prosser, B. Seidler, J. Bauer, M. Heikenwalder, E. Metzakopian, A. Krug, U. Ehmer, G. Schneider, T. Knosel, P. Rummele, D. Aust, R. Grutzmann, C. Pilarsky, Z. Ning, L. Wessels, R. M. Schmid, M. A. Quail, G. Vassiliou, I. Esposito, P. Liu, D. Saur, and A. Bradley. 2015. 'A conditional piggyBac transposition system for genetic screening in mice identifies oncogenic networks in pancreatic cancer', *Nat Genet*, 47: 47-56.

Ratner, L., T. A. Waldmann, M. Janakiram, and J. E. Brammer. 2018. 'Rapid Progression of Adult T-Cell Leukemia-Lymphoma after PD-1 Inhibitor Therapy', *N Engl J Med*, 378: 1947-48.

Ribas, A., and J. D. Wolchok. 2018. 'Cancer immunotherapy using checkpoint blockade', *Science*, 359: 1350-55.

Rigby, S., Y. Huang, B. Streubel, A. Chott, M. Q. Du, S. D. Turner, and C. M. Bacon. 2009. 'The lymphoma-associated fusion tyrosine kinase ITK-SYK requires pleckstrin

homology domain-mediated membrane localization for activation and cellular transformation', *J Biol Chem*, 284: 26871-81.

Riley, J. L. 2009. 'PD-1 signaling in primary T cells', *Immunol Rev*, 229: 114-25.

Roemer, M. G., R. H. Advani, A. H. Ligon, Y. Natkunam, R. A. Redd, H. Homer, C. F. Connelly, H. H. Sun, S. E. Daadi, G. J. Freeman, P. Armand, B. Chapuy, D. de Jong, R. T. Hoppe, D. S. Neuberg, S. J. Rodig, and M. A. Shipp. 2016. 'PD-L1 and PD-L2 Genetic Alterations Define Classical Hodgkin Lymphoma and Predict Outcome', *J Clin Oncol*, 34: 2690-7.

Rohr, J., S. Guo, J. Huo, A. Bouska, C. Lachel, Y. Li, P. D. Simone, W. Zhang, Q. Gong, C. Wang, A. Cannon, T. Heavican, A. Mottok, S. Hung, A. Rosenwald, R. Gascoyne, K. Fu, T. C. Greiner, D. D. Weisenburger, J. M. Vose, L. M. Staudt, W. Xiao, G. E. Borgstahl, S. Davis, C. Steidl, T. McKeithan, J. Iqbal, and W. C. Chan. 2016. 'Recurrent activating mutations of CD28 in peripheral T-cell lymphomas', *Leukemia*, 30: 1062-70.

Rossy, J., D. J. Williamson, and K. Gaus. 2012. 'How does the kinase Lck phosphorylate the T cell receptor? Spatial organization as a regulatory mechanism', *Front Immunol*, 3: 167.

Rougerie, P., and J. Delon. 2012. 'Rho GTPases: masters of T lymphocyte migration and activation', *Immunol Lett*, 142: 1-13.

Ruland, J., and L. Hartjes. 2018. 'CARD-BCL-10-MALT1 signalling in protective and pathological immunity', *Nat Rev Immunol*.

Sarver, A. L., J. Erdman, T. Starr, D. A. Largaespada, and K. A. Silverstein. 2012. 'TAPDANCE: an automated tool to identify and annotate transposon insertion CISs and associations between CISs from next generation sequence data', *BMC Bioinformatics*, 13: 154.

Sharma, P., K. Wagner, J. D. Wolchok, and J. P. Allison. 2011. 'Novel cancer immunotherapy agents with survival benefit: recent successes and next steps', *Nat Rev Cancer*, 11: 805-12.

Sharpe, A. H., and K. E. Pauken. 2018. 'The diverse functions of the PD1 inhibitory pathway', *Nat Rev Immunol*, 18: 153-67.

Sheppard, K. A., L. J. Fitz, J. M. Lee, C. Benander, J. A. George, J. Wooters, Y. Qiu, J. M. Jussif, L. L. Carter, C. R. Wood, and D. Chaudhary. 2004. 'PD-1 inhibits T-cell receptor induced phosphorylation of the ZAP70/CD3zeta signalosome and downstream signaling to PKCtheta', *FEBS Lett*, 574: 37-41.

Shlapatska, L. M., S. V. Mikhalap, A. G. Berdova, O. M. Zelensky, T. J. Yun, K. E. Nichols, E. A. Clark, and S. P. Sidorenko. 2001. 'CD150 association with either the

SH2-containing inositol phosphatase or the SH2-containing protein tyrosine phosphatase is regulated by the adaptor protein SH2D1A', *J Immunol*, 166: 5480-7.

Sledzinska, A., S. Hemmers, F. Mair, O. Gorka, J. Ruland, L. Fairbairn, A. Nissler, W. Muller, A. Waisman, B. Becher, and T. Buch. 2013. 'TGF-beta signalling is required for CD4(+) T cell homeostasis but dispensable for regulatory T cell function', *PLoS Biol*, 11: e1001674.

Spinelli, L., S. Carpentier, F. Montanana Sanchis, M. Dalod, and T. P. Vu Manh. 2015. 'BubbleGUM: automatic extraction of phenotype molecular signatures and comprehensive visualization of multiple Gene Set Enrichment Analyses', *BMC Genomics*, 16: 814.

Streubel, B., U. Vinatzer, M. Willheim, M. Raderer, and A. Chott. 2006. 'Novel t(5;9)(q33;q22) fuses ITK to SYK in unspecified peripheral T-cell lymphoma', *Leukemia*, 20: 313-8.

Tanaka, Y., A. M. Maeshima, J. Nomoto, S. Makita, S. Fukuhara, W. Munakata, D. Maruyama, K. Tobinai, and Y. Kobayashi. 2018. 'Expression pattern of PD-L1 and PD-L2 in classical Hodgkin lymphoma, primary mediastinal large B-cell lymphoma, and gray zone lymphoma', *Eur J Haematol*, 100: 511-17.

Tarakhovsky, A., M. Turner, S. Schaal, P. J. Mee, L. P. Duddy, K. Rajewsky, and V. L. Tybulewicz. 1995. 'Defective antigen receptor-mediated proliferation of B and T cells in the absence of Vav', *Nature*, 374: 467-70.

Tseng, S. Y., M. Otsuji, K. Gorski, X. Huang, J. E. Slansky, S. I. Pai, A. Shalabi, T. Shin, D. M. Pardoll, and H. Tsuchiya. 2001. 'B7-DC, a new dendritic cell molecule with potent costimulatory properties for T cells', *J Exp Med*, 193: 839-46.

Tubo, N. J., and M. K. Jenkins. 2014. 'TCR signal quantity and quality in CD4(+) T cell differentiation', *Trends Immunol*, 35: 591-96.

Ungewickell, A., A. Bhaduri, E. Rios, J. Reuter, C. S. Lee, A. Mah, A. Zehnder, R. Ohgami, S. Kulkarni, R. Armstrong, W. K. Weng, D. Gratzinger, M. Tavallaee, A. Rook, M. Snyder, Y. Kim, and P. A. Khavari. 2015. 'Genomic analysis of mycosis fungoides and Sezary syndrome identifies recurrent alterations in TNFR2', *Nat Genet*, 47: 1056-60.

Vallois, D., M. P. Dobay, R. D. Morin, F. Lemonnier, E. Missiaglia, M. Juilland, J. Iwaszkiewicz, V. Fataccioli, B. Bisig, A. Roberti, J. Grewal, J. Bruneau, B. Fabiani, A. Martin, C. Bonnet, O. Michielin, J. P. Jais, M. Figeac, O. A. Bernard, M. Delorenzi, C. Haioun, O. Tournilhac, M. Thome, R. D. Gascoyne, P. Gaulard, and L. de Leval. 2016. 'Activating mutations in genes related to TCR signaling in angioimmunoblastic and other follicular helper T-cell-derived lymphomas', *Blood*, 128: 1490-502.

Vallois, D., A. Dupuy, F. Lemonnier, G. Allen, E. Missiaglia, V. Fataccioli, N. Ortonne, A. Clavert, R. Delarue, M. C. Rousselet, B. Fabiani, F. Llamas-Gutierrez, S. Ogawa,

M. Thome, Y. H. Ko, K. Kataoka, P. Gaulard, and L. de Leval. 2018. 'RNA fusions involving CD28 are rare in peripheral T-cell lymphomas and concentrate mainly in those derived from follicular helper T cells', *Haematologica*, 103: e360-e63.

Van Arnam, J. S., M. S. Lim, and K. S. J. Elenitoba-Johnson. 2018. 'Novel insights into the pathogenesis of T-cell lymphomas', *Blood*, 131: 2320-30.

van der Veeken, J., A. J. Gonzalez, H. Cho, A. Arvey, S. Hemmers, C. S. Leslie, and A. Y. Rudensky. 2016. 'Memory of Inflammation in Regulatory T Cells', *Cell*, 166: 977-90.

Vaque, J. P., G. Gomez-Lopez, V. Monsalvez, I. Varela, N. Martinez, C. Perez, O. Dominguez, O. Grana, J. L. Rodriguez-Peralto, S. M. Rodriguez-Pinilla, C. Gonzalez-Vela, M. Rubio-Camarillo, E. Martin-Sanchez, D. G. Pisano, E. Papadavid, T. Papadaki, L. Requena, J. A. Garcia-Marco, M. Mendez, M. Provencio, M. Hospital, D. Suarez-Massa, C. Postigo, D. San Segundo, M. Lopez-Hoyos, P. L. Ortiz-Romero, M. A. Piris, and M. Sanchez-Beato. 2014. 'PLCG1 mutations in cutaneous T-cell lymphomas', *Blood*, 123: 2034-43.

Vose, J. M. 2008. 'Peripheral T-cell non-Hodgkin's lymphoma', *Hematol Oncol Clin North Am*, 22: 997-1005, x.

Wang, L., X. Ni, K. R. Covington, B. Y. Yang, J. Shiu, X. Zhang, L. Xi, Q. Meng, T. Langridge, J. Drummond, L. A. Donehower, H. Doddapaneni, D. M. Muzny, R. A. Gibbs, D. A. Wheeler, and M. Duvic. 2015. 'Genomic profiling of Sezary syndrome identifies alterations of key T cell signaling and differentiation genes', *Nat Genet*, 47: 1426-34.

Watatani, Y., Y. Sato, H. Miyoshi, K. Sakamoto, K. Nishida, Y. Gion, Y. Nagata, Y. Shiraishi, K. Chiba, H. Tanaka, L. Zhao, Y. Ochi, Y. Takeuchi, J. Takeda, H. Ueno, Y. Kogure, Y. Shiozawa, N. Kakiuchi, T. Yoshizato, M. M. Nakagawa, Y. Nanya, K. Yoshida, H. Makishima, M. Sanada, M. Sakata-Yanagimoto, S. Chiba, R. Matsuoka, M. Noguchi, N. Hiramoto, T. Ishikawa, J. Kitagawa, N. Nakamura, H. Tsurumi, T. Miyazaki, Y. Kito, S. Miyano, K. Shimoda, K. Takeuchi, K. Ohshima, T. Yoshino, S. Ogawa, and K. Kataoka. 2019. 'Molecular heterogeneity in peripheral T-cell lymphoma, not otherwise specified revealed by comprehensive genetic profiling', *Leukemia*, 33: 2867-83.

Weiss, A., and D. R. Littman. 1994. 'Signal transduction by lymphocyte antigen receptors', *Cell*, 76: 263-74.

Whitfield, M. L., G. Sherlock, A. J. Saldanha, J. I. Murray, C. A. Ball, K. E. Alexander, J. C. Matese, C. M. Perou, M. M. Hurt, P. O. Brown, and D. Botstein. 2002. 'Identification of genes periodically expressed in the human cell cycle and their expression in tumors', *Mol Biol Cell*, 13: 1977-2000.

Whittaker, S., R. Hoppe, and H. M. Prince. 2016. 'How I treat mycosis fungoides and Sezary syndrome', *Blood*, 127: 3142-53.

Wieman, H. L., J. A. Wofford, and J. C. Rathmell. 2007. 'Cytokine stimulation promotes glucose uptake via phosphatidylinositol-3 kinase/Akt regulation of Glut1 activity and trafficking', *Mol Biol Cell*, 18: 1437-46.

Yokosuka, T., M. Takamatsu, W. Kobayashi-Imanishi, A. Hashimoto-Tane, M. Azuma, and T. Saito. 2012. 'Programmed cell death 1 forms negative costimulatory microclusters that directly inhibit T cell receptor signaling by recruiting phosphatase SHP2', *J Exp Med*, 209: 1201-17.

Yoo, H. Y., M. K. Sung, S. H. Lee, S. Kim, H. Lee, S. Park, S. C. Kim, B. Lee, K. Rho, J. E. Lee, K. H. Cho, W. Kim, H. Ju, J. Kim, S. J. Kim, W. S. Kim, S. Lee, and Y. H. Ko. 2014. 'A recurrent inactivating mutation in RHOA GTPase in angioimmunoblastic T cell lymphoma', *Nat Genet*, 46: 371-5.

Zhan, H. Q., X. Q. Li, X. Z. Zhu, H. F. Lu, X. Y. Zhou, and Y. Chen. 2011. 'Expression of follicular helper T cell markers in nodal peripheral T cell lymphomas: a tissue microarray analysis of 162 cases', *J Clin Pathol*, 64: 319-24.

Zhao, Y., D. L. Harrison, Y. Song, J. Ji, J. Huang, and E. Hui. 2018. 'Antigen-Presenting Cell-Intrinsic PD-1 Neutralizes PD-L1 in cis to Attenuate PD-1 Signaling in T Cells', *Cell Rep*, 24: 379-90 e6.

6 Acknowledgements

This PhD thesis is the result of the effort and support of multiple people to whom I am deeply grateful.

First, I would like to thank Professor Jürgen Ruland for introducing me to field of Immunology and everything he has taught me about inspiration, scientific thinking and writing, designing experiments, interpretation of data, motivation, patience and persistence. I also want to say thank you for his trust, generosity, guidance, personal support and for the freedom he offered to explore my scientific curiosity in our experiments.

Next, I want to thank Professor Roland Rad and Professor Mathias Heikenwälder for being great mentors for the PhD program. I am deeply thankful for having had such brilliant researchers on my side from whom I have received great advice and inspiration.

In addition, I am also tremendously grateful for the work of my co-authors and their substantial contribution to generate and interpret the data presented in this thesis. Thanks, Dr. Zsuzsanna Kurgyis, Dr. Selina Keppler, Dr. Konstanze Pechloff, Dr. Erik Hameister, Dr. Ruppert Öllinger, Dr. Roman Maresch, Prof. Thorsten Buch, Dr. Katja Steiger, Dr. Dr. Christof Winter and Prof. Roland Rad. I am delighted to have worked with you and I look forward to working with you again.

Also, I am deeply appreciative to the Ruland lab members for being wonderful collogues and friends. Special thanks for many enjoyable and memorable moments I owe to Dr. Zsuzsanna Kurgyis, Dr. Konstantin Neumann, Miriam Schulz, Dr. Erik Hameister, Marie Arens, Dr. Paul König, Dr. Kai Lee and Dr. Lara Hartjes.

Finally, I wish to sincerely thank all those of you who have contributed to this study. It has been a privilege to work with you.

7 Publications

Wartewig, T., Z. Kurgyis, S. Keppler, K. Pechloff, E. Hameister, R. Öllinger, R. Maresch, T. Buch, K. Steiger, C. Winter, R. Rad, and J. Ruland. 2017. '*PD-1 is a haploinsufficient suppressor of T cell lymphomagenesis'*, Nature, 552: 121-25.

Wartewig, T., and J. Ruland. 2019. *'PD-1 Tumor Suppressor Signaling in T Cell Lymphomas'*, Trends Immunol, 40: 403-14.

8 Table and Figure List